

COMPUTER SIMULATION OF CAM SYSTEM DYNAMICS  
AND SENSITIVITY STUDIES

By

© PARAMJIT SINGH GREWAL, M. Eng.

A Thesis

Submitted to the School of Graduate Studies

in Partial Fulfilment of the Requirements

for the Degree

Doctor of Philosophy

McMaster University

July 1986

DOCTOR OF PHILOSOPHY (1986)  
(Mechanical Engineering)

McMASTER UNIVERSITY  
Hamilton, Ontario

TITLE : Computer Simulation of Cam System Dynamics  
and Sensitivity Studies

AUTHOR : Paramjit Singh Grewal  
B.Sc. Eng. Honours (Punjab University)  
M.E. Honours (University of Roorkee)  
M.Eng. (McMaster University)

SUPERVISOR: Professor W.R. Newcombe

NUMBER OF PAGES: x, 195.

## ABSTRACT

This thesis deals with the dynamics of cam systems, and stems from the need to integrate the dynamic design with the quality of manufacture of the cam profile. The objective is to provide a better insight into the high-speed dynamic performance of the system, and generate more refined qualitative and quantitative information for the dynamic design and the manufacturing of cams. A simulation approach has been used, and a stochastic model has been proposed for the generation of the input signal, which comprises the desired lift and the lift error due to manufacturing errors in the cam profile. The stochastic model employs the techniques of random number generation and spline smoothing. The input signal is integrated with the seven degrees-of-freedom dynamic model considered for the common cam-follower system.

A comprehensive study of the popular cam motions has been conducted to investigate their high-speed performance. In particular, the effects of cam profile manufacturing errors on the dynamic behaviour of the cam-follower system are examined. Sensitivity studies have been performed to investigate the effects of critical system parameters on the system behaviour.

The study has demonstrated that for semi-rigid follower cam systems, the combined effects of system flexibility and cam profile errors are significantly greater than that of flexibility

alone, and that the effects of profile errors are dominating. The dynamic response is critically dependent on the waviness of the lift error. It has been established that at high speeds, it is not the vibrational response, but the jump behaviour which determines the dynamic performance. The Modified-Sine, Simple Harmonic, and 3-4-5 Polynomial motions have been shown to exhibit superior high-speed performance to that of the popular Cycloidal and Modified-Trapezoidal motions. It has also been demonstrated that, for the flexible follower system, the dynamic effects of cam profile errors are small. This is probably the reason why previous investigators have neglected the effects of cam profile errors in their modelling.

This thesis makes a significant contribution in the field of design of cam-follower systems and the manufacture of cams. A versatile, user-oriented software system - COSCAD has been developed which can be a very useful tool for the cam designer to search for the best cam motion, the system parameters, and the production quality of cams to achieve optimum dynamic performance. Using this program, the system behaviour can be predicted during the design development stage without setting up a complex experimental rig.

### ACKNOWLEDGEMENTS

The author gratefully thanks Prof. W.R. Newcombe for his guidance, encouragement, continued assistance, and supervision during the course of this work. He also thanks Prof. J.N. Siddall, Dr. R.L. Judd, and Dr. A.A. Smith of Civil Engineering, members of his supervisory committee, for their understanding and friendly interest.

The financial assistance provided by the Natural Sciences and Engineering Research Council of Canada, and the Department of Mechanical Engineering through a Teaching Assistantship, is gratefully acknowledged.

The author is highly thankful to Messers Eonic Inc., Detroit for allowing visits to their cam design, manufacturing, and inspection departments, and for making available a variety of inspection lift error charts for high-speed cams.

Lastly, the author is indebted to his employer at Punjab Agricultural University, Ludhiana, India, for granting an uninterrupted study leave.

## TABLE OF CONTENTS

	PAGE
ABSTRACT	iii
ACKNOWLEDGEMENTS	v
NOMENCLATURE	ix
CHAPTER 1 INTRODUCTION	1
1.1 General Background	1
1.2 Objectives and Scope of Research	2
1.3 Method of Approach	5
1.4 Organization of the Work	6
CHAPTER 2 LITERATURE REVIEW	8
2.1 Introduction	8
2.2 Investigations in Cam System Dynamics	9
CHAPTER 3 PERFORMANCE CHARACTERISTICS IN CAM DYNAMICS	39
3.1 Introduction	39
3.2 Performance Criteria	39
3.2.1 Frequency-Domain Response	40
3.2.2 Time-Domain Response	41
3.2.3 Dynamic Characteristics at the Cam	42
CHAPTER 4 SYSTEM IDENTIFICATION	43
4.1 Introduction	43
4.2 Cam-Follower System	44
4.3 Idealized Dynamic Model	44

TABLE OF CONTENTS (continued)

	PAGE
CHAPTER 4 (continued)	
4.4 Mathematical Model - Formulation of Equations of Motion	47
4.4.1 Torsional System	49
4.4.2 Contact Force	50
4.4.3 Return Spring Preload	50
4.4.4 Contact Stiffness	52
4.4.5 Translational System - Motion with No-Jump	55
4.4.6 Energy Dissipation	55
4.4.7 Jump Criterion	58
4.4.8 Translational System - Motion during Jump	59
4.5 Simulation of the Excitation	60
4.5.1 Machining Process of Cam Profile - Cam Production	60
4.5.2 Model of the Input Signal - The Lift Function	63
4.5.3 Smoothing by Spline Interpolation	70
CHAPTER 5 IMPLEMENTATION	75
5.1 Introduction	75
5.2 Solution of Equations of Motion	75
5.3 Generation of Lift Error Function	76
5.4 System Parameters	77
5.5 Calculation of Natural Frequencies	81
CHAPTER 6 RESULTS AND DISCUSSION	83
6.1 Introduction	83
6.2 Comparison of Cam Motions	84
6.2.1 Comparison Based on Flexibility Alone	84
6.2.2 Comparison Based on Profile Errors (Tolerance) Alone	97
6.2.3 Comparison Based on Combined Flexibility and Tolerance Effects	102

TABLE OF CONTENTS (continued)

	PAGE
CHAPTER 6 (continued)	
6.3 Effect of Varying the Cam Profile Error	134
6.4 Response Sensitivity to System Parameters	140
6.4.1 Speed Effects	140
6.4.2 Effects of Return Spring Stiffness	146
6.4.3 Effects of Follower Mass	153
6.4.4 Effects of Damping	153
6.4.5 Effects of Camshaft Torsional Stiffness	159
6.5 Effects of System Dynamics and Cam Profile Errors for a Flexible Follower System	163
CHAPTER 7 CONCLUSIONS	170
7.1 Conclusions and Recommendations	170
7.2 Comparison with the Results of Previous Work	175
7.3 Contributions in the Area of Research	180
7.3 Suggestions for Further Research	184
REFERENCES	185
APPENDICES	190
A.1 Calculation of System Properties	190
A.2 Random Number Generation	193
A.3 Return Spring Idealization	194
A.4 Software System - COSCAD, User's Manual	-



## NOMENCLATURE

$C_b$	:	Damping coefficient of camshaft bearing
$C_{cb}$	:	Coulomb friction damping coefficient at the follower-guide interface
$C_f$	:	Internal friction damping coefficient of follower
$C_{rs}$	:	Internal friction damping coefficient of return spring
$C_{sf}$	:	Damping coefficient for drive shaft in torsion
$C_{vs}$	:	Damping coefficient for drive shaft in transverse vibrations
$e$	:	Follower offset
$F_c$	:	Contact force between cam and follower at their contact
$F_{cb}$	:	Coulomb friction force on the follower
$F_p$	:	Return spring preload
$F_w$	:	External work load
$I_c$	:	Cam inertia plus inertia of the camshaft considered at the cam
$I_{cs}$	:	Inertia of the camshaft considered at the cam
$K_f$	:	Follower stiffness
$K_h$	:	Contact stiffness
$K_{rs}$	:	Stiffness of the return spring
$K_{sf}$	:	Drive shaft stiffness in Torsion
$K_{vs}$	:	Transverse stiffness of the drive shaft
$l$	:	Cam thickness

- $M_c$  : Mass of the cam plus that of the camshaft considered at the cam  
 $M_{cs}$  : Mass of camshaft considered at the cam  
 $M_{f1}$  : Follower mass  
 $M_r$  : Mass of the follower roller - may also include a part of the follower mass  
 $M_{rs}$  : Mass of the return spring  
 $R_b$  : Cam base circle radius  
 $R_r$  : Roller radius  
 $T_c$  : Cam torque  
 $y, \dot{y}, \ddot{y}$  : Theoretical lift (displacement), velocity, and acceleration of the follower  
 $(y_i, \dot{y}_i, \ddot{y}_i; i=1,6)$  : Vertical displacements, velocities, and accelerations of various masses  
 $\theta_i, \dot{\theta}_i$  : Input angular displacement, and velocity  
 $\theta_c, \dot{\theta}_c, \ddot{\theta}_c$  : Angular displacement, velocity, and acceleration of the cam  
 $\delta_{rs}$  : Return spring compression in assembly  
 $c_f$  : Damping factor for the follower  
 $c_{rs}$  : Damping factor for the return spring  
 $\phi$  : Pressure angle  
 $\omega_c$  : Cam rotational speed ( $\dot{\theta}_c$ )

## CHAPTER 1

### INTRODUCTION

#### 1.1 General Background

Cams are used extensively in automotive industry and in high-speed, automated, special-purpose production machinery for transmitting a desired motion to a follower by direct contact. They provide an unlimited range of applications and a compact system which is easy to design and manufacture. However, the accuracy of machining the cam profile becomes critical in high-speed applications because of the sensitivity of the desired follower motion to these errors, and combined with the vibration effects of system elasticity, cam profile errors produce bad dynamic behaviour of the system. Consequently, increased vibration, jump, shock, fatigue, and wear problems occur.

The dynamics of high-speed cam-follower systems remains an active field of research and development with the ever-increasing demand of achieving high performance at minimum weight and cost. Computer simulation studies are an important analytical tool in the cam design field. They have long been used to predict the dynamic behaviour of new designs, or in the development of existing systems. This form of computer-aided design drastically reduces the need for an expensive and time consuming exercise of constructing and testing prototypes. Sensitivity information can be easily generated to gain a basic understanding of the system behavioural characteristics, and to evaluate design trade-offs.

As the demands on the cam system increase, the designer's understanding of the system dynamics must also improve. It is, therefore, important to refine the simulation models continuously to describe the physical system as accurately as possible, within the constraints of mathematical complexity and computational effort.

1.2 Objectives and Scope of Research

The output motion of the follower in a cam-follower system deviates from the motion designed into the cam because of the vibrations of driving and driven elements in the mechanism, and the manufacturing errors in the cam profile. Earlier investigations have followed either a pure dynamic approach, considering the cam profile as perfect, or have considered only kinematics to study the influence of profile errors on the follower response for a perfectly rigid system. The most general case ( IV in Fig. 1.1 ), where both dynamics and profile errors are taken into account, has seldom been studied. Considering the realities of cam manufacture and its high-speed operation, this case presents the actual situation in practice.

	Ideal Profile	Real Profile
Kinematics	I	II
Dynamics	III	IV

Fig. 1.1 Possible combinations for investigation of cam mechanisms.

Most of the previous studies have considered the system as an oversimplified single degree-of-freedom (d.o.f.) system with idealizations which would seriously affect the information obtained and the conclusions drawn. It has been felt that a greater insight into the dynamic behaviour of the cam system can be achieved when the system is considered in its entirety, accounting for all the important factors that influence the system response. This forms the basis of the investigations undertaken in this work.

A comprehensive design procedure requires trade-offs between the dynamic response at the cam such as driving torque, contact forces, etc., and at the output in the form of motion distortion, vibration, and jump, during the complete cam cycle in the steady-state. Direct optimization would involve multi-objectives and highly nonlinear analysis equations in the parametric form because of continuous cam rotation. It is, however, convenient to simulate the system behaviour and conduct sensitivity analysis to study the effect of system parameter changes on various design criteria. Based on the studies on different cam motions, an optimal design giving the most desirable cam profile and the system parameters, can thus be approached.

In this investigation, the high-speed dynamic performance of all the popular cam motions will be evaluated and compared using similar system specifications. The desired theoretical cam motion cannot be reproduced in manufacturing, and machining errors do occur in the profile which seriously affect the system performance.

The effects of these errors have generally been neglected in the past because most studies were done on very flexible follower systems of the push-rod type valve-gear in automotive engines, where these errors have been observed to have no significant effects on the system dynamics. In the present study, the main emphasis will be laid on the dynamic effects of machining errors in cam profiles and their relation to the cam motion specification and operating cam speeds. A comprehensive dynamic model will be considered to account for the effects of cam speed variations, compliance at the cam-follower interface, return spring vibrations, and Coulomb friction, etc. Sensitivity analysis will be performed to study the effects of changes in critical system parameters. It will be possible to study the effects of system flexibility and machining errors separately as well as in combination. Wherever possible, the results will be compared with those of the previous investigators.

Important qualitative and quantitative information on the high-speed dynamic performance of the most common type of cam-follower mechanism and for all the popular cam motion programs will be provided. In addition, the software system to be developed within these objectives will be of significant value to the cam designer to predict, without setting up a complex experimental rig, the system performance during the design development stage. It is important to note here that for a comparative study of cam motions, an experimental approach cannot duplicate the lift error for cams produced to different motion specifications.

### 1.3 Method of Approach

The analysis approach used here is the simulation technique. A multi-degree-of-freedom dynamic model for the cam-follower system along with a stochastic model to simulate the excitation, taking into account the lift error due to cam profile machining inaccuracy, has been developed for the dynamic analysis of the system. An actual input signal (excitation), obtained by superimposing on the theoretical lift, the inspection lift error data acquired from quality cam manufacturers, is also employed to determine the dynamic effects in a more realistic situation. The error data at discrete cam angle positions has been smoothed by spline interpolation. The dynamic model includes all the significant factors that influence the system response characteristics. An appropriate model has been considered to simulate the return spring vibrations, and expressions are developed to compute the compliance at the contact between cam and follower surfaces.

The performance criteria comprise the dynamic response at the output in the form of acceleration oscillations and jump, and at the cam in the form of contact force, cam torque, pressure angle, and cam-speed variations. Because of the consideration of nonlinearities, like Coulomb friction, numerical integration has been employed to obtain the dynamic response. The results are presented in the tabular form and plotted for the visual interpretation of the system response.

#### 1.4 Organization of the Work

Here a summary of the subjects presented and discussed is given.

Chapter 2 gives a comprehensive survey of the investigations in cam system dynamics. The literature has been covered under three broad areas; namely, the consideration of system dynamics alone, consideration of manufacturing effects, and optimization studies in cam dynamics. A critical review, pointing out the weaknesses and omissions in these works, has been presented.

Chapter 3 deals with the performance characteristics generally used to describe the system response. Other behavioural characteristics which more specifically determine the cam system dynamic performance are also defined.

System modelling is covered under Chapter 4, which presents a detailed development of the dynamic system model for the cam mechanism, and the stochastic model to generate the input signal. Expressions are derived for the contact compliance and the contact force at the cam-follower interface, and the criterion has been developed to define the follower jump. System equations are derived for both the normal follower-cam contact mode and the situation where follower jump has occurred.

Chapter 5 contains the method of solution employed for the system of equations, the actual generation of the lift error, the specifications for the cam-follower system under investigation, and the calculation of approximate system natural frequencies.



The results of the study are presented in Chapter 6. Logical discussions on the results are also provided. Finally, conclusions are drawn and recommendations made in Chapter 7. The results are compared with those of previous investigations, and extensions of the research are suggested.

CHAPTER 2  
LITERATURE REVIEW

2.1 Introduction

The importance of cam system dynamics was recognized only in the late 1940's. Early studies dealt with the merits of various motion curves for cam shapes. In general, the criteria of a successful profile have been - that its acceleration be continuous, the rate of change of acceleration be small, and the magnitudes of acceleration and velocity be small. Consequently, higher order polynomials, Cycloidal, Modified-Trapezoidal, and Modified-Sine motions have been considered as superior choices. However, the dynamic performance (the output motion, and contact stresses, etc.) and relative merits of any one of these cam motions depend on many parameters in the cam-follower system. The important factors that contribute to the observed response characteristics, and the difference between the real output motion of the system and the theoretical motion designed into the cam can be identified as:

- the basic acceleration form of the designed cam motion,
- manufacturing errors in cam profile,
- other imperfections, clearances and backlash,
- inertia and flexibility of the follower system,
- energy dissipation through friction at interfaces and the internal friction,
- speed of rotation,

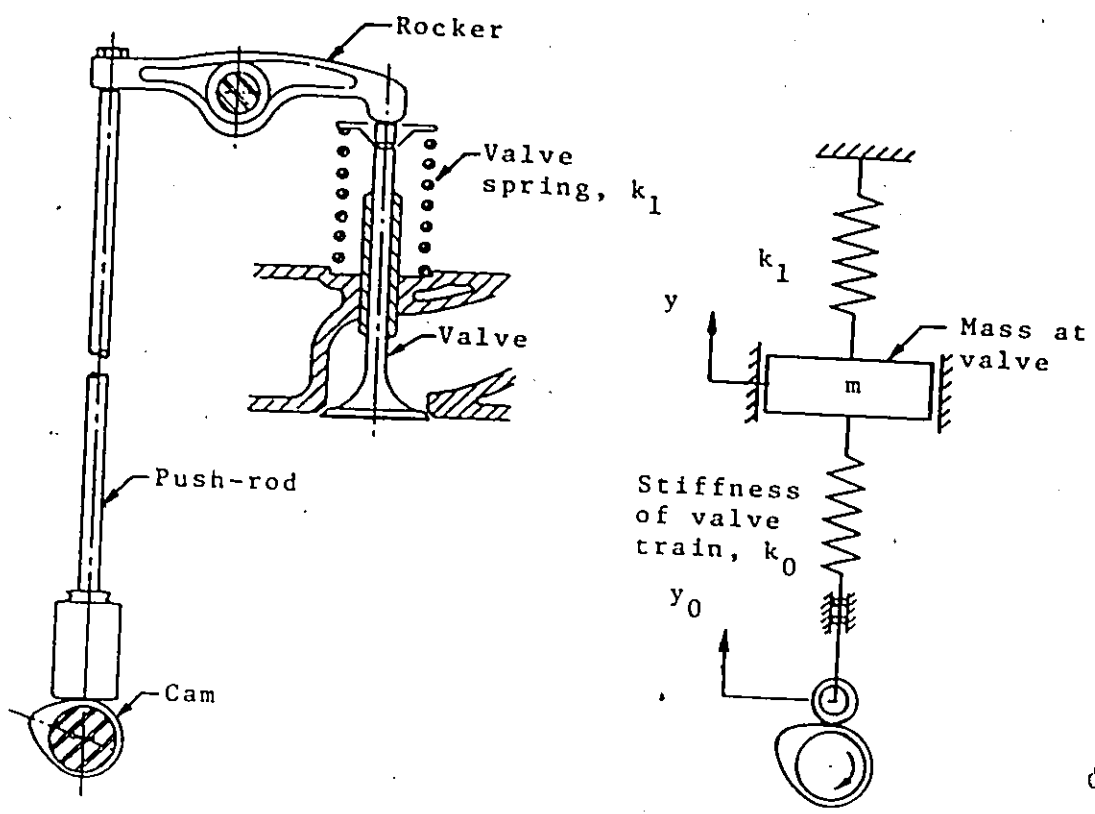
- variations in cam rotational speed due to shaft flexibility and drive characteristics,
- work-function (load) characteristics,
- preload and resonant vibrations of the return spring, if used,
- spring behaviour of the elastic zone at the contact of the cam follower interface,
- pressure angle and cam size (base radius),
- various system inertias,
- type of follower.

## 2.2 Investigations in Cam System Dynamics

Over the years, serious efforts have been made to obtain a better understanding of the influence of various factors on the dynamic behaviour of cam driven mechanisms. A literature review is presented here in chronological order, and different studies are grouped under three main areas, namely, the consideration of system dynamics alone, consideration of manufacturing error effects, and optimization studies in cam system dynamics.

### Consideration of System Dynamics Alone

Dudley [1] developed what is known as the "polydyne" method, by introducing follower system dynamics into the cam synthesis problem. This resulted in an excellent approach to the design of high-speed, highly flexible systems of the automotive valve-gear (Fig. 2.1a) and textile machinery. The method involved specifying the desired output (valve) motion, and adjusting the cam profile



(a) Automotive overhead (push-rod) valve train [6]

(b) Dynamically equivalent system [1]

Fig. 2.1 A high-speed, high flexibility cam-follower linkage.

through the solution of the differential equations of motion for that dynamic system to achieve the required output motion  $y$  - Fig. 2.1b. Polynomials are used for the cam motion because of their inherent flexibility. The principal drawbacks of the method, however, are the lack of local motion control, and that the method is precise only at the design speed, whereas speed variations always occur in most applications. Though extremely popular in automotive industry, the method does not result in quantitative correlation between the designed dynamic response and the true dynamic response at high speeds because of the unaccounted system imperfections in the form of machining errors, clearances, nonlinearities and variations in cam speed, etc.

Hrones [2] was probably the first to employ dynamic simulation of the cam-follower system to account for system flexibilities. Of the three basic motion curves popular at that time, the Cycloidal was shown to have much smaller amplitudes of oscillations than either of Parabolic and the Simple Harmonic motions.

On the basis of tests conducted with the three basic motions - Parabolic, Simple Harmonic (SH), and Cycloidal, Mitchell [3] demonstrated the superior dynamic performance of the Cycloidal motion with its smooth acceleration curve, thus experimentally supporting the findings of Hrones [2]. Resonance was observed at forcing frequencies approaching the odd integral multiples of the natural frequency of the follower system. The tolerances achieved averaged less than  $\pm 0.001$  in. Although the importance of extreme machining accuracy required for good operation of the Cycloidal cam is mentioned, the

profile error effects are not discussed. Sufficiently long dwell periods were considered so that the follower transient vibrations damped out before the start of the next cam cycle.

Commenting on Mitchell's paper [3], Barkan supported the conclusions that a successful cam profile must have a continuous acceleration, and added that the derivative of the acceleration curve (jerk) should also be continuous. This condition was, however, greatly limited by the accuracy to which cam profiles were produced.

Hrones commented that it was surprising, and at the same time comforting to observe that the inaccuracies in cam contour and backlash in the actual system caused little deviation from his own analytical predictions of the dynamic response [2].

Stoddart [4] expanded on the "polydyne" method and derived 24th and 40th order polynomials to improve the automotive valve cam design.

Barkan [5] modelled an engine overhead valve linkage by an equivalent single d.o.f. system and studied the dynamic response considering system flexibility, inertia, and damping effects. The effect of the force produced by resonant vibrations of the valve spring (return spring) was also included. For the flexible system under study, the spring vibrations were shown to have little effect. The comparison between the predicted acceleration response and the electronically measured acceleration showed significant deviations throughout the cam cycle. The observed deviation was mainly due to the vibration effects of a highly flexible follower system. In the simulation, the cam speed was assumed constant, and no consideration

was given to the cam profile errors and the compliance at the cam follower contact.

Turkish [6] compared the measured response of a push-rod valve-gear arrangement with the simulated response of an equivalent single d.o.f. model. It was demonstrated that in the case of constant acceleration (Parabolic) cam motion, a large amount of valve-gear vibrations occurred even with a valve gear of high frequency (rigid follower), and that a smooth acceleration curve was very beneficial in producing good valve-gear dynamics. On the basis of a critical analysis of the transient vibrations in springs, it was recommended that the best way to keep the spring surge to a minimum was to operate at high harmonic orders ( $> 12$ ) by using a relatively high valve spring frequency (stiff spring).

During the discussion on valve symposium papers [5,6], Barkan commented that with highly flexible systems (push-rod automotive) the valve linkage vibrations had a much greater significance than the spring vibrations. With highly rigid systems, however, spring surges were of first order importance at high speeds.

Neklutin [7] analyzed many acceleration diagrams based on Harmonic Series, but without considering follower system dynamics. The studies resulted in the development of the popular Modified-Trapezoidal and Modified-Sine acceleration curves having reasonable magnitudes of maximum acceleration, and finite jerk characteristics.

The design procedure developed by Johnson [8] allows the designer to approximate, quantitatively, a general acceleration curve by finite-differences. The displacement curve is generated from

the desired acceleration curve using numerical integration and curve-fitting.

Mercer and Holowenko [9] simulated the residual vibrational characteristics of various cam motions over a range of follower system natural frequencies. Many important factors were not considered in their rather simple single d.o.f. model. They concluded that there was no best-of-all possible cam motion. However, the 7th order Polynomial motion resulted in low residual vibrations over the widest range of follower system natural frequencies.

Rothbart, commenting on their contribution, pointed out the significance of including cam surface irregularities, cam speed variations, and damping effects as important factors.

Freudenstein [10] suggested the use of harmonic series as an alternative to polynomials as a means for establishing profile specifications for high-speed cams. To account for system dynamics, a dynamic acceleration factor was defined, which could be evaluated when the acceleration profile was known. Using finite Fourier Series, he developed functions having minimum components in the higher order harmonics, the lowest order of which was the Cycloid (sine acceleration). The harmonic profile could be optimized between the extremes of a Cycloid and a constant acceleration (Parabolic) motion to yield minimum acceleration factor. Curves similar to the Modified-Trapezoidal motion have been suggested.

Baumgarten [11] derived equations for the preload force necessary to maintain contact of the follower on the cam for simple types of cam motions. In the simple dynamic model, the follower is



assumed rigid, damping is ignored, and the profile is considered as perfect. Only the rise portion is investigated, whereas the jump is more likely to occur on return. Static weight of the follower is wrongly considered in the dynamic equilibrium equations.

Allais [12] compared the dynamics of the Cycloidal and Modified-Trapezoidal cams. The Modified-Trapezoidal motion yielded lower peak forces for  $n > 7$  and the Cycloidal motion had the advantage for flexible systems with  $n$  lying between 3 and 6, where  $n$  is the ratio of cam rise time to the natural vibration period of the follower system. Neither curve was suitable for very flexible systems, where the polydyne procedure, employing the polynomial motions, was recommended. The analysis assumed an undamped system, no return spring vibrations, and the cam machined to the mathematical accuracy.

Eiss [13] formulated a two d.o.f. dynamic model of the cam-follower system, considering the elastic deflection of the cam follower interface and cam support flexibility. Two techniques are identified to reduce the vibrations, namely, (a) to select an acceleration function which causes minimum vibration, and (b) to adjust the system parameters to obtain minimum vibration for a given acceleration function. System damping, cam speed variations, return spring vibrations, and cam profile errors are neglected. Analytical solutions are presented for six acceleration pulses, and, through an example, it is demonstrated as to how the parameters could be selected to give minimum vibration amplitudes.

As an extension to the Dudley's polydyne cam synthesis technique, Johnson [14] presented a numerical method of synthesizing

motion considering the dynamics of a system of n-degrees of freedom. He developed polynomials wherein interior motion requirements could be controlled in addition to the consideration of the usual boundary conditions. The derived polynomials gave quite high values of maximum acceleration as compared to that of the Parabolic and Cycloidal motions.

Barkan, in his discussion on the paper, questioned the general benefits of a more refined approach considering response to the nth harmonic. He pointed out that in most real cam systems, the dynamic response was dominated by the fundamental harmonic - an observation supported by many authors. Also, it was quite impossible to manufacture cams with sufficient accuracy to control even the third derivative (jerk) with any real precision. Based on his own investigations [5], he concluded that significant errors in the manufactured acceleration curve did not affect, substantially, the response of a flexible system at high speeds because, at high speeds, they constituted a higher order excitation of frequencies, much higher than the system was capable of following.

Johnson himself pointed in his closure to the discussion that a profile tolerance of  $\pm 0.002$  in. produced no measurable error in the output of the very flexible mechanism studied by him. He noted that the required precision of cam manufacture was inversely proportional to the natural period of vibration so that high precision was demanded for rigid systems.

Erisman [15] used Fourier Series in the development of a continuous function to express cam lifts and accelerations in flexible automotive valve linkages. The smooth acceleration diagram was duplicated with a finite series of odd sine terms and the resulting harmonic expression for the cam profile  $y_c$  was combined with the differential equation of system dynamics involving dynamic valve lift  $y_v$  and dynamic valve acceleration  $\ddot{y}_v$ . An undamped single d.o.f. cam-follower system model was considered. The solution of the resulting equation yielded the valve motion  $y_v$ . The characteristics of the valve spring in relation to the complete valve train linkage have been investigated. Many interrelated variables could be presented as dimensionless parameters. It was found that for the flexible system under study, the spring surge had little effect on the complete dynamic system, but in general the selection of a high ratio ( $n > 12$ ) of the valve spring natural frequency to the cam shaft speed was recommended. It was also recognized that the cam speed had a definite influence on the ultimate choice of the cam profile. Profile error effects and cam follower contact condition were not considered.

Meeusen [16] has presented a computer based formulation for evaluating the overhead-cam valve train system dynamics. The valve train is assumed as infinitely rigid, and the effects of valve spring surge are considered. No damping is accounted for. Theoretically predicted results are correlated with the experimental data on the basis of no-follow (jump) speed criterion. Although the program has the provision to use the inspection cam lift data as the input, the results do not show cam lift error effects.

Crutcher [17] developed a computer program to study the dynamic behaviour of the poppet valve mechanism. An equivalent single d.o.f. system, subjected to internal damping and Coulomb friction, was considered. Through comparison with measured results, it was shown that the simulation studies predicted the valve motion and linkage forces quite satisfactorily. The effects of changes in internal friction, Coulomb friction factor, and valve spring stiffness were also studied. Whereas the Coulomb friction at the guides was shown to have adverse effects, the internal damping of the follower system was useful in controlling the amplitude of vibrations.

Wagstaff [18] considered a multi-mass model of the valve spring to include the spring surge effects in the simulation of push-rod valve-gear dynamics. The cam profile provided the forcing function, and was read into the computer program in the form of the tappet displacement (lift) for each degree of cam rotation. It was concluded that the simulation of the valve spring was a very important factor in obtaining accurate agreement with experimental response, especially at high speeds where the spring vibrations were significant. Also the simulation must be carried through several cycles to arrive at a steady state.

Based on an extension of Hertz theories, Smith [19] presented an analysis of the elastic deformation at the point of contact between the cam surface and the follower so that the contact spring constant could be determined.

Sakai and Tsuda [20] observed that the analysis of valve motion would reduce a great deal of experimental work preceding the final decision of valve-gear design. They investigated the valve jump characteristics considering a single d.o.f. model of the valve-gear, taking into account the dry friction at valve guide and the hysteresis damping of the equivalent push-rod. They recorded the valve motion at various speeds experimentally and observed jump at about 2300 rpm camshaft speed, which was shown to support the analytical results obtained from their model. They also stressed the need to take into account the valve spring vibrations.

Bagci [21] used a single d.o.f model to test the dynamic performance of three different cam motion curves through several cycles of cam rotation and at a series of cam speeds. Stiffness at the cam-follower interface was accounted for. Based on the simulation studies, the following conclusions were drawn.

- The actual motion of the follower system can only be simulated after several cycles of cam rotation and that the use of only the rise period of a cam cycle yields unreliable information for the complete response analysis of the cam-follower system.
- Motion curves that result in favourable dynamic behaviour of the follower system at a particular cam speed may not be good choices at different cam speeds.
- The follower system experiences certain cam speeds as critical (as experimentally observed by Mitchell [3]).

The effects of return spring vibrations, camshaft flexibility, Coulomb friction at the guides, and cam profile errors were not considered.

Fawcett and Fawcett [22] studied the effects of variations in cam speed due to the flexibility of the camshaft and its drive. This had a significant effect on the valve dynamics, and was an important consideration in rigid follower systems typical of high-speed production machinery and overhead camshaft valve gears in engines.

Matthew and Tesar [23] developed a matrix method for specification of Trapezoidal motion characteristics, allowing control of  $y$ ,  $\dot{y}$ ,  $\ddot{y}$ , ... at specific points during cam rotation. They point out the very significant differences between the push-rod type automotive valve-gear and the typical high-speed production machinery cam-follower systems, namely that

- automatic production machinery cams have very rigid follower systems compared to the relatively flexible automotive follower systems, so that only modest proportions of the total energy is absorbed by deformations,
- production machinery cams are seldom decoupled from the follower at any part of the cycle, and thus require precise and smooth motion at the end points. Automotive valve-gear has intentional clearances, so that the motion control at the boundaries is not critical.

The specification of the output motion properties for effectively rigid systems, therefore, requires a unique philosophy different from that for the flexible automotive cam systems. Here it is important that the motion has well controlled local properties in terms of velocity, acceleration, and shock, etc.

Kanzaki and Itao [24] investigated the residual vibration characteristics of the cam mechanism for typehead positioning in high-speed teleprinters. The polynomial equations of motion are determined upon the consideration of the boundary conditions and the characteristics of residual vibrations. The results obtained by a single d.o.f. viscous damped follower system are verified by the experiment. By the use of higher order polynomials, the residual vibrations are shown to be reduced over a comparatively wider range of rise times.

Chen [25] studied the dynamic response of a cam driven system, considering a lumped multi-d.o.f. model containing nonlinear parameters. He identified two factors that had definite influence on the system response characteristics as the basic acceleration form, and the system internal parameters of mass, stiffness, and damping.

Reeve and Rees-Jones [26] studied the dynamic performance of the family of standard motions having a sine-constant-cosine acceleration (SCCA) function. The standard motions like SH, constant acceleration-retardation (Parabolic), Cycloidal, Modified-Sine, and Modified-Trapezoidal, fit into this family. The important dynamic parameters studied included the maximum and minimum

acceleration, residual vibration, and torque requirements during lift. A single d.o.f. simulation model was used, and a constant rotational speed of the cam was assumed. They concluded that no single motion could completely satisfy all the necessary requirements, and selecting a motion was a matter of compromise. Although the authors recommend the Modified-Trapezoidal motion as the most useful general purpose motion, yet their ratings in Table 2.1 indicate the Modified-Sine and the Simple Harmonic motions to be the superior choices, with the Cycloidal motion being preferred for flexible systems.

TABLE 2.1  
COMPARISON OF CAM MOTIONS [26]

Motion	Deviation in Lift Accel.		Velocity	Impact	Input Torque		Residual Vibration 2<n<10
	Nominal	2<n<10			Nominal	2<n<10	
Parabolic	5	1	2	1	1	1	1
Modified- Trapezoidal	3	3	2	2	2	2	4
Simple Harmonic	3	2	5	5	5	3	1
Modified- Sine	2	3	3	4	4	4	4
Cycloidal	1	5	2	3	3	4	5

n: ratio of the lift period to the natural period of vibration of the follower system.

Ratings 1 to 5 correspond to a range from relatively bad to excellent, respectively.



Matthew and Tesar [27] posed the synthesis problem as that of determining the cam shape factor 'S' to produce the specified response  $y(t)$ . The cam shape factor was defined in terms of the output motion  $y$ ,  $\dot{y}$ , and  $\ddot{y}$  and the dimensionless parameters  $\mu_m$ ,  $\mu_c$ , and  $\mu_k$  which depend on the system coefficients  $M$ ,  $C_r$ ,  $K_r$ ,  $K$  and the rotational design speed  $\omega_d$  - Fig. 2.2. They classified the cam-follower systems into low, medium, and high speed depending on the

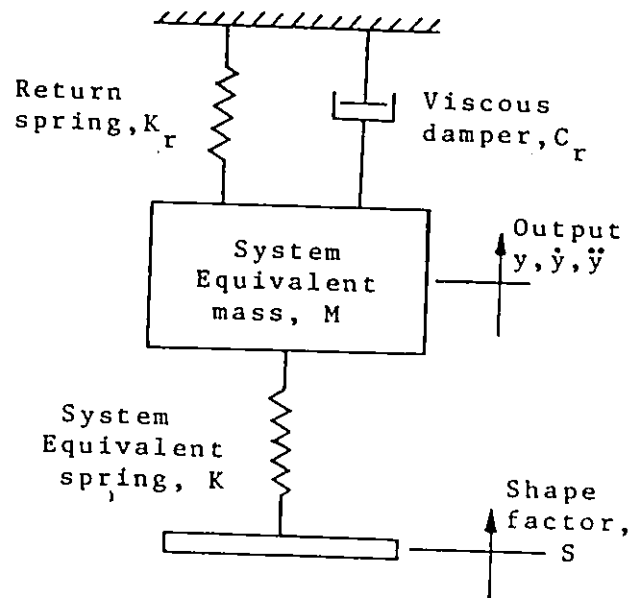


Fig. 2.2 The one d.o.f. cam-follower model [27].

TABLE 2.2  
CLASSIFICATION OF SYSTEMS BY  $\mu_m$  [27]

Type of Cam System	Weight (lb)	System Spring (lb/in)	Speed (rev/min)	$\mu_m$	$\mu_m$ (general)
Low-speed industrial	10.00	$0.5 \times 10^7$	300	$5.2 \times 10^{-6}$	$10^{-5} - 10^{-6}$
Automobile (overhead-cam)	0.75	$1.0 \times 10^6$	3000	$2.0 \times 10^{-4}$	$10^{-4}$
High-speed industrial	2.00	$0.5 \times 10^6$	3000	$1.0 \times 10^{-3}$	$10^{-3}$
Automobile (push-rod)	1.35	12,650	3000	$2.7 \times 10^{-2}$	$2 - 7 \times 10^{-2}$

$$\mu_m = \left( \frac{\omega_d}{\omega_n} \right)^2$$

$\omega_d$  - Design speed

$\omega_n$  - Natural frequency of the follower system

parameter  $\mu_m$  which was defined as the squared ratio of the design speed  $\omega_d$  to the natural frequency of the follower system  $\omega_n$ , Table 2.2. They recommended the use of higher order polynomial motion specification and highest possible accuracy of cam manufacture ( $\pm 0.0001$  in. or better) for high-speed cams. Their model assumed constant cam speed, perfect profile, and massless return spring.

Reeve, commenting on the manufacturing accuracy, stated that the very best that could be achieved in practice for industrial cams was commonly 0.001 in. in absolute error range, and a rate of change of error of 0.0002 in/deg.

The authors concluded the discussion with the following remarks - "Many important questions remain to be answered when considering a complete system and they form the basis of a worthwhile investigation".

Rao and Raghavacharyulu [28] studied the jump characteristics of various standard cam motions experimentally. A rigid follower and a very soft return spring were used. Simple Harmonic motion was shown to give much better jump characteristics than the Cycloidal and the Polynomial cams as indicated by the higher cam speeds at which jump started. The higher the order of the polynomial, the poorer was its performance in relation to jump behaviour. This is expected because of the high accelerations, and consequently, high inertia forces in higher order polynomials, although their vibration characteristics are better.

Koster [29] developed a four d.o.f. simulation model to investigate the dynamics of a cam-operated transfer mechanism. The follower linkage was represented by a single mass and a single stiffness, but additional freedoms were included to account for the camshaft flexibility in torsion and transverse vibrations. It was shown that the transient vibrations characterized the dynamic behaviour of the cam mechanism. The effects of the non-uniform cam speed, backlash, and lubricant squeeze were accounted for and a close correlation between the simulated and the measured response was demonstrated.

Chen [30] has given a comprehensive review of the state of the art of cam system dynamics. Discussing the trend for future developments, it is suggested that future efforts must be directed towards the study of more refined and realistic models which considered the combined dynamic effects of many parameters involved. It is finally remarked that much work needed to be done concerning system identification and sensitivity analysis in the cam mechanism field.

To predict the automotive valve train behaviour at high speeds, Akiba et al. [31] have used a single d.o.f. model, with three additional masses to simulate the valve spring effects. They substantiated their findings with experimental results. It was observed that the valve jump and bounce phenomenon would occur within the speed ranges where the modern high-speed engines were driven with a considerable probability. They suggested a two mass model for the valve train to predict the jump phenomenon more adequately.

Through experimental investigations, Pisano and Freudenstein [32] demonstrated that the operating speed of the cam-follower system of an automotive valve-gear was limited not by excessive dynamic forces or vibrations, but by a loss of load on the push-rod and the resulting valve toss (jump). They also created a single d.o.f. dynamic model, considering most linkage elements as rigid and the return spring as a distributed parameter element, and compared the simulation results with their experimental results. The effects of Coulomb friction at guides, cam follower contact stiffness, nonuniform cam speed, and profile errors were not considered.

### Consideration of Manufacturing Error Effects:

Although the importance of machining accuracy in cam system dynamics is well recognized, very little work has been done in studying the dynamic effects of cam profile errors and the sensitivity of popular motion curves to such errors.

In a purely kinematic study, Johnson [33] applied the method of finite-differences to establish the approximate acceleration effects of profile inaccuracies. No sound basis was given for determining the actual follower displacement which was assumed to deviate from the desired curve in a cyclic and smooth fashion between the limits of tolerance specification.

Rothbart [34] conducted dynamic tests to study the dynamic effect of single non-periodic errors in the cam profile, and observed large variations in the acceleration curve when the rate of change of error was high. He observed that accuracies as close to  $\pm 0.0003$  in. may be necessary in high-speed applications. Further, in a survey on cam manufacturing techniques, Rothbart [35] has given a complete list of methods popular at that time, along with the probable accuracy that could be obtained from each.

Nourse [36] identified cam production tolerances as made up of the following two components:

- (i) A maximum allowable deviation with which the profile "as made" can be permitted to deviate from the designed profile. Normally, this bandwidth changes with the location along the profile.

- (ii) The profile waviness which indicated the rate at which the profile "as made" can be permitted to deviate from the designed profile.

He developed an analytical procedure for profile random error smoothing. The smoothest profile was defined mathematically as that profile, within the random error limits, for which the higher order derivatives (acceleration and its rate of change) had the least numerical value. This was achieved through the use of polynomials and application of the method of least squares. The smoothed lift error and its kinematic effects on acceleration are shown in Fig. 2.3. In practice, the lift error function is not as smooth as shown, and has high frequency pulses.

Brittain and Horsnell [37] studied the effect of grinding wheel wear and setting-up errors on the accuracy of profiles produced on a copy grinding machine. The analysis does not account for the randomness error, and the smooth error variation follows the changes in velocity over the rise and return periods, with the maximum variation occurring near the middle of these periods. Using the dynamic analysis program of Barkan [5], it was shown that these smooth errors had very little effect on the dynamics.

Dhande and Chakraborty [38] analyzed the effect of manufacturing and assembly errors on the output displacement characteristics of the cam-follower systems using a probabilistic approach. In this purely kinematic study, the stochastic model considered the contact between two random surfaces and all input

# CAMCHECK —

## CAM PROFILE EVALUATION NEW METHODS

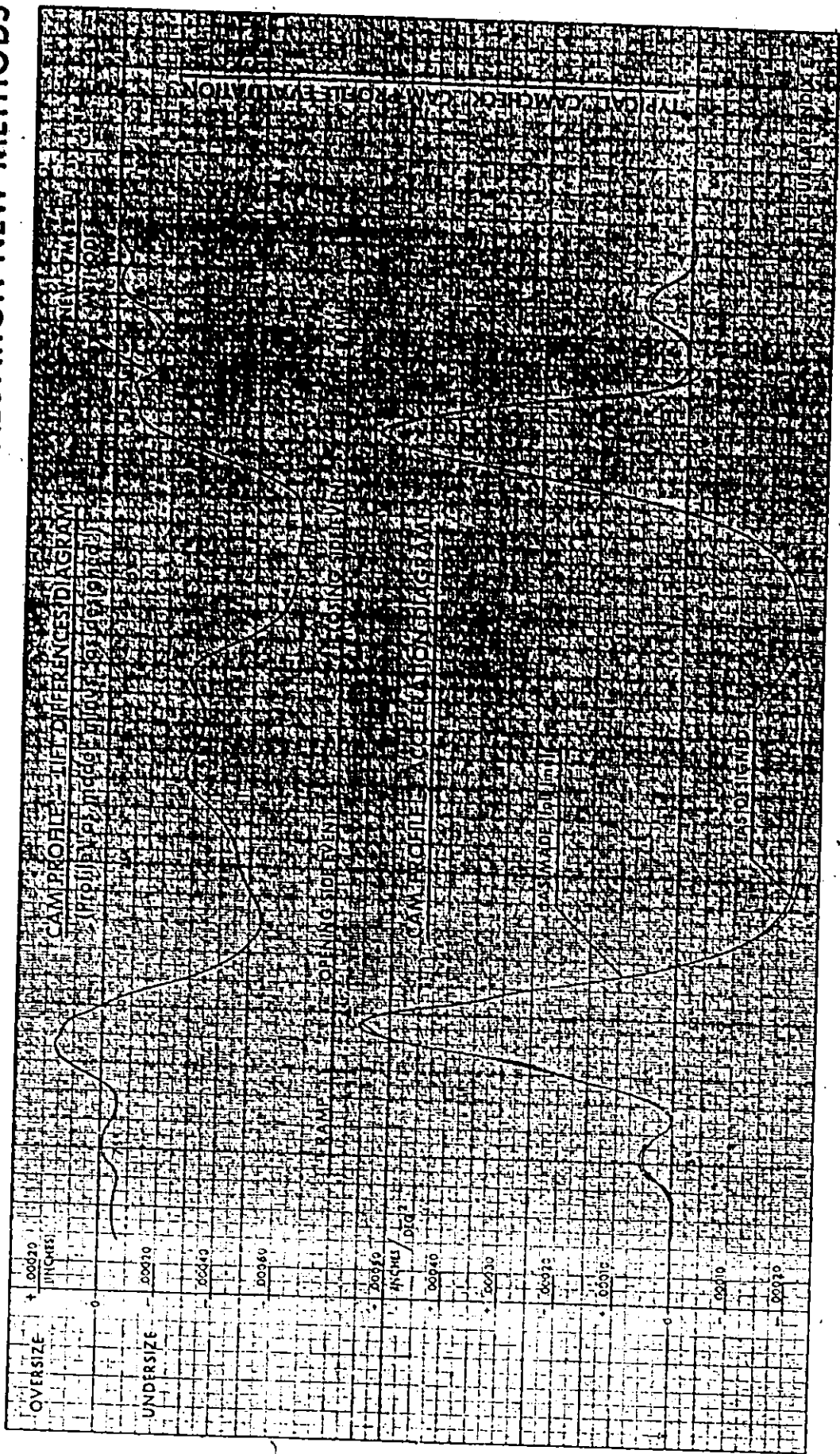


Fig. 2.3 Smoothed lift error and its kinematic effects on acceleration [36].

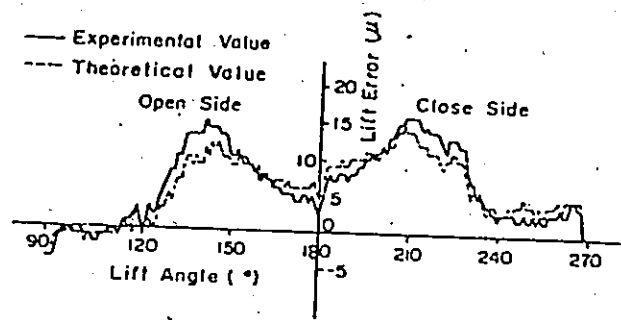
variables as random and normally distributed. It was observed that maximum error occurred at the angular positions of the cam where the pressure angle as well as the velocity of the follower was maximum.

Kawaski et al. [39] presented an analytical procedure for computing the lift error of the cam profile produced by the inverse profile copy method using the oscillating cam grinding machine. Three principal factors were identified to contribute to the lift error - the diameter of the cam grinding wheel, precision of model cam profile, and process errors. Typical lift-error functions are shown in Fig. 2.4.

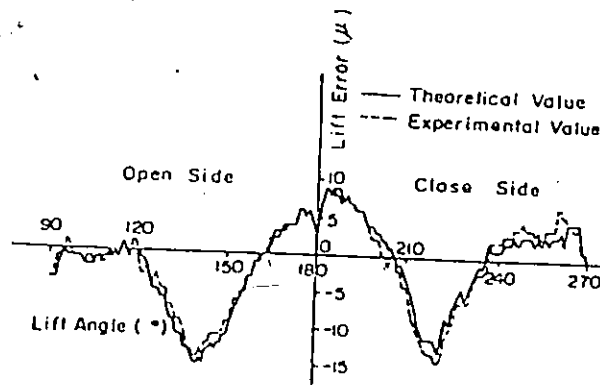
An automatic system for kinematic evaluation of the cam profile has been developed by Krawczynski et al. [40]. The measured sequence of follower displacements, for equally spaced values of the cam angle, is smoothed utilizing the concept of movable mean used in time-series analysis. They employ a third-order piecewise polynomial fit with least square minimization. Stirling's formula is used to obtain acceleration variation over the cam cycle and the smoothed acceleration thus obtained is compared with the theoretical acceleration - Fig. 2.5b. The acceleration deviations lie within  $\pm 10$  percent of the theoretical acceleration. System dynamics are not considered in this study.

Kim and Newcombe [41] investigated the kinematic effects of cam profile tolerances on the follower displacement, velocity, and acceleration using a stochastic approach, finite differences, and the maximum likelihood theory. A uniform tolerance was considered over the cam cycle.





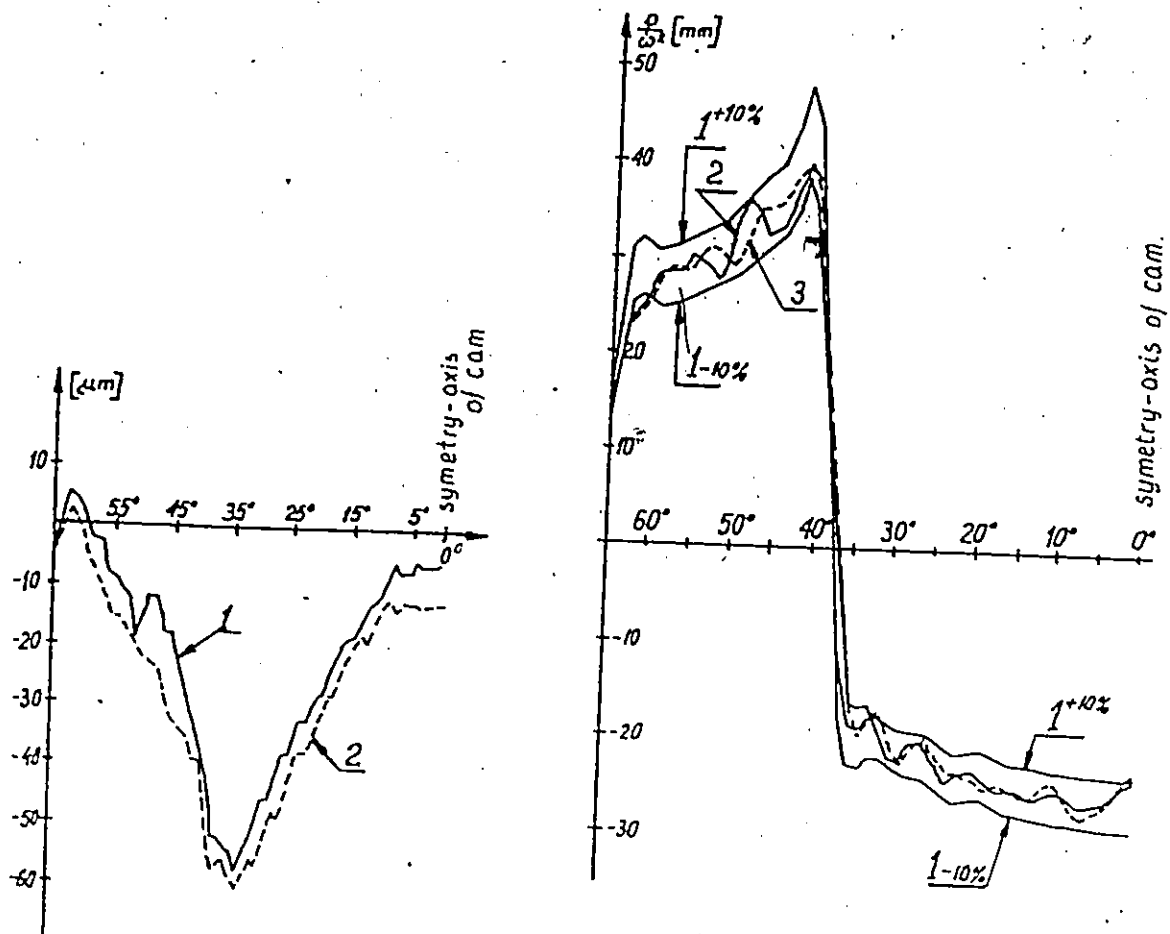
$d = 628 \text{ mm}$



$d = 710 \text{ mm}$

$d$ : grinding wheel size

Fig. 2.4 Lift error functions [39].



(a) Lift error over a portion of the cam cycle  
 1 - measured  
 2 - from automatic system

(b) Acceleration diagram  
 1 - theoretical curve  
 2 - curve obtained from measurements  
 3 - curve obtained from automatic system

Fig. 2.5 Lift error and its kinematic effects on acceleration [40].

Bialkowicz et al. [42] presented the results of experimental investigations for the effects of wear on the dynamic characteristics of real cam profiles. They concluded that even a significant wear (after 1500 hrs. running) did not markedly change the dynamic properties of the cam. They stressed the importance of the simulation approach and the modelling of the input signal (cam profile) based on probabilistic data obtained from numerous newly machined cams. In their analytical investigations, they employed the automatic system of cam profile control developed by Krawczynski et al. [39].

In their survey on cam manufacturing methods, Grant and Soni [43] indicate that even with all the advances made in the state of the art, basic machining with most NC machines and common mills and lathes was still in the tolerance band of  $\pm 0.0005$  to  $\pm 0.001$  in. Of course tolerances of the order of  $\pm 0.00005$  in. have been achieved where absolutely necessary.

Giordana et al. [44] studied the influence of construction errors in the law of motion (Trapezoidal) of cam mechanisms. The analysis carried out was purely kinematic, with the elements of the mechanism considered perfectly rigid. The lift error distribution had a typical trend, similar to the behaviour of the pressure angle or the follower velocity, with the maximum error occurring in the middle of the rise and return portions. The effect of other dimensional errors, and variations in the cam rotational speed were also investigated. They concluded that the profile errors and other dimensional inaccuracies introduced only slight variations (less

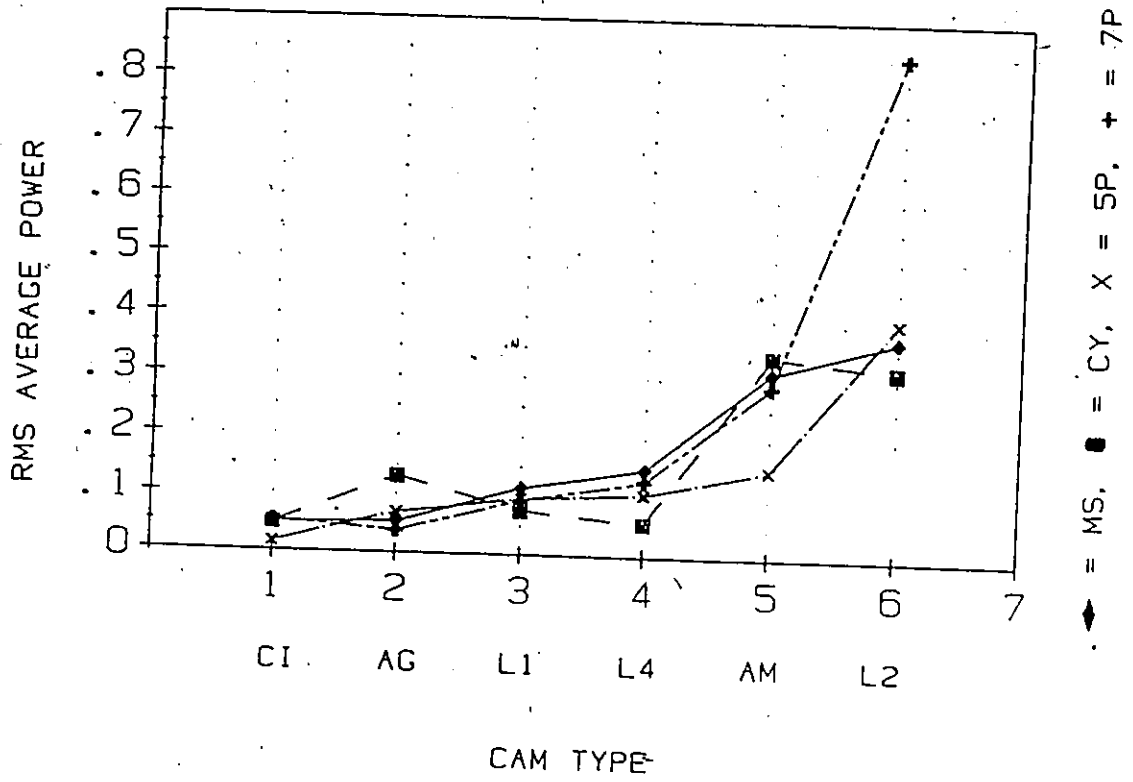
than 10 %) into the law of motion and that changes in angular speed had a noticeable influence.

Sankar and Osman [45] simulated the dynamics of a two dimensional hybrid profiling mechanism used in cam manufacturing, and studied the effect of system parameters in controlling the manufacturing error. The cam profile error was identified to be due to static, kinematic, and transient behaviour of the mechanism. The manufactured profile indicated undercutting on the rise portion and overcutting on the return side. Maximum error of the order of 0.01 in. occurred in the midspan of the rise and return portions.

In a comprehensive investigation, Kim and Newcombe [46] developed an eleven d.o.f. model to simulate the response of the cam-follower-drive system so that the effects of system flexibility and cam profile tolerances could be investigated separately, as well as in combination. The simulation results showed high frequency vibrations with large variations in the follower acceleration caused by the waviness frequency in profile errors. The simulation was carried out at a single rotational speed of 800 rpm and the spring surge effects were neglected which is an important consideration for rigid follower system used in the investigation. The machining tolerance was considered uniform over the cam cycle.

Norton [47], in a review work, explained the significance of cam manufacture and observed the lack of research integrating the theoretically superior cam motions with the realities of cam manufacture.

In a more recent work, Norton [48] has conducted experimental investigations to study the effect of cam manufacturing methods on the dynamic performance of double-dwell cams. Four motions - Modified-Sine (MS), Cycloidal (CY), 3-4-5 Polynomial (5P) and 4-5-6-7 Polynomial (7P), were all cut on the same cam as rise, return, rise, return and six such cams, produced by different manufacturing methods, were tested for their acceleration characteristics. The shaft speed was 3.2 Hz. Even at this low speed, the acceleration plots showed significant oscillations. Large differences were observed in the noise (RMS error in the acceleration waveform) generated by cams produced with different manufacturing methods - Fig. 2.6. Clearly some methods (CI) were far superior to others (L2) in producing quality cams. It was also concluded that there was significant difference in the noise associated with the different cam motions produced by the same manufacturing technique. The 3-4-5 Polynomial motion was observed to be the quietest, and the 4-5-6-7 Polynomial, the noisiest. This conclusion is based on the RMS average power for all manufacturing methods taken together. The results with separate manufacturing methods, however, do not show any significant noise differences for various motions - Fig. 2.6.



- CI - Circular Interpolation CNC
- AG - Analog Ground
- L1 - Linear Interpolation CNC 1 deg.
- L4 - Linear Interpolation CNC 1/4 deg.
- AM - Analog Milled
- L2 - Linear Interpolation CNC 1/2 deg.

Fig. 2.6 Effects of cam manufacturing methods and cam motions on follower acceleration [48].


### Optimization Studies in Cam System Dynamics:

Recent studies in cam synthesis have considered the problem as one of optimization, and have emphasized the minimization of some or many of the dynamic response characteristics at a prescribed speed or over a range of cam speeds.

Kwakernaak and Smit [49] employed a single d.o.f. undamped system and formulated the problem of finding a suitable cam profile to minimize the residual vibrations over a prescribed range of cam speeds, with limiting constraints on the follower velocity, acceleration, and jerk. The optimized profile compared favourably with the popular Cycloidal profile.

Based on the polydyne procedure for cam synthesis, and considering a single d.o.f. dynamic model, Berzak and Freudenstein [50] described a procedure for determining optimum performance for the output motion in a cam driven system. Inclusion of extra terms in the polynomials provided additional freedoms that could be used for the imposition of appropriate constraints to satisfy the optimization criteria such as peak velocity, peak acceleration, residual vibrations, and symmetry, etc. A balanced set of performance criteria could be obtained through trade-offs by scanning the domain of feasible polynomial cam curves.

Rao [51] considered a single d.o.f. undamped system including the return spring and minimized the least square flexibility error (defined as the difference between the motion machined into the cam and the follower response), subject to prevention of separation between the cam and the follower.



A method of calculating the variance of the dynamic response, using a stochastic approach by coupling numerical integration and probability principles, has been presented by Rao and Gavane [52]. The problem of allocation of tolerances on the cam profile and other geometrical parameters, and variations in system parameters like mass, stiffness, and damping has been formulated as a nonlinear programming problem. A measure of the manufacturing cost is minimized, subject to constraints on the allowable deviation in the dynamic response. It is concluded that the variations in the mass mainly govern the optimum point.

Chew et al. [53] considered a single d.o.f. model with viscous damping and included the roller follower mass to provide a realistic description of contact force and stress at the cam follower interface. To achieve a balance between the system characteristics at the output (motion distortion and vibration) and at the cam follower interface (contact stresses), they developed an optimality criterion with suitable weighting factors and bounds, and evaluated the criterion with the aid of optimal control theory. Design parameters for the synthesis of high-speed cam-follower systems could be evaluated to yield the best characteristics included in the criterion. Shaft flexibility, cam manufacturing errors, and return spring vibration effects have not been considered in this development.



## CHAPTER 3

### PERFORMANCE CHARACTERISTICS IN CAM DYNAMICS

#### 3.1 Introduction

The behaviour of the end member (the follower) of the cam mechanism, caused by the input motion excitation (cam), is known as its response. Design evaluation of a high-speed cam-actuated system requires an assessment of the response of the follower to the input motion excitation. To determine the response of a typical dynamic system, one generally considers both the steady-state and the transient response. For cam-follower systems, however, it is the transient response that characterizes the system, because the cyclic forcing frequency is very low in comparison with the natural frequency of the follower system [29]. Non-periodic, high frequency pulses due to cam profile errors also induce transients. The vibrations are characterized by the fundamental frequency of the follower system. If dwell periods are short and damping small, the initial conditions of every new cam cycle are determined by the residual vibrations of the preceding motion.

#### 3.2 Performance Criteria

Follower response is generally described in one of the two ways -

- (a) Frequency-domain response.
- (b) Time-domain response.

3.2.1 Frequency-Domain Response

Frequency-domain response, also termed as the Dynamic Response Spectra (DRS), is formally defined as the plot of the peak accelerations (primary or residual) of a multitude of single d.o.f. undamped spring-mass systems, of different natural frequencies (period  $T_n$ ), w.r.t. a specified excitation (period  $T_1$ ). The dimensionless ratio of the response amplitude to the static displacement, termed as the dynamic magnification factor (D) is plotted versus the frequency ratio (or period ratio  $T_1/T_n$ ) - Fig. 3.1. Such a response spectrum analysis provides unique information to help the designer quickly visualize the effects of mechanical shock (pulse) on a system, indicating the maximum dynamic loads expected.

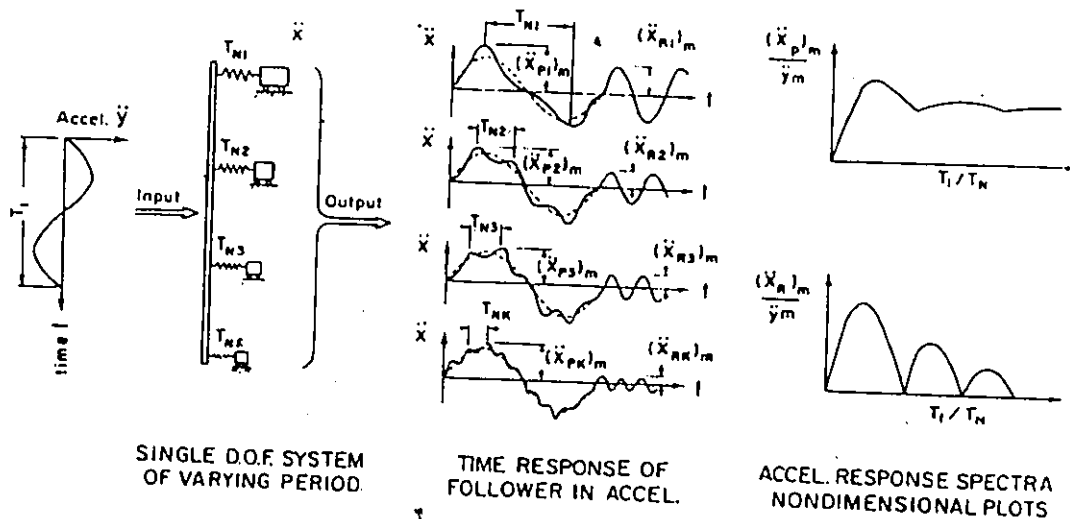


Fig. 3.1 Graphic definitions of Dynamic Response Spectra (DRS) [56].

### 3.2.2 Time-Domain Response

In the time-domain, the response characteristics are defined with respect to real time or the cam angle. Time response at the follower comprises its displacement, velocity, and acceleration variations over the cam cycle. Follower jump describes the condition of separation of the follower from the cam surface because of high inertia, vibrations, or a soft retaining spring.

Follower response in displacement provides information on the positional accuracy of the follower at the end of rise and return periods. However, the response in acceleration (Fig. 3.2) is most important because of the inertia forces which are produced.

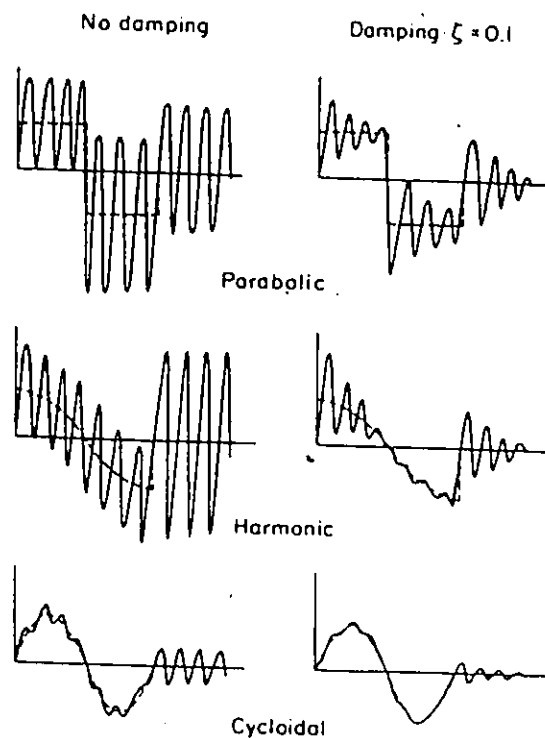


Fig. 3.2 Vibratory response characteristics of cam-follower for Parabolic, Simple Harmonic and Cycloidal input (a) no damping, and (b) with 10% damping.

### 3.2.3 Dynamic Characteristics at the Cam

In addition to the output time-response in the form of follower acceleration variations, one would be concerned with certain important behavioural characteristics at the cam. These comprise the contact force, cam torque, pressure angle, and the cam speed variations with respect to cam angle over a cycle. These characteristics determine the contact stresses and power requirements, and thus affect the efficiency, wear, and life of the mechanism.

The present investigation considers the time-response of the follower acceleration, and the behavioural characteristics at the cam as the performance criteria.

## CHAPTER 4

### SYSTEM IDENTIFICATION

#### 4.1 Introduction

A model is a combination of idealized components used to describe the behaviour of a real physical system. Modelling is one of the major tasks in the study of cam dynamics and the usefulness of the solution is greatly dependent on how closely the model represents the system. A very complex model may not be warranted because of mathematical complexity and solution economy, however, it must be elaborate enough to provide accurate information necessary for engineering action.

While earlier investigations indicated that the simple one d.o.f. linear model was adequate for the study of cam system dynamics [29], the dynamic behaviour of cam-actuated systems in modern high-speed applications can only be expressed realistically by means of more refined multi-degree-of-freedom nonlinear models. Such models must include the important effects of cam manufacturing errors, cam speed variations, return spring vibrations, Coulomb friction, and the compliance at the cam follower interface.

Two models are necessary for the physical simulation of cam system dynamics:

- (a) a representative dynamic model of the cam mechanism to be investigated,
- (b) the model of the input signal - the lift function.

#### 4.2 Cam-Follower System

Many different cam-follower configurations are in use in industry. No particular application is intended for simulation in this work. Because the idea is to present a comprehensive comparison of popular cam motions, and perform sensitivity studies, only a representative system has been chosen. This is a two-dimensional disk cam mechanism, with a flexible camshaft and driving a spring-controlled translating roller follower - see Fig. 4.1. This is a popular and versatile model which is easy to analyze kinematically, and is best applied to automotive cam systems and many similar applications.

#### 4.3 Idealized Dynamic Model

Although the system, in reality, is a continuous system, it is more convenient to idealize it as a discrete system with lumped masses, inertias, elasticity and damping. The motion, described by ordinary differential equations, can be easily obtained and nonlinearities can be directly included.

For the cam-follower system under study, a seven d.o.f. dynamic simulation model, as shown in Fig. 4.2, has been proposed. It comprises a single d.o.f. torsional system and a six d.o.f. translational system. The torsional system represents the inertia of the cam along with a portion of the camshaft, and the torsional flexibility of the drive shaft. The translational system considers the effects of transverse flexibility of the camshaft, contact compliance

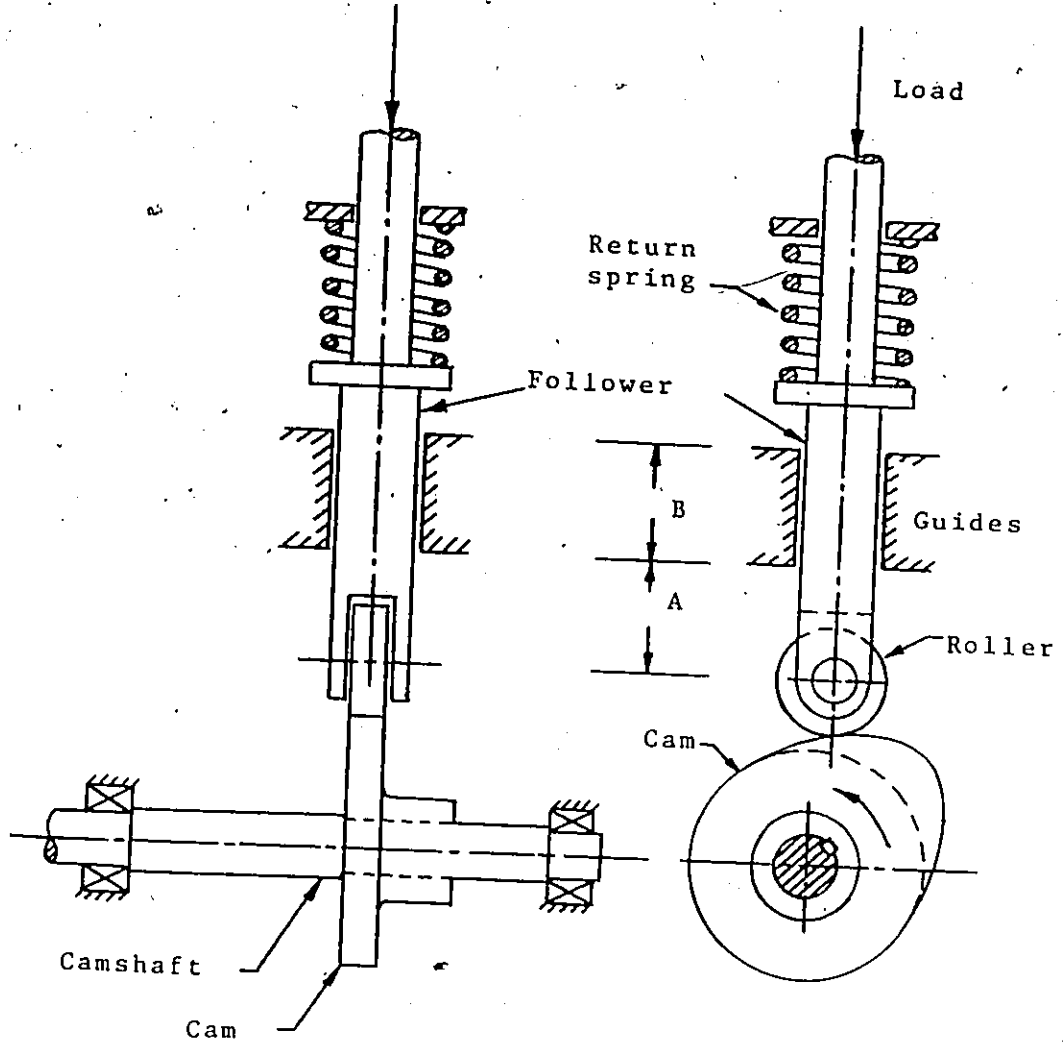


Fig. 4.1 Representative cam-follower system.

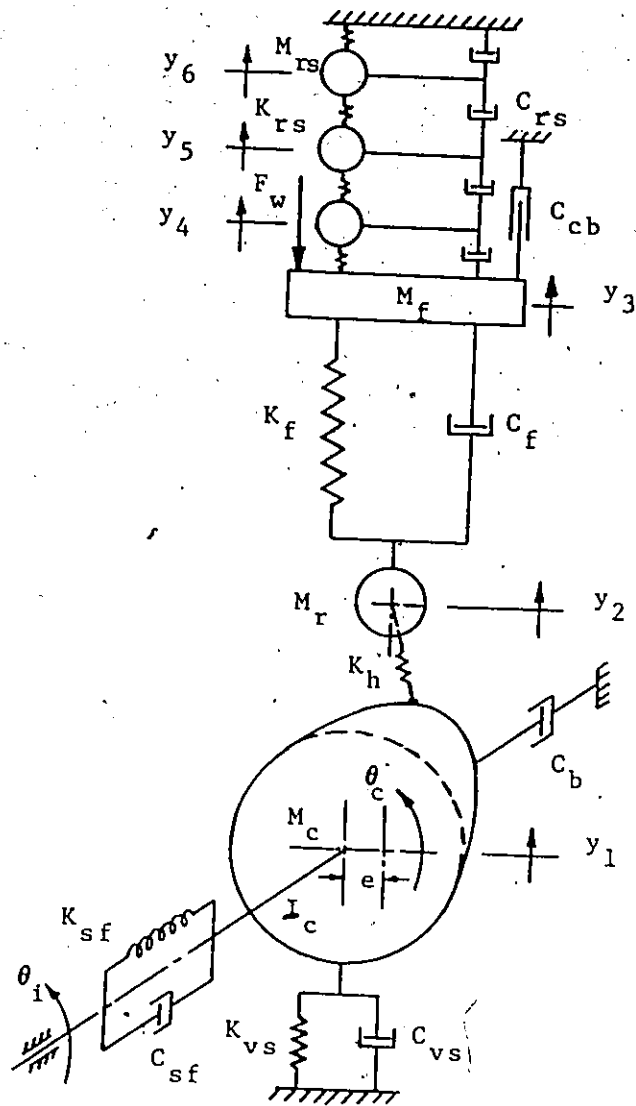


Fig. 4.2 Dynamic system model.



at the cam follower interface, follower flexibility, and the return spring vibrations, and includes the important factors of internal damping in the follower system, Coulomb friction at the guides, internal friction in the return spring and the external work load.

Since the return spring vibrations interact strongly with the follower vibrations, particularly at high speeds, they must be simulated, and solved simultaneously with the follower behaviour. Coil spring vibrations are often compared to the longitudinal vibrations of an elastic bar and for convenience can be treated mathematically by a discrete mass system. To simulate the return spring, a triple mass model satisfies the requirements for appropriate modelling [31]. It has its second and third natural frequencies twice and three-times the fundamental frequency, respectively - Appendix A3.

The internal friction can be considered as viscous [32]. The only other assumption made is that there are no clearances. This can be easily realized unless intended for a particular application, like the automotive valve-gear.

#### 4.4 Mathematical Model - Formulation of Equations of Motion

The free-body diagrams, corresponding to the dynamic model considered, are shown in Figs. 4.3a and 4.3b. The governing equations of motion are derived employing Newton's second law of motion.

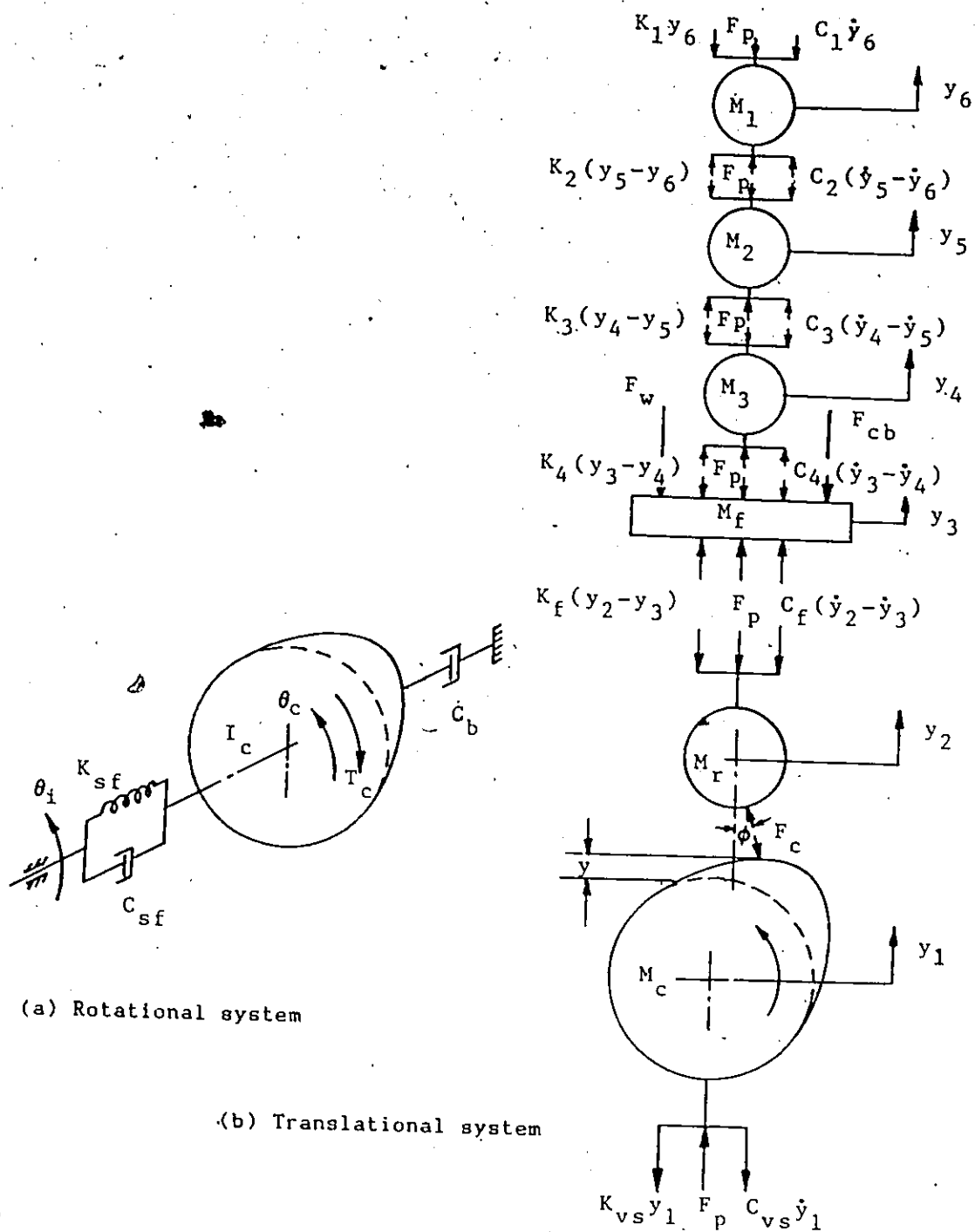


Fig. 4.3 Free-body diagrams for the dynamic model of Fig. 4.2.



#### 4.4.2 Contact Force

The contact force  $F_c$ , between the follower roller and the cam at their point of contact - Fig. 4.2 and 4.3b, is given as follows:

$$F_c \cos\phi = K_h \cos^2\phi (y+y_1-y_2) + F_p \quad (4.4)$$

where

$K_h \cos^2\phi$  = vertical contact stiffness

$(y+y_1-y_2)$  = contact spring compression

$F_p$  = return spring preload.

Therefore

$$F_c = K_h \left[ (y+y_1-y_2) + \frac{F_p}{\cos^2\phi} \right] \cos\phi \quad (4.5)$$

#### 4.4.3 Return Spring Preload

In nonpositive-drive cam mechanisms, the return spring is an important element used to control the follower motion during the return stroke. Adequate preload is necessary to hold the follower on the cam, and avoid separation. To provide the preload, the spring is assembled in compression.

To determine the preload  $F_p$ , let  $\delta_{rs}$  be the compression of the spring of stiffness  $K_{rs}$ . It causes a deformation  $\Delta$  of the equivalent spring ( $K_{eq}$ ) due to the follower stiffness  $K_f$ , contact stiffness  $K_h$ , and the camshaft transverse stiffness  $K_{vs}$ . The return spring is relaxed by the same length  $\Delta$ .

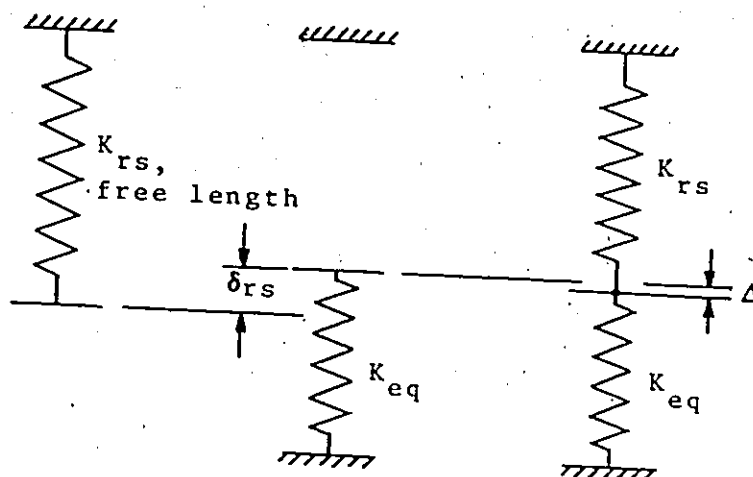


Fig. 4.5 Return spring preload.

With reference to Fig. 4.5, the static equilibrium equation can be written as

$$K_{eq} \Delta = K_{rs} (\delta_{rs} - \Delta). \quad (4.6)$$

For the springs in series,

$$K_{eq} = \frac{K_f K_h K_{vs}}{K_f K_h + K_h K_{vs} + K_f K_{vs}}$$

From equation (4.6)

$$\Delta = \frac{K_{rs} \delta_{rs}}{K_{eq} + K_{rs}}$$

Therefore, the preload force  $F_p$  is given by

$$F_p = K_{eq} \Delta$$

or

$$F_p = \frac{K_{eq} K_{rs} \delta_{rs}}{K_{eq} + K_{rs}} \quad (4.7)$$

#### 4.4.4 Contact Stiffness

The elastic deformation at the contact between the cam surface and the follower is an important consideration in cam design for high-speed applications. The load-deformation relationship in the contact region can be defined by a nonlinear spring because the radius of curvature of the cam varies with the cam angle.

The spring constant for the contact between cam and follower has been analytically determined from the theory of contact of two elastic bodies. Smith [19] has given separate expressions for the diametral and local deformations of cylinders in contact. Burr [58] has given a more realistic analysis and considered the total deformation between the centers of two contacting cylindrical surfaces as consisting of the local Hertz deformation at the point of contact, and the radial elastic deformations of the bodies.

Consider two cylindrical surfaces of radii  $R_1$  and  $R_2$  ( $>R_1$ ), and of length  $l$ , subjected to load  $P$  as shown in Fig. 4.6.

The half-width  $b$  of the rectangle of contact between parallel cylinders is given by [58],

$$b = \sqrt{\frac{4}{\pi} \left(\frac{P}{l}\right) (\eta_1 + \eta_2) R} = 1.13 \sqrt{\left(\frac{P}{l}\right) 2 \eta R}, \quad (4.8)$$

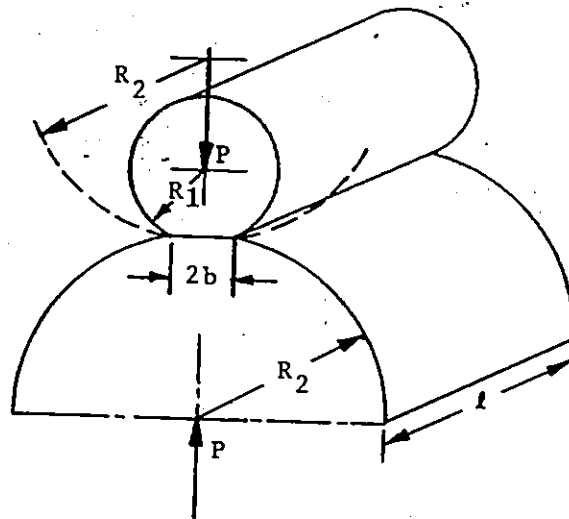


Fig. 4.6 Contact between two elastic bodies.

where

$$R = 1 / \left( \frac{1}{R_1} + \frac{1}{R_2} \right).$$

For the contacting bodies of the same material,

$$\eta_1 = \eta_2 = \frac{1 - \nu}{E} = \eta$$

$\nu$  = Poisson's ratio

$E$  = modulus of elasticity.

For steel  $\eta = 4.40 \times 10^{-6} \text{ mm}^2 / \text{N}$ .

The total deformation (approach of bodies) is given by [58] -

$$\delta = 0.638 \left( \frac{P}{l} \right) \eta \left[ \frac{2}{3} + \ln \frac{2 R_1}{b} + \ln \frac{2 R_2}{b} \right]. \quad (4.9)$$

In the cam-follower system under consideration,  $R_1$  is the radius of the follower roller ( $R_r$ ), and  $R_2$  is the radius of

curvature of the cam profile ( $R_c$ ), which varies according to the contact position, and is given by [56,57]

$$R_c = \frac{[(R_0+y)^2 + (e - \frac{\dot{y}}{\omega_c})^2]^{3/2}}{(R_0+y)^2 + (e - \frac{\dot{y}}{\omega_c}) [2(e - \frac{\dot{y}}{\omega_c}) - e] - (R_0+y) \frac{\ddot{y}}{\omega_c^2}} - R_r \quad (4.10)$$

where

$$R_0 = R_b + R_r.$$

The radius  $R_2$  is taken as negative for the concave surface (shown dotted in Fig. 4.6), and infinity for the plane surface, except in the expression for deformation. In expression (4.9),  $R_2$  is taken as a large positive number for any value negative or infinity. It has been observed by the author, as also by Smith [19] in his analysis, that the deformation was relatively insensitive to the variable radius of the cam.

Computing the deformation  $\delta$  in metres under a unit load  $P = 1N$ , the contact stiffness will be given by

$$K_h = 1/\delta \quad N/m. \quad (4.11)$$



#### 4.4.5 Translational System - Motion with No-Jump

From Fig. 4.3b, the equations of translational motion are derived as follows :

$$\begin{aligned}
 M_C \ddot{y}_1 &= - C_{vs} \dot{y}_1 - K_{vs} y_1 - F_C \cos\phi + F_p \\
 M_F \ddot{y}_2 &= - C_f(\dot{y}_2 - \dot{y}_3) - K_f(y_2 - y_3) + F_C \cos\phi - F_p \\
 M_F \ddot{y}_3 &= C_f(\dot{y}_2 - \dot{y}_3) + K_f(y_2 - y_3) - C_4(\dot{y}_3 - \dot{y}_4) - K_4(y_3 - y_4) \\
 &\quad - F_w - F_{cb} \\
 M_3 \ddot{y}_4 &= C_4(\dot{y}_3 - \dot{y}_4) + K_4(y_3 - y_4) - C_3(\dot{y}_4 - \dot{y}_5) - K_3(y_4 - y_5) \\
 M_2 \ddot{y}_5 &= C_3(\dot{y}_4 - \dot{y}_5) + K_3(y_4 - y_5) - C_2(\dot{y}_5 - \dot{y}_6) - K_2(y_5 - y_6) \\
 M_1 \ddot{y}_6 &= C_2(\dot{y}_5 - \dot{y}_6) + K_2(y_5 - y_6) - C_1 \dot{y}_6 - K_1 y_6 \quad (4.12)
 \end{aligned}$$

where

$F_w$  = external work load

$F_{cb}$  = Coulomb friction force, always opposing the motion of the follower.

#### 4.4.6 Energy Dissipation

There are several points in the cam mechanism at which relative motion, and hence friction, can develop. This includes the drive shaft, bearings, cam follower interface, the follower, sliding pair at the follower guide, and return spring, etc. However, only the damping mechanisms that affect the response of the system to a noticeable extent have been included in the modelling. For the

translational system, the damping in the follower (material damping) and the Coulomb friction at the follower guide interface are of significant importance. The phenomenon can be modelled by simple descriptions; that is, a viscous type of damping for the follower and the damping force proportional to the normal load for the Coulomb friction as shown in Fig. 4.7.

The damping coefficient for the material friction can be obtained from experimentally determined damping ratio  $\zeta$ , given by

$$\zeta = \frac{C}{C_{cr}}$$

where,  $C_{cr}$  is the critical damping, which depends on the mass and stiffness values.

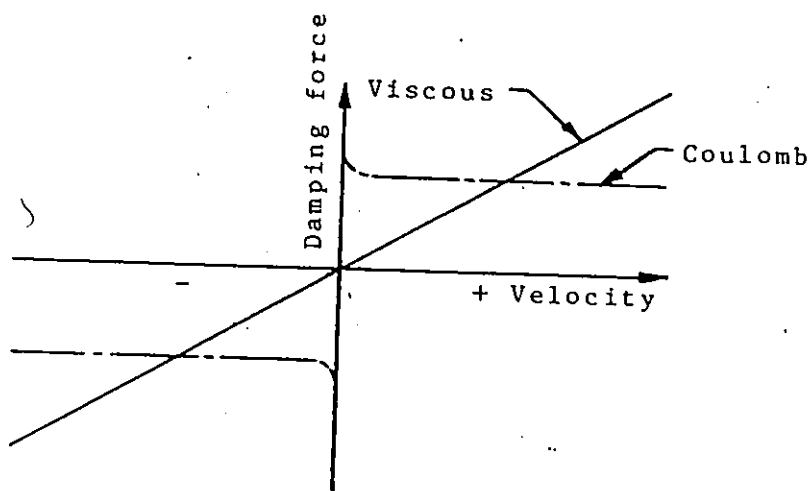


Fig. 4.7 Damping mechanisms.

For the follower, we have

$$C_f = \zeta_f C_{cr} = \zeta_f 2 \sqrt{K_f M_f} \quad (4.13)$$

The values of  $\zeta_f$  for cam-follower system have been found to range from 0.05 to 0.15 [3,17,18,56]. In the present investigation,  $\zeta_f$  is taken as 0.10.

For the return spring,

$$C_{rs} = \zeta_{rs} 2 \sqrt{2 K_{rs} M_{rs}} \quad (4.14)$$

where  $\zeta_{rs}$  is taken as 0.01 [18].

#### Coulomb Friction

The normal contact force between the cam and the follower acts at an angle  $\phi$  (the pressure angle) with the vertical. This results in side thrust between the follower and its guide. Referring to Fig. 4.8, the thrust reactions are given by

$$\begin{aligned} N_1 &= \frac{A + B}{B} F_c \sin \phi \\ N_2 &= \frac{A}{B} F_c \sin \phi \end{aligned} \quad (4.15)$$

The friction forces  $F_1$  and  $F_2$  are given as

$$\begin{aligned} F_1 &= C_{cb} N_1 \\ F_2 &= C_{cb} N_2 \end{aligned} \quad (4.16)$$

where  $C_{cb}$  is the sliding friction coefficient. A value of 0.08 has been selected for the coefficient  $C_{cb}$ .

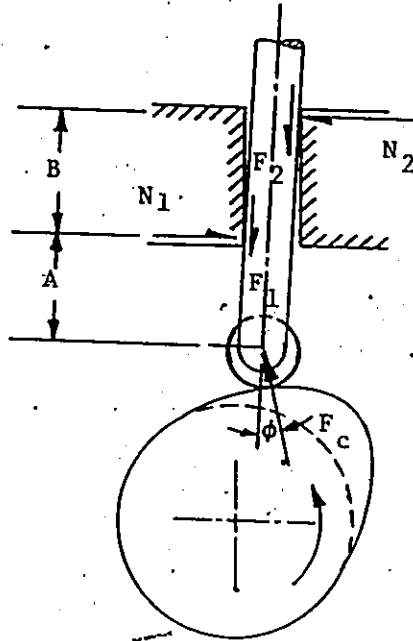


Fig. 4.8 Coulomb friction at the follower guide.

The total friction force  $F_{cb}$  is given by

$$F_{cb} = F_1 + F_2 \quad (4.17)$$

All the coefficients are allowed as variables in the software system so that any user-defined values can be entered.

#### 4.4.7 Jump Criterion

The contact between cam and follower is maintained for  $F_c$  positive. Therefore, for no jump to occur, we can write from equation (4.5), the inequality

$$(y + y_1 - y_2) + \frac{F_p}{\cos^2 \phi} > 0$$

or

$$y + y_1 + \frac{F_P}{\cos^2 \phi} > y_2 \quad (4.18)$$

Separation between the cam and follower occurs when  $F_C = 0$ . Alternatively,

$$y_2 > y + y_1 + \frac{F_P}{\cos^2 \phi} \quad (4.19)$$

#### 4.4.8 Translational System - Motion During Jump

When the follower leaves the cam surface,  $F_C$  equals zero and the springs  $K_f$  and  $K_{vs}$  are no longer compressed by the return spring preload. The follower essentially rides on the return spring and the system will vibrate at a new low frequency determined mainly by the return spring stiffness. The first three equations of motion for the translational system (4.12), are changed as follows:

$$\begin{aligned} M_C \ddot{y}_1 &= -C_{vs} \dot{y}_1 - K_{vs} y_1 \\ M_r \ddot{y}_2 &= -C_f(\dot{y}_2 - \dot{y}_3) - K_f(y_2 - y_3) \\ M_f \ddot{y}_3 &= C_f(\dot{y}_2 - \dot{y}_3) + K_f(y_2 - y_3) - C_4(\dot{y}_3 - \dot{y}_4) \\ &\quad - K_4(y_3 - y_4) - F_w - F_p \end{aligned} \quad (4.20)$$

The Coulomb friction force  $F_{cb}$  becomes zero, because  $F_C = 0$ .

#### 4.5 Simulation of the Excitation

The cam profile provides the forcing function for the follower. In addition to the theoretical motion cut on the cam, the profile errors due to cam manufacturing influence the nature of the excitation.

##### 4.5.1 Machining Process of Cam Profile - Cam Production

Several methods are used for cam production [35,43]. For the manufacture of precision cams, the two most common methods are:

- (i) Analog duplication of a master cam.
- (ii) Direct Continuous Numerically Controlled (CNC) cutting of production cams.

When a number of cams of the "same design" are to be produced, as in automotive camshaft production, a master cam is first cut by the common incremental cutting method. This is usually done on rotary-table milling machines, or mills that are numerically controlled. After the master cam leaves the milling machine, it will have a series of scallops or flats on its contour as shown in Fig. 4.9. For the next step, a skilled workman "hand-dresses" the master with abrasives to remove the scallops or flats, and create a smooth, continuous contour. The master cams are commonly produced to tolerances of  $\pm 0.0001$  to  $\pm 0.0002$  in. To produce the required cam, the master cam is placed in an analog, duplicating cam production machine which traces its contour and drives a cutter continuously against the final workpiece to cut a similar shape. Master cams are generally made oversize so that the inaccuracies in the master will be

decreased by the ratio of the master to the production cam size. The copying process has its own dynamics which contribute to the distortion between the master and the workpiece profile. Precision cams are first machined soft, then hardened, and finally ground using copy-grinding or NC grinders.

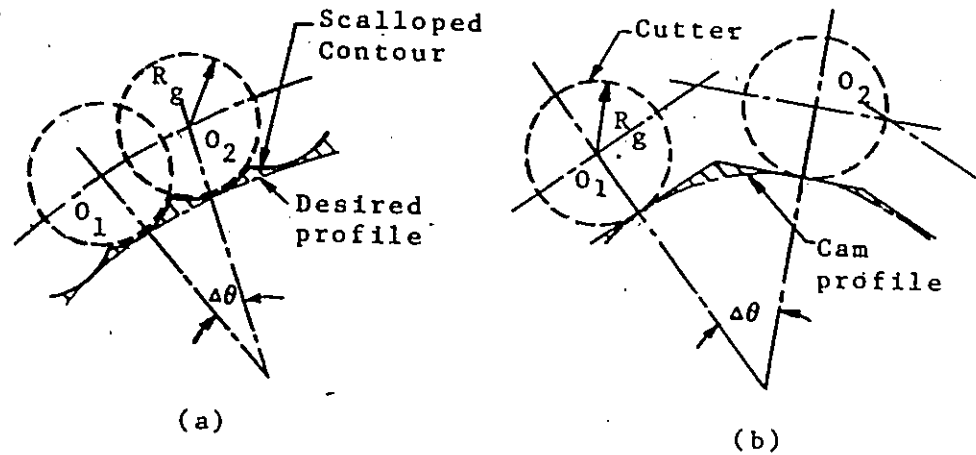


Fig. 4.9 Scallops (a), and Flats (b) on cam contour as a result of incremental cutting.

In the CNC method of cam manufacture, no master cam is involved. Each production cam is a separate operation. An NC tape is first made, which contains all the cam profile (displacement) information encoded in either polar or cartesian coordinates depending on the particular machine to be used. The cutter moves in a step-wise fashion according to the programmed data points, creating either a piece-wise linear approximation or circular interpolation of the original function. The higher derivatives of such a function tend to infinite pulses. However, the subsequent grinding, also on a CNC grinder, removes these sharp errors and produces a fairly smooth and continuous profile.

Quality cam manufacturers, like Eonic, Inc. - Detroit, have computer programs that perform the basic engineering analysis required in cam design, and also prepare NC tapes used in cam production. This cuts cost, and reduces the production times.

Each manufacturing method introduces its own noise into the resultant cam motion. There are a variety of machines used to inspect the finished cam. At Eonic, their Digital Cam Inspection Machine records the deviation from theoretical cam data (lift) to actual cam data, to twenty-millionths of an inch. It employs the actual follower size, can check a camshaft lobe at 360 points ( $1^\circ$  interval) and print out the deviation at each point. Commonly achieved accuracies, with most of the NC machines and common mills and lathes, range between  $\pm 0.001$  to  $\pm 0.005$  in. [43].



#### 4.5.2 Model of the Input Signal - The lift Function

In industry practice, the lift error, defined as the difference between the actual lift and the theoretical lift, is measured as a function of the cam angle over the cam cycle. In order to quantify the effects resulting from the cam profile errors, this lift error must be superimposed on the ideal desired lift function. However, since the lift error depends on so many factors of the manufacturing process, such as the grinding wheel size, and the dynamics of the machinery used, the error generated for different cams, produced to the same specifications, is of random nature, as shown in Figs. 4.10 and 4.11. These are typical cam profile error measurement charts for automotive cams obtained from Eonic, Inc., Detroit, Michigan - USA, which were produced from their Digital Cam Inspection Machine.

To simulate the input signal generated by a real cam, a stochastic model has been considered. The deviation in the follower displacement (lift error) due to cam profile errors, measured as a function of cam angle, is a random function. Engineering specifications for the production cam tolerances consist of a maximum allowable deviation in lift, and an allowable rate of deviation. Typical values for quality automotive cams are:

maximum allowable deviation (Size tolerance specification)	:	$\pm 0.001$ in.
allowable rate of deviation (Waviness specification)	:	0.0001 in/deg.

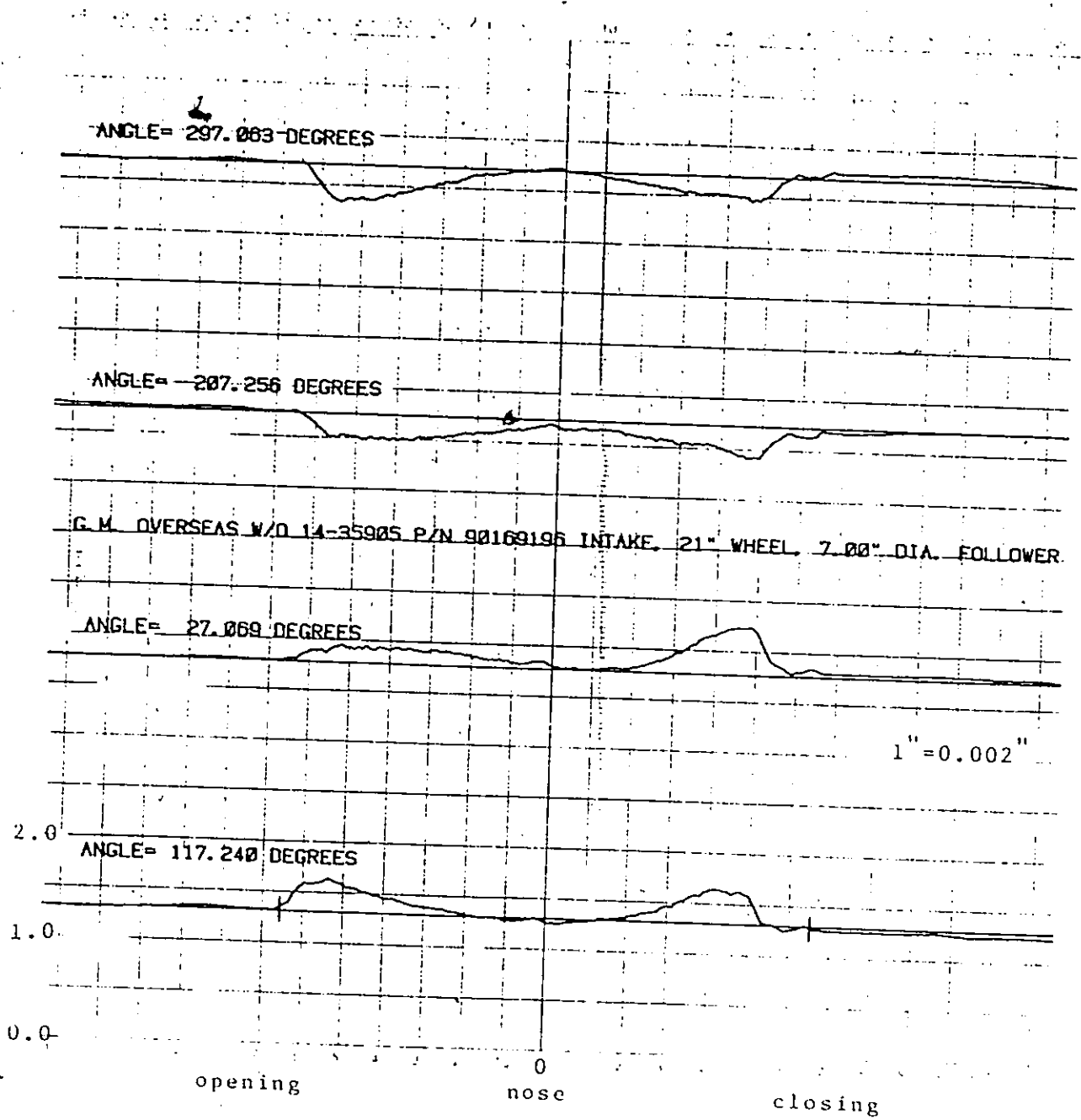


Fig. 4.10 Inspection lift error for automotive cams - Eonic, Inc., Detroit.



There can be two approaches to the generation of data for the lift function;

- (i) from the real sequences of lift error measurements,
- (ii) assuming a distribution for the random errors.

(i) If sufficient information on cam profile checking is available, Fig. 4.11, real sequences of cam lift error measurement data (inspection lift error) can be employed. For  $n$ -independent realizations of the random function  $X(\theta)$  - Fig. 4.12, the mean and standard deviation at angle  $\theta_k$  can be calculated in the following way - Ref. Table 4.1.

$$\text{Mean, } \overline{X(\theta_k)} = \frac{\sum_{i=1}^n X_i(\theta_k)}{n} \quad (4.21)$$

$$\text{Variance, } D_x(\theta_k) = \frac{\sum_{i=1}^n [X_i(\theta_k) - \overline{X(\theta_k)}]^2}{n-1} \quad (4.22)$$

Then, representing the data by a probability distribution, a sequence can be sampled randomly.

(ii) If, however, enough data is not available, it is convenient and necessary to make realistic assumptions about the distribution of values, and then sample randomly from these distributions. The assumptions made in the present simulation are based on the available literature on cam profile errors, as shown in Figs. 2.3-2.5, and the records of deviations obtained from quality cam manufacturers, Figs. 4.10, 4.11, and 4.13. The lift error is characterized by a variable-

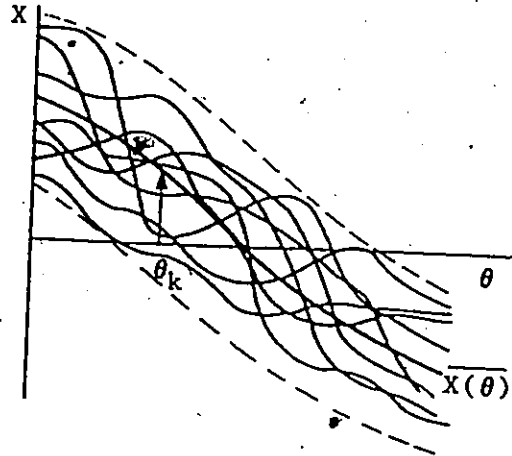


Fig. 4.12 The expectation (mean) of a random function.

TABLE 4.1

THE RESULTS OF THE MEASUREMENTS

$X(\theta)$	$\theta_1$	$\theta_2$	...	$\theta_k$	...	$\theta_m$
$X_1(\theta)$	$x_1(\theta_1)$	$x_1(\theta_2)$	...	$x_1(\theta_k)$	...	$x_1(\theta_m)$
$X_2(\theta)$	$x_2(\theta_1)$	$x_2(\theta_2)$	...	$x_2(\theta_k)$	...	$x_2(\theta_m)$
...	...	...	...	...	...	...
$X_i(\theta)$	$x_i(\theta_1)$	$x_i(\theta_2)$	...	$x_i(\theta_k)$	...	$x_i(\theta_m)$
...	...	...	...	...	...	...
$X_n(\theta)$	$x_n(\theta_1)$	$x_n(\theta_2)$	...	$x_n(\theta_k)$	...	$x_n(\theta_m)$

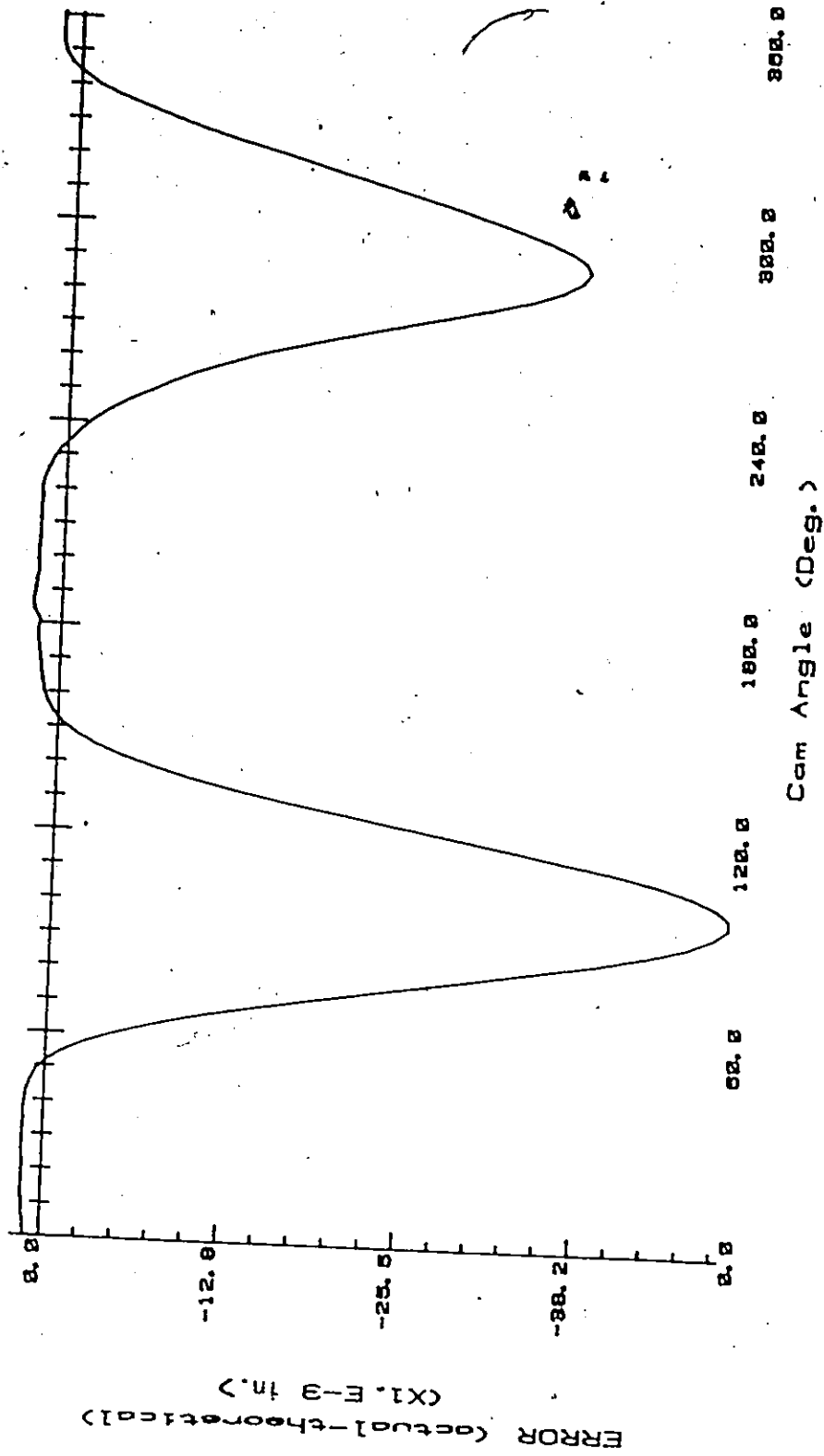


Fig. 4.13 Deviation between real and theoretical roller displacement (lift error) [46].

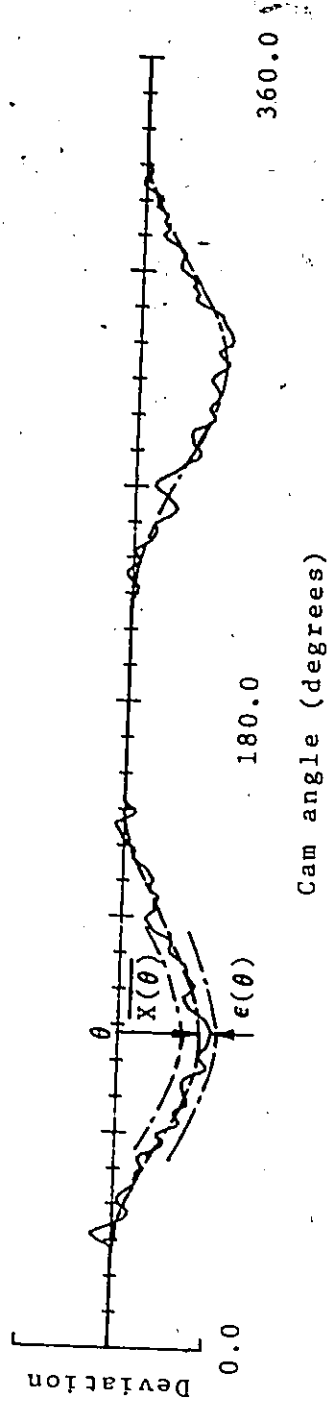


Fig. 4.14 Lift error characterized by a variable-mean deviation and a superimposed waviness.

mean deviation or "size-error" and a superimposed waviness of random nature - Figs. 4.12 and 4.14. The general lift error function can be written as

$$X(\theta) = \overline{X(\theta)} + \epsilon(\theta). \quad (4.23)$$

The mean  $\overline{X(\theta)}$  is assumed to follow the pressure angle (or velocity) variations over the complete cam cycle, with a maximum defined by the maximum allowable size tolerance, and the waviness error  $\epsilon(\theta)$  has been assumed to be normally distributed between the 3 $\sigma$  limits of randomness deviation about the variable mean.

With the variable mean and randomness deviation determined at fixed incremental angles, random number generation is employed to determine discrete values of the simulated lift error. This error is added to the ideal lift to give the simulated discrete lift function. The two approaches for generating the lift function have been implemented in the software system developed for the simulation of the cam dynamics. The system is also programmed so that the measured lift error data from a single cam can be input to study the dynamic influence of the profile errors for a particular cam design.

#### 4.5.3 Smoothing by Spline Interpolation

Spline functions are used extensively as approximating functions because they permit local curve fitting, and hence are suited to the characterization of complex waveforms. They are computationally easy to handle; their derivatives and integrals are



also spline functions, of one degree lower and higher, respectively. Smoothing spline interpolation [59-62] replaces strict interpolation by a blending of the adjacent splines at their junctions. This has been employed here to obtain a smooth piece-wise polynomial fit to the discrete data obtained with either of the two approaches described earlier in the main section.

Referring to Fig. 4.15, let  $\theta_0, \theta_1, \dots, \theta_n$  be distinct values of the independent variable (cam angle positions), and  $y_0, y_1, \dots, y_n$  denote the corresponding values of the dependent variable (discrete lift function values). In this development, a knot (where polynomials join) will be considered to be placed at each data point  $\theta_i, i=0, 1, \dots, n$ , so that each point is treated equivalently.

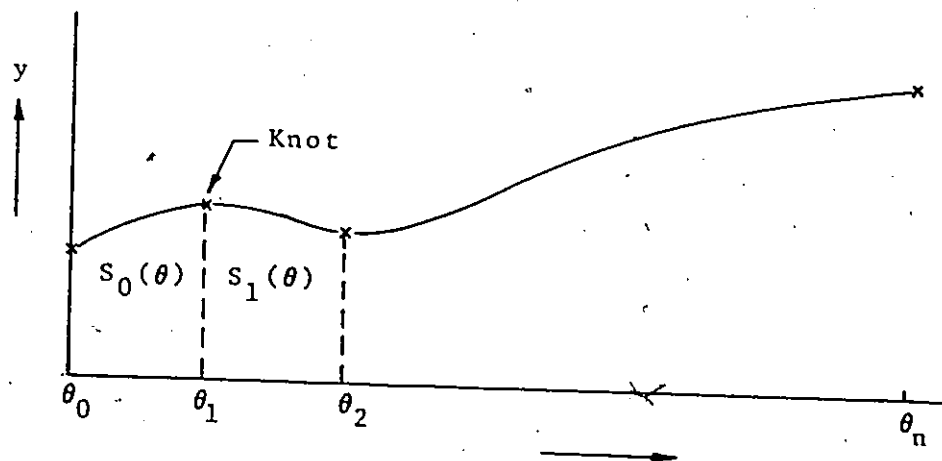


Fig. 4.15 Spline interpolation.

A mathematical spline  $S(\theta)$  is, by definition [59,60], a piece-wise polynomial of degree  $k$ , and has the following properties:

- (i) The polynomials (all of degree  $k$ ) join in the knots, i.e.,  $S(\theta_i) = y_i$ ,  $i = 0, 1, \dots, n$ .
- (ii) The polynomial and its first  $(k-1)$  derivatives obey continuity condition at the joints (knots), i.e., for a cubic spline  $S(\theta)$ ,  $S'(\theta)$ , and  $S''(\theta)$  are continuous on  $[\theta_0, \theta_n]$ .

In terms of the flexible strip mechanical spline, these properties can be described as follows:

- (i) The spline must pass through the knots.
- (ii) The spline does not break, nor does it bend into sharp angles.

Also the theory of thin beams shows that, between the knots, the mechanical spline approximates a cubic polynomial.

A cubic spline function  $S_i(\theta)$  is defined within  $\theta_i \leq \theta \leq \theta_{i+1}$ ,  $0 \leq i \leq n-1$  as

$$S_i(\theta) = a_i + b_i(\theta - \theta_i) + c_i(\theta - \theta_i)^2 + d_i(\theta - \theta_i)^3, \quad (4.24)$$

satisfying conditions (i) and (ii).

To provide smoothing, the method developed by Reinsch [59] has been employed. Cubic spline fitting provides one free parameter which is responsible for smoothing the fit within the given bounds. The smoothing function  $S(\theta)$  shall be constructed so as to minimize the smoothing integral

$$I = \int_{\theta_0}^{\theta_n} S''(\theta)^2 d\theta, \quad (4.25)$$

under the boundary conditions that

$$\sum_{i=0}^n \left\{ [S(\theta_i) - y_i] / \delta y_i \right\}^2 \leq SM; \quad \delta y_i > 0 \\ \equiv \sigma(y_i). \quad (4.26)$$

That is,  $\delta y_i$  is an estimate of the standard deviation of the ordinate  $y_i$ . The constant  $SM > 0$ , called the smoothing parameter, controls the extent of smoothing. Choosing  $SM$  equal to zero leads to simple interpolation by cubic spline functions, without smoothing.

Condition (4.25) states that the spline assumes the shape that minimizes its potential energy, which is approximately proportional to the curvature, i.e., the second derivative. All the spline functions do not necessarily pass through the measured values  $y_i$ , however, the curvature is minimized. This requires that [60],

$$S''(\theta) = S''(\theta_n) = 0. \quad (4.27)$$

The solution of (4.25) and (4.26) may be obtained by the method of calculus of variations. Introducing an auxiliary variable  $z$  together with a Lagrangian parameter  $p$ , we require to minimize the functional

$$\int_{\theta_0}^{\theta_n} S''(\theta)^2 d\theta + p \left\{ \sum_{i=0}^n \left[ (S(\theta_i) - y_i) / \delta y_i \right]^2 + z^2 - SM \right\}. \quad (4.28)$$

The optimization procedure for (4.28), and an ALGOL program have been developed by Reinsch [59]. The same algorithm has been implemented here in Fortran 77.

The first two derivatives, i.e., the velocity and acceleration required in the dynamic simulation, are directly available from the spline interpolation. This displacement, velocity, and acceleration information, rather than that from the theoretical ideal cam motion function, is then used to simulate the cam system dynamics for the most general case when the dynamic effects and the influence of errors in the cam profile are taken into account.

## CHAPTER 5

### IMPLEMENTATION

#### 5.1 Introduction

The multi-degree-of-freedom system of equations, involving nonlinearities, must be solved by a suitable numerical method. The lift error function has been generated using practical values for the maximum allowable size tolerance and random error confidence limits. For the system parameters selected, approximate natural frequencies have been computed for the return spring, follower system, and the torsional drive system.

#### 5.2 Solution of Equations of Motion

The nonlinear second-order differential equations for the dynamic model have been transformed into a system of first-order equations. Over the years, many efficient methods have been developed for the solution of such a system of equations. This implementation employs the most widely used fourth-order Runge-Kutta method. The method is self-starting, easy to program, quite stable, and has small truncation error per step. A step size of 0.1 degree of cam angle (0.00001 sec. time-step at a cam speed of 1500 RPM) has been used. This gave an accurate and economical solution, which was determined by experimenting with different step sizes and comparing the results with the solution obtained by the application of a more accurate fifth order Runge-Kutta method with an adjustable step size [63,64]. A solution time of less than two minutes was taken for simulation over

one cam cycle, if only dynamic effects for a perfect profile were desired. For the combined effects of profile errors and system dynamics, the solution time taken was less than four minutes.

### 5.3 Generation of Lift Error Function

The continuous lift error function has been generated in two ways;

- (a) from the measured values, of the lift error for a single cam, obtained from industry, and
  - (b) through simulation, by assuming a maximum deviation for the smooth mean error (size tolerance) and a distribution for the waviness error.
- (a) In this case the lift error data was obtained from Eonic, Inc., Detroit in tabular form at  $1^\circ$  cam angle intervals. The system program is capable of accepting this data from a file. This discrete data is internally interpolated using spline fitting, without smoothing ( $SM=0$ ), to generate the continuous lift error function.
- (b) For simulation, the smooth size-error is assumed to vary as the pressure angle over the cam cycle. For the comparative study of cam motions and for the sensitivity analysis, the maximum allowable tolerance on the size-error, at the location of the maximum pressure angle is fixed as 0.0127 mm (0.0005 in. or 5 tenths). The waviness error, is assumed to be normally distributed within a tolerance band ( $3\sigma$ ) of  $\pm 0.00254$  mm ( $\pm 0.0001$  in.). These tolerances are representative of those obtainable in industrial practice. As is observed from

inspection lift error plots obtained from industry, there is no significant waviness error over the dwell periods. Therefore, a very small confidence interval is chosen for the waviness error over these portions.

The frequency of the waviness error (WE) depends on the cam incremental angle selected for lift error simulation, whereas its amplitude depends on the  $3\sigma$  limits. For the chosen  $3\sigma$  limits of waviness error, it is found from several tests, that a large cam angle interval ( $5^\circ$  to  $10^\circ$ ) generates a waviness of much lower frequency than observed in inspection lift error plots. An incremental angle of  $1^\circ$  gives a closer approximation to the waviness frequency observed in plots obtained from industry. This, however, results in severe vibrations of the semi-rigid follower system considered for the investigation. Results are presented for the lift error simulated with  $1^\circ$  and  $2^\circ$  cam angle intervals.

To study the effects of profile errors for a particular motion, the size-error tolerance is varied, and the smoothness parameter (SM) changed to get different rate of deviation (mm/deg.) or the sharpness of profile irregularities.

#### 5.4 System Parameters

The critical system parameters of follower mass and its stiffness have been chosen for a typical semi-rigid system used in high-speed industrial applications and in overhead-cam automotive designs [27]. The return spring stiffness has been selected so as to provide adequate contact force over the rise and return periods at the

selected design speed. The total lift has been fixed so as to keep the maximum acceleration at a reasonable level for the selected cam speed. Cam speed was typical of a high-speed application. Basic cam and roller follower sizes, and the drive parameters were taken from a study conducted by Kim and Newcombe [46]. The drive parameters represent an essentially rigid drive. The system damping factors and Coulomb friction coefficient have been based on the typical experimental values obtained in cam-follower systems of the type considered in this investigation [17,18,56]. For the sake of comparison, results have also been given for a typical flexible system, representative of push-rod automotive designs.

Although the system has been programmed for the general case of a spring-constrained roller follower, driven by any of the radial cam types, e.g., Dwell-Rise-Dwell-Return (D-R-D-R), Dwell-Rise-Return-Dwell (D-R-R-D), or a Rise-Return-Rise (R-R-R); results have been presented for the most common D-R-D-R cams. Unless specified otherwise, the following input data and system parameters have been chosen for the system under consideration.



Basic Input Data

Cam motion program : D-R-D-R-D

	Dwell	Rise	Dwell	Return	Dwell
Cam angle interval (deg.)	0-30	30-150	150-210	210-330	330-360

Total rise	: 0.02540 m
Diameter of cam base circle	: 0.07620 m
Diameter of follower roller	: 0.01905 m
Cam thickness	: 0.00635 m
Initial return spring compression	: 0.01270 m
Mass of camshaft considered at the cam, $M_{CS}$	: 4.668 kg
Inertia of camshaft considered at the cam, $I_{CS}$	: 0.000454 kg.m <sup>2</sup>
Reference to Fig. 4.1	A = 0.111125 m
	B = 0.0762 m
Maximum allowable size tolerance	: 0.127E-4 m
Standard deviation of waviness error	
-- over rise and return	: 0.762E-6 m
-- over dwell periods	: 0.020E-6 m
Smoothing parameter - SM	: 35.0
Cam speed	: 1500 RPM

Dynamic System Parameters:

$I_C$  = Internally computed for each motion - APPENDIX A.1  
(0.000664 kg.m<sup>2</sup> for Cycloidal cam)

$M_C$  = Internally computed for each motion - APPENDIX A.1  
(0.42365 kg for Cycloidal cam)

$M_r$  = 0.02276 kg

$M_f$  = 0.340 kg

$M_{rB}$  = 0.068 kg

$K_{Bf}$  = 2.26E+4 N.m/rad

$K_{vB}$  = 2.60E+9 N/m

$K_h$  — internally computed (Section 4.4.4), and  
nonlinear because cam radius changes continuously

$K_f$  = 1.751E+8 N/m

$K_{rB}$  = 2.10E+4 N/m

$C_{Bf}$  = 0.01356 N.m-sec/rad

$C_{vB}$  = 752.9 N-sec/m

Damping factor - follower  $\zeta_f = 0.1$

Damping factor - return spring  $\zeta_{rB} = 0.01$

$C_f$  and  $C_{rB}$  are internally computed using the damping factors  
 $\zeta_f$  and  $\zeta_{rB}$

$C_b$  = 0.113 N.m-sec/rad

Coulomb friction coefficient,  $C_{cb} = 0.08$

## 5.5 Calculation of Natural Frequencies

### Torsional System

$$K_{gf} = 2.26E+4 \text{ N.m/rad}, \quad I_c = 0.00112 \text{ kg.m}^2$$

(including  $I_{cs}$ )

Natural frequency is given by

$$\omega_{nt} = \sqrt{\frac{K_{gf}}{I_c}} = 4492.0 \text{ rad/sec}$$

(observed frequency  $\approx 4710 \text{ rad/sec}$ ).

### Follower System

Although the contact stiffness  $K_h$  varies with the cam radius, the variation has been found to be less than 10%. For the contact stiffness  $K_h$  corresponding to the cam base circle radius, the equivalent follower stiffness ( $K_e$ ) is given by

$$K_e = K_{rs} + \frac{K_f K_h}{K_f + K_h} = 0.706 \times 10^8 \text{ N/m}$$

$$M_f = 0.34 \text{ kg}$$

Therefore,

$$\omega_{nf} = \sqrt{\frac{K_e}{M_f}} = 14410.0 \text{ rad/sec}$$

(observed frequency  $\approx 14130 \text{ rad/sec}$ ).

### Return Spring - Fundamental natural frequency (APPENDIX A.3)

$$f_{rs} = \frac{1}{\pi} \sqrt{\frac{K_{rs}}{M_o}} \text{ Hz}, \quad M_o = \frac{M_{rs}}{2}$$

$$= 250.1 \text{ Hz. or } 1571.0 \text{ rad/sec.}$$

(observed frequency  $\approx 245 \text{ Hz}$ ).

The natural frequencies for the follower system and the return spring were also checked through a modal analysis for the translational system, and very close results were obtained. This was done to provide a means of checking the frequencies to be observed in the graphs resulting from the simulation process.

Implementation has been done in FORTRAN 77 on the VAX-730 computer. The available options are interactively selected, whereas the input data is given in input files. The results can be plotted on an HP plotter and/or printed out.

The following popular cam motions have been studied - Parabolic, Simple Harmonic, Cycloidal, Modified-Trapezoidal, 3-4-5 Polynomial, 4-5-6-7 Polynomial, and Modified-Sine.

## CHAPTER 6

### RESULTS AND DISCUSSION

#### 6.1 Introduction

In this chapter, the simulation results are presented and discussed. The results are covered under three headings, namely,

- comparison of cam motions,
- effects of cam profile errors, and
- response sensitivity to system parameters.

Most simulation results are presented for the third cycle of cam rotation, at which time a steady state was achieved in the absence of significant return spring vibrations. The tabulated results comprise - the root mean square (RMS) deviation of the actual follower acceleration from the theoretical acceleration over a cam cycle, the deviation at the peak acceleration, maximum and minimum contact force, and the maximum cam torque over the rise and return periods. The RMS deviation has been taken as the index of comparison of motions, but the deviation at peak acceleration is always useful information. Cam speed variations are discussed wherever important and no significant deviations are observed in the pressure angle.

Graphic output is of most use to the designer to visualize the response characteristics. The various dynamic response criteria have been plotted on the HP-7221A plotter and are given along with the tabulated data.

## 6.2 Comparison of Cam Motions

The maximum values of the theoretical characteristics of various motions are given in Table 6.1 and the acceleration curves for various cam motion programs are shown in Table 6.1a. The selected cam motions are compared with respect to;

- the effects of system dynamics alone (flexibility effects) for a perfect cam profile,
- the effects of cam profile errors alone (tolerance effects) for a perfectly rigid system, and
- the combined effects of system dynamics and profile errors (flexibility + tolerance) for the most general case.

The same system parameters and the simulated (or inspection) lift error function have been used for each cam motion. It is important to note that the same lift error cannot be realized in experimental studies because cams with different motions will be cut with different random profile errors.

### 6.2.1 Comparison Based on Flexibility Alone

The performance criteria are given in Tables 6.2 and 6.3, and selected response characteristics are shown in Figs. 6.1-6.4. The acceleration response shows a well-defined transient occurring at the natural frequency of the follower system - Fig. 6.1. No significant return spring vibrations occur at the cam speed of 1500 RPM. However, at a higher speed of 2100 RPM, low frequency return spring vibrations are clearly observed even for the smooth Cycloidal motion - Fig. 6.4. A very small contact force is available on the

TABLE 6.1 THEORETICAL CHARACTERISTICS - MAXIMUM VALUES

Cam Speed — 1500 RPM

Motion	Velocity (m/sec)	Acceleration (m/sec.sq.)	Pressure Angle (deg.)	Cam Torque (N.m)
1. Parabolic	3.81	571.50	21.9	13.0
2. Simple Harmonic	2.99	705.06	17.9	11.2
3. Cycloidal	3.81	897.71	22.3	14.0
4. Modified Trap.	3.81	698.39	22.1	13.7
5. 3-4-5 Poly.	3.57	824.76	21.0	13.2
6. 4-5-6-7 Poly.	4.17	1073.39	24.1	15.3
7. Modified Sine	3.35	789.81	19.9	12.5

TABLE 6.1a ACCELERATION CHARACTERISTICS OF THEORETICAL CAM MOTIONS

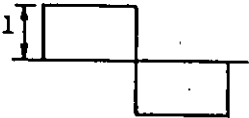
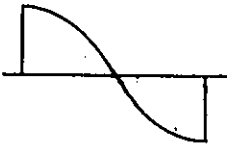
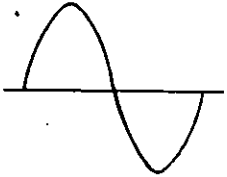
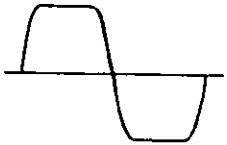
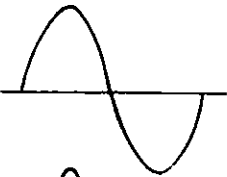
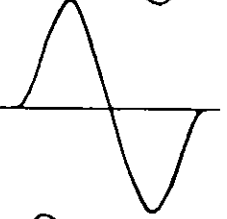
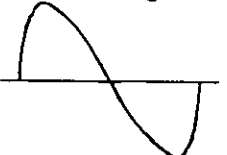
Motion	Acceleration Curve	Relative Max. (Min.)
Parabolic		1.00
Simple Harmonic		1.23
Cycloidal		1.57
Modified-Trapezoidal		1.22
3-4-5 Polynomial		1.44
4-5-6-7 Polynomial		1.88
Modified-Sine		1.38



TABLE 6.2 FLEXIBILITY EFFECTS ON FOLLOWER ACCELERATION

Cam Speed -- 1500 RPM

Motion	Deviation at Peak Acceleration (m/sec.sq.)		RMS Deviation (m/sec.sq.)
	Max. Rise	Max. Return	
1. Parabolic	908.78	968.63	277.32
2. Simple Harmonic	613.47	677.75	201.93
3. Cycloidal	9.94	13.01	8.86
4. Modified Trap.	23.12	28.47	14.64
5. 3-4-5 Poly.	16.94	17.48	13.25
6. 4-5-6-7 Poly.	1.04	2.58	2.56
7. Modified Sine	26.60	33.47	15.99

TABLE 6.3 FLEXIBILITY EFFECTS AT THE CAM

Cam Speed — 1500 RPM

Motion	Contact Force (N)					Max. Cam Torque (N.m)	
	Rise Min.	Max.	Upper Dwell Max.	Return Max.	Min.	Rise	Return
1. Parabolic	0.0	1004.4	1022.4	999.8	254.6	22.6	-20.6
2. Simple Harmonic	531.7	746.7	1032.9	539.6	297.1	12.2	-9.8
3. Cycloidal	434.6	792.2	812.1	638.3	374.9	16.0	-12.4
4. Modified Trap.	434.4	834.3	828.6	654.8	354.9	17.4	-13.4
5. 3-4-5 Poly.	474.8	733.3	818.3	601.1	413.9	14.4	-11.3
6. 4-5-6-7 Poly.	360.5	881.5	801.4	704.9	311.8	18.7	-14.2
7. Modified Sine	502.8	680.7	824.7	565.9	454.0	13.2	-10.5

FLEXIBILITY

ACCELERATION

THEORETICAL ACCEL.

CYCLE - 3

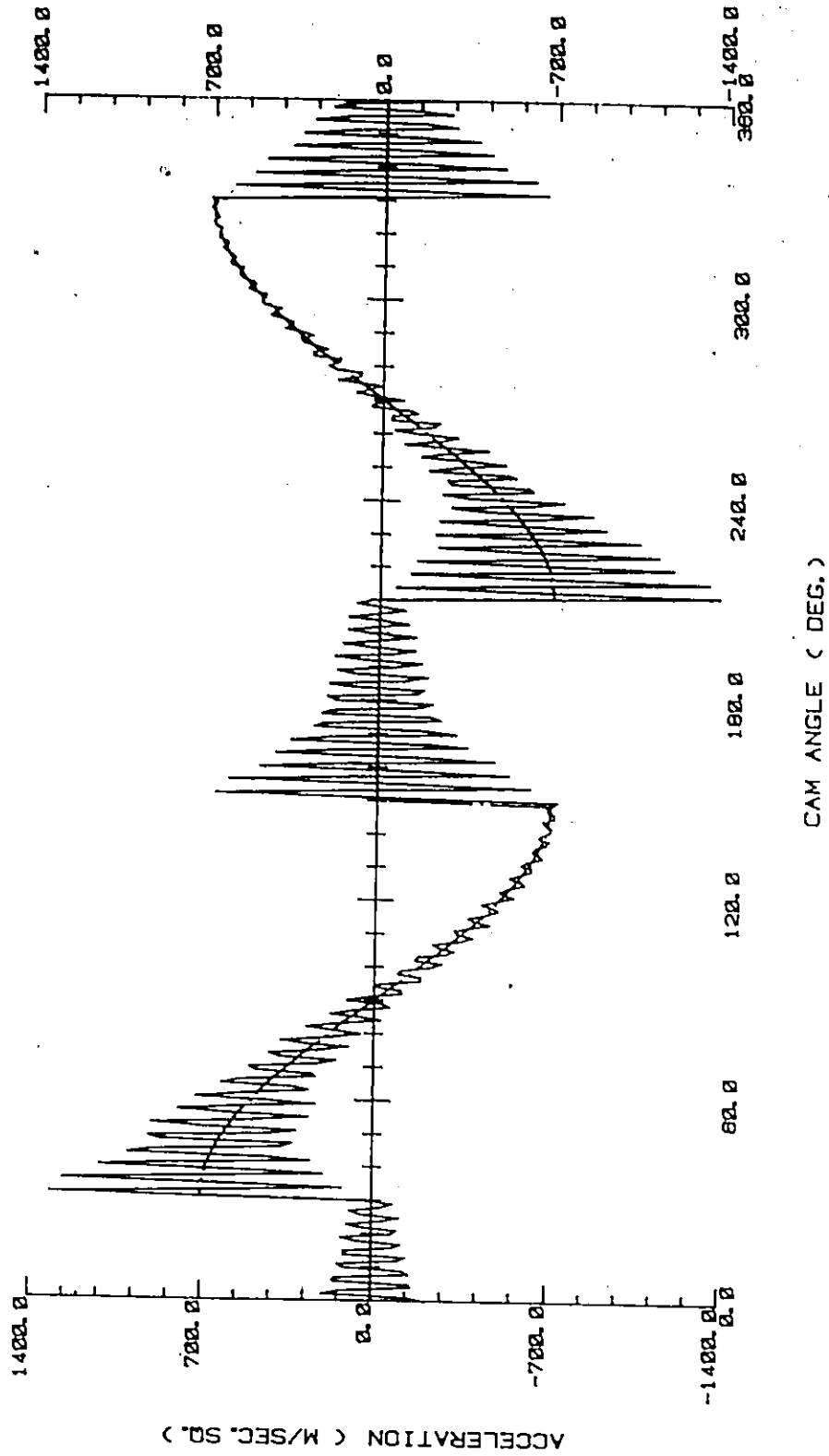


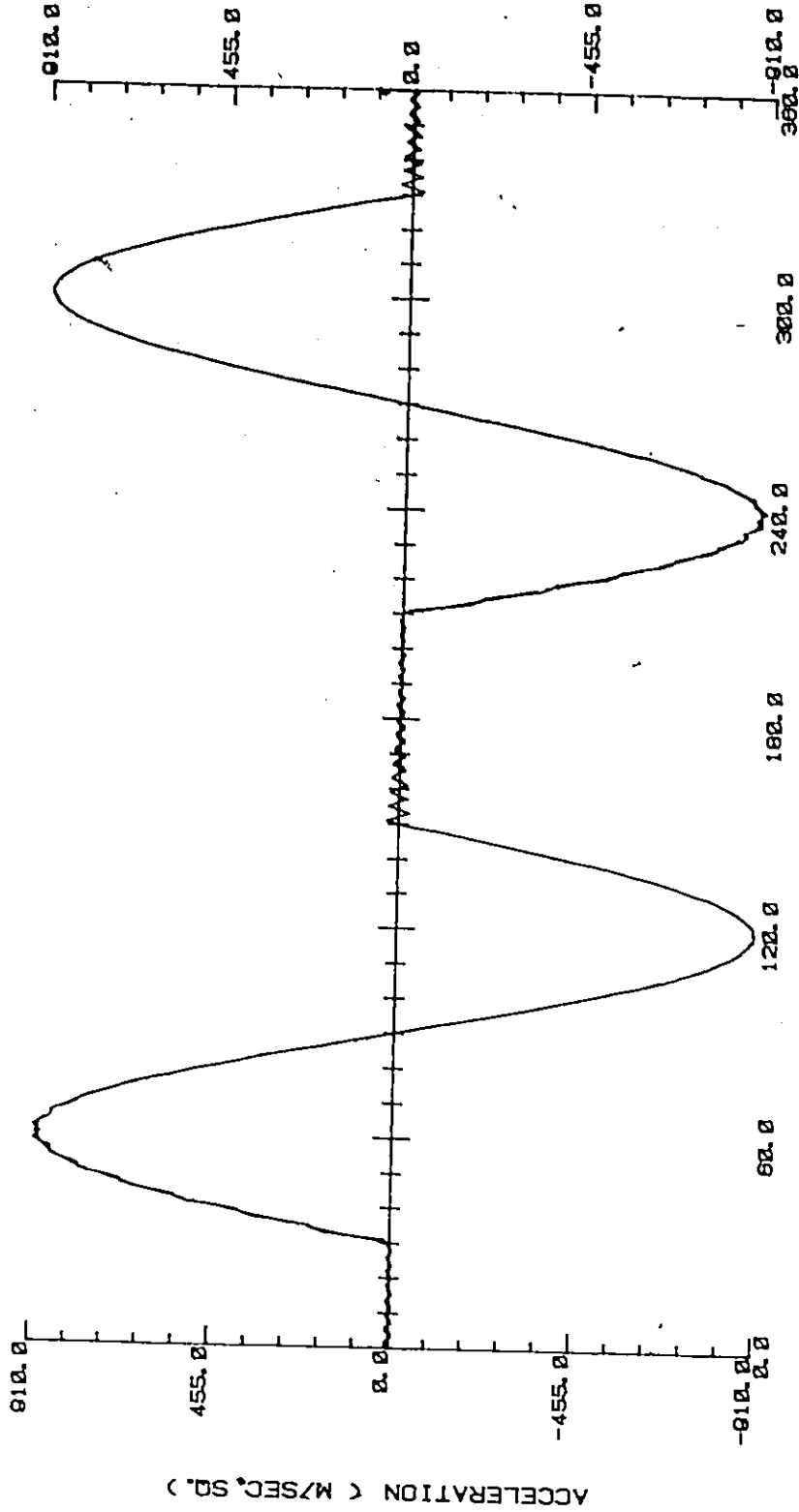
Fig. 6.1 Flexibility effects on follower acceleration - SH motion, 1500 RPM.

FLEXIBILITY

ACCELERATION

THEORETICAL ACCEL.

CYCLE - 3



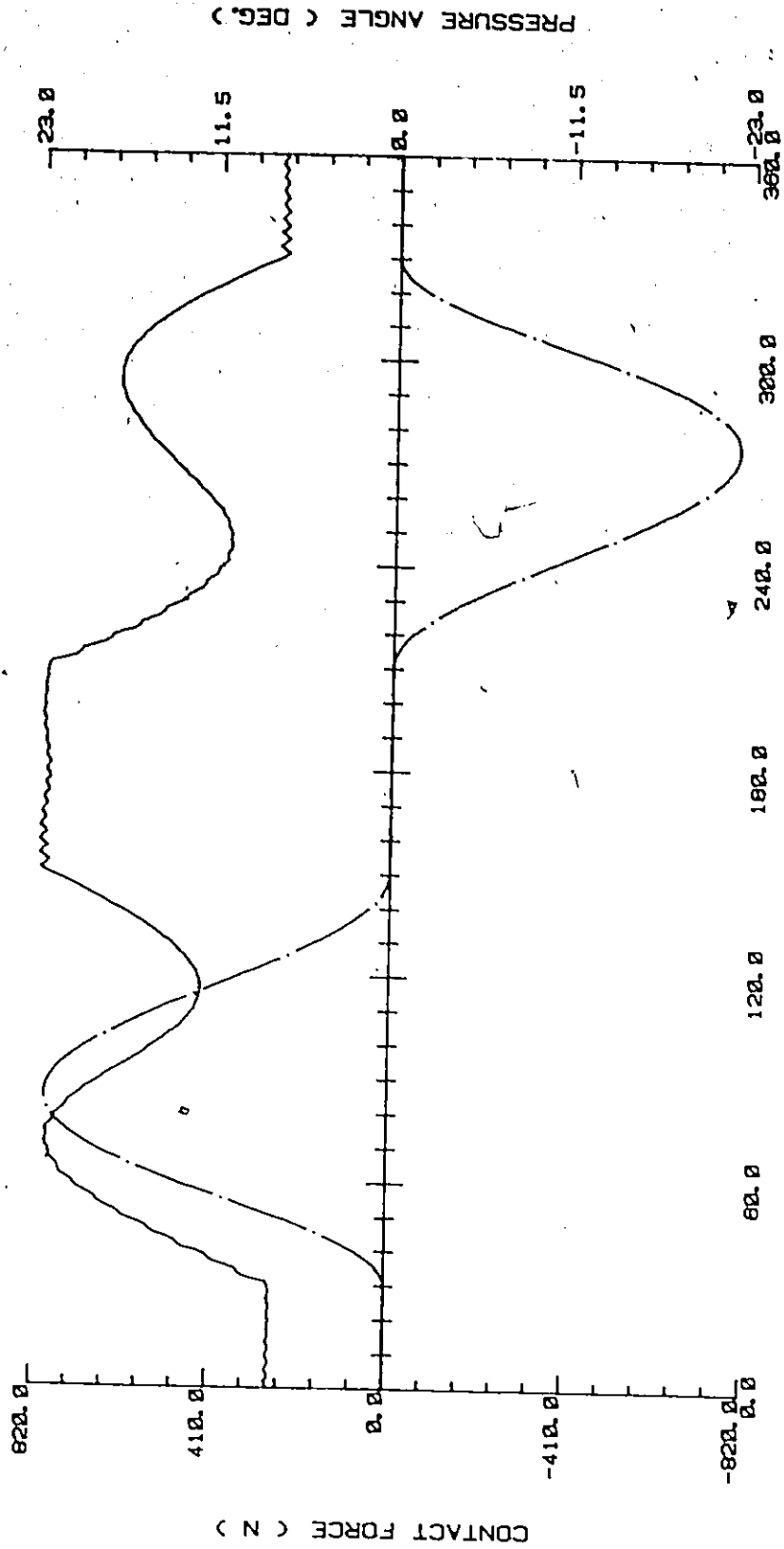
CAM ANGLE ( DEG. )

Fig. 6.2 Flexibility effects on follower acceleration - Cycloidal motion, 1500 RPM.

FLEXIBILITY

— CONTACT FORCE  
 - - - - - PRESSURE ANGLE

CYCLE - 3



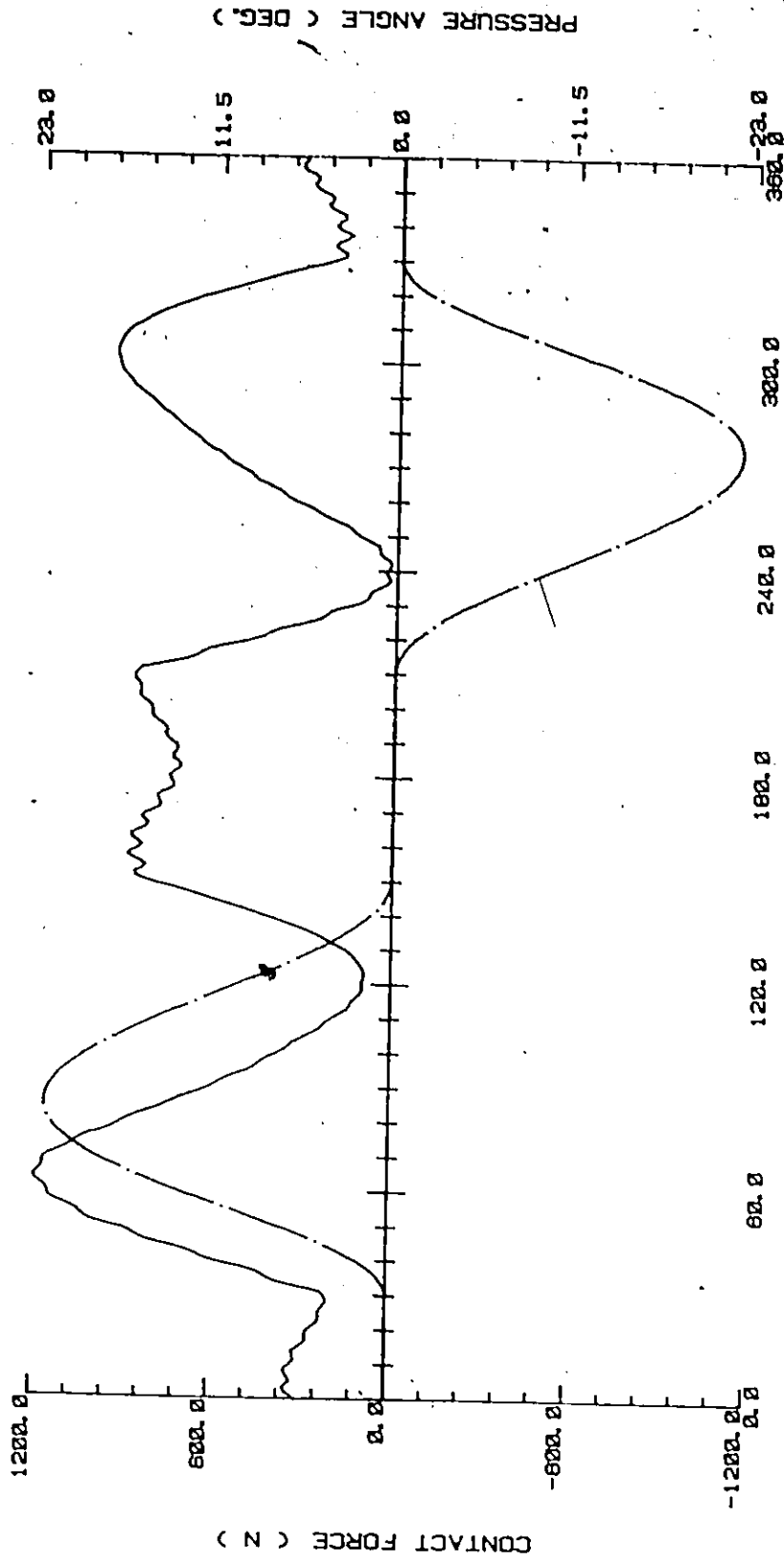
CAM ANGLE ( DEG. )

Fig. 6.3 Flexibility effects on contact force - Cycloidal motion, 1500 RPM.

FLEXIBILITY

— CONTACT FORCE  
- - - PRESSURE ANGLE

CYCLE - 3



CAM ANGLE ( DEG. )

Fig. 6.4 Flexibility effects on contact force - Cycloidal motion, 2100 RPM.

return, and follower jump occurs just above this speed.

An assessment of the relative merits of cam motions is presented in Table 6.4, where the numbers 1 to 7 correspond to ratings of excellent to bad. The comparison of various cam motions, based on system dynamics alone, is given under the following five headings.

#### 1. Transient Vibrations

The programs are listed in the order of increased vibrations as:

4-5-6-7 Poly., Cycloidal, 3-4-5 Poly., Modified-Trapezoidal, Modified-Sine, Simple Harmonic, Parabolic.

Clearly, the cam motions with smooth acceleration characteristics induce only small oscillations in the follower acceleration - Fig. 6.2, whereas the motions containing high frequency components (Parabolic) result in severe vibrations. This observation is obvious, but is made here for the sake of comparison when the effects of cam profile errors are accounted for along with the flexibility effects.

#### 2. Pitting Performance - Maximum Contact Force

For most motions, the maximum contact force occurs on the upper dwell, rather than the lower flank of rise, because of low inertia force at the speed considered. The maximum depends on the smoothness of the cam motion and hence its residual vibration characteristics. The maximum contact force on the lower flank of the rise, however, depends on the theoretical maximum acceleration of the cam motion, the amplitude of vibrations, and the shape of the

TABLE 6.4 COMPARISON OF CAM MOTIONS - FLEXIBILITY EFFECTS ALONE

Cam Speed -- 1500 RPM

Motion	1-Excellent		7-Bad		Torque Requirement
	Transient Vibration	Pitting Tendency	Jump Rise	Jump Return	
1. Parabolic	7	7	7 (YES)	7	7
2. Simple Harmonic	6	3	1	6	1
3. Cycloidal	2	4	4	3	4
4. Modified Trap.	4	5	5	4	5
5. 3-4-5 Poly.	3	2	3	2	3
6. 4-5-6-7 Poly.	1	6	6	5	6
7. Modified Sine	5	1	2	1	2



acceleration curve. For the Parabolic and SH motions, very high contact forces occur due to sudden jump in the acceleration of these motions at the transition points and the resulting high vibrations.

In the order of increased maximum contact force on the rise portion, the motions are listed as below:

Modified-Sine, 3-4-5 Poly., Simple Harmonic, Cycloidal,  
Modified-Trapezoidal, 4-5-6-7 Poly., Parabolic.

### 3. Jump Characteristics

The jump characteristics are defined by the minimum contact force over the rise and return periods. The Parabolic motion causes the follower to jump on the rise portion, as indicated by the zero contact force in Table 6.3. This happens due to the high amplitude of vibration in the beginning of the negative acceleration, caused by infinite jerk. Modified-Sine motion is observed to give the best jump characteristics because of the early and late peaks in its acceleration curve (Table 6.1a). The spring force is high near the end of rise and in the beginning of return, and on subtracting the maximum inertia force, results in a high minimum contact force to avoid jump. Theoretically, in the absence of flexibility effects, the SH motion should give best jump behaviour because of its low theoretical maximum acceleration which occurs at the end points of rise and return periods (Table 6.1a). This is clearly observed on the rise (Table 6.3) where a high minimum contact force is available because the vibrations have almost damped out near the end of the rise period. However, because of very high vibration amplitudes (hence high inertia force) in the beginning of return (Fig. 6.1), the minimum contact force reduces

substantially resulting in poor jump behaviour.

In the order of increased jump tendency, the various motions are rated as follows :

Modified-Sine, 3-4-5 Poly., Cycloidal, Modified-Trapezoidal,  
4-5-6-7 Poly., Simple Harmonic, Parabolic.

The motions with bad jump characteristics have either a high theoretical maximum acceleration (4-5-6-7 Poly.) or produce high transient vibrations (Parabolic), and their acceleration peaks occur towards the middle of the rise and return periods (Table 6.1a).

#### 4. Maximum Torque Requirements

Maximum cam torque determines the power requirements for the drive. It depends directly on the theoretical maximum values of the velocity, pressure angle, and the maximum contact force.

The motions are rated according to the cam torque requirements, from superior to bad, as follows :

Simple Harmonic, Modified-Sine, 3-4-5 Poly., Cycloidal,  
Modified-Trapezoidal, 4-5-6-7 Poly., Parabolic.

The superior motions have low maximum values of velocity, pressure angle (Table 6.1) and contact force (Table 6.3). These motions have their peak acceleration skewed to the left on rise.

#### 5. Cam Speed Variations

For most motions, the variation in cam speed is observed to be less than 0.3% because of the rigid drive used. For Parabolic motion, the fluctuation is of the order of 2.3% because of high vibrations and jump occurring on the rise portion.

### 6.2.2 Comparison Based on Profile Errors (Tolerance) Alone

Since system dynamics are not involved, only the kinematic effects of cam profile errors, on the follower motion, are to be considered. Any error in the lift function is magnified in the acceleration response because of the second derivative involved. The simulated lift error function is shown in Fig. 6.5 and the results on its effects on follower acceleration are given in Table 6.5 and shown for SH and Cycloidal motions in Figs. 6.6 and 6.7, respectively. The acceleration fluctuations are not so severely magnified because of the relatively smooth lift error function.

The step change of acceleration in Parabolic and SH motions, giving rise to infinite jerk, is smoothed because of the cam profile errors, i.e., a perfect step is impossible to manufacture. This should help to limit the vibration amplitudes for these motions. Referring to Table 6.5, no significant differences are observed in the RMS deviations in accelerations for various motions. The relatively high values for the Parabolic and SH motions are due to high deviations at the transition points to the dwells.

This comparison is only of academic importance because, in practice, system dynamics are always involved.

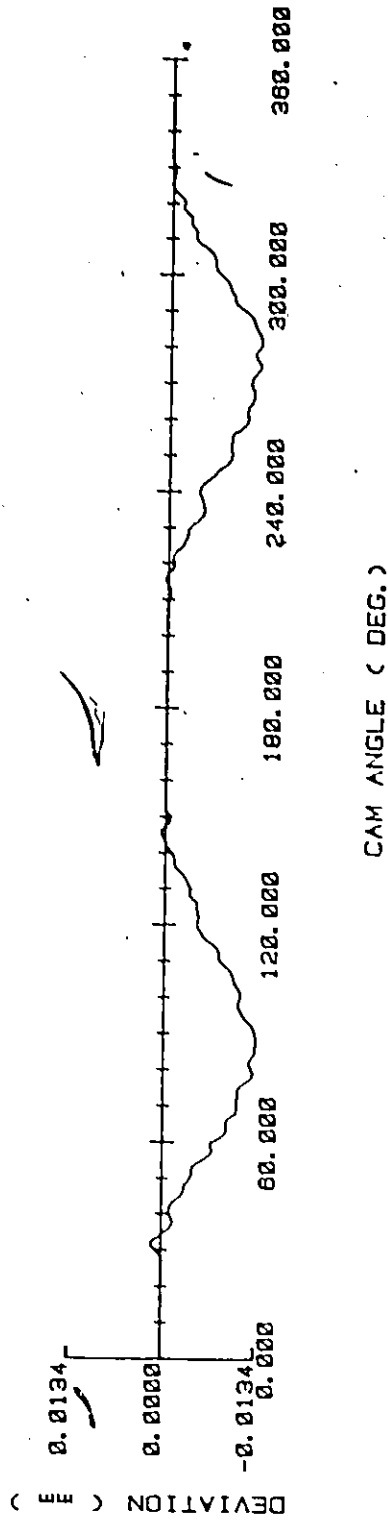


Fig. 6.5 Simulated lift error function - Size Tolr. = 0.0127 mm,  
 Waviness SD = 0.000762 mm, SH = 35.0, 2° cam angle interval.

TABLE 6.5 TOLERANCE EFFECTS ON FOLLOWER ACCELERATION

Cam Speed — 1500 RPM,

Size Tolr. = 0.0127 mm, Waviness SD = 0.000762 mm, SM = 35.0

Max. Rate of Deviation = 0.00092 mm/deg.

Motion	Deviation at Peak Acceleration (m/sec.sq.)		RMS Deviation (m/sec.sq.)
	Max. Rise	Max. Return	
1. Parabolic	95.60	94.13	68.50
2. Simple Harmonic	90.47	48.10	50.45
3. Cycloidal	58.49	38.55	18.51
4. Modified Trap.	60.35	60.57	19.20
5. 3-4-5 Poly.	45.61	16.73	18.81
6. 4-5-6-7 Poly.	57.90	38.29	18.42
7. Modified Sine	37.83	61.03	19.25

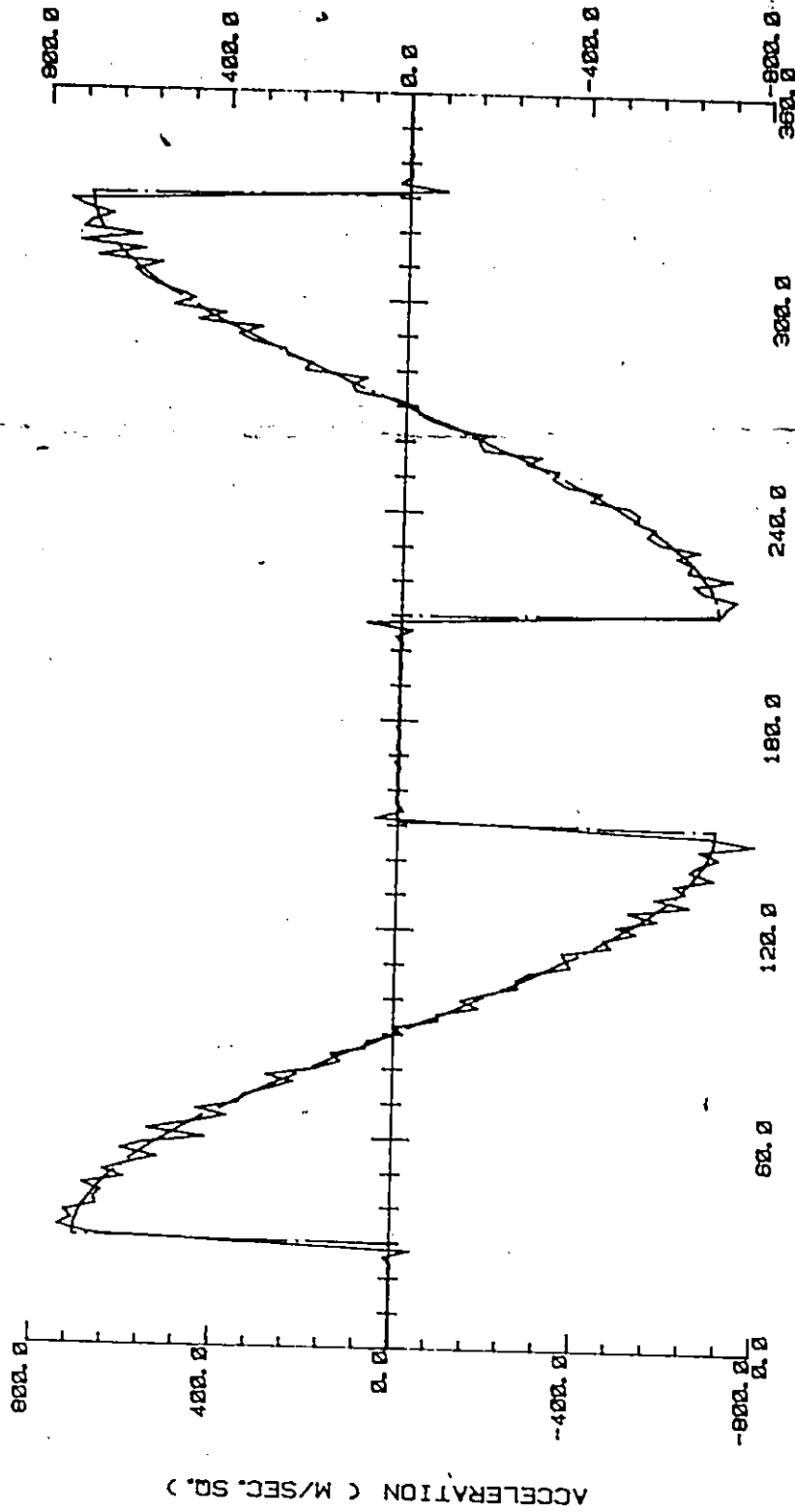
\* SD - Standard Deviation  
SM - Smoothing Parameter

TOLERANCE

ACCELERATION

THEORETICAL ACCEL.

CYCLE - 1

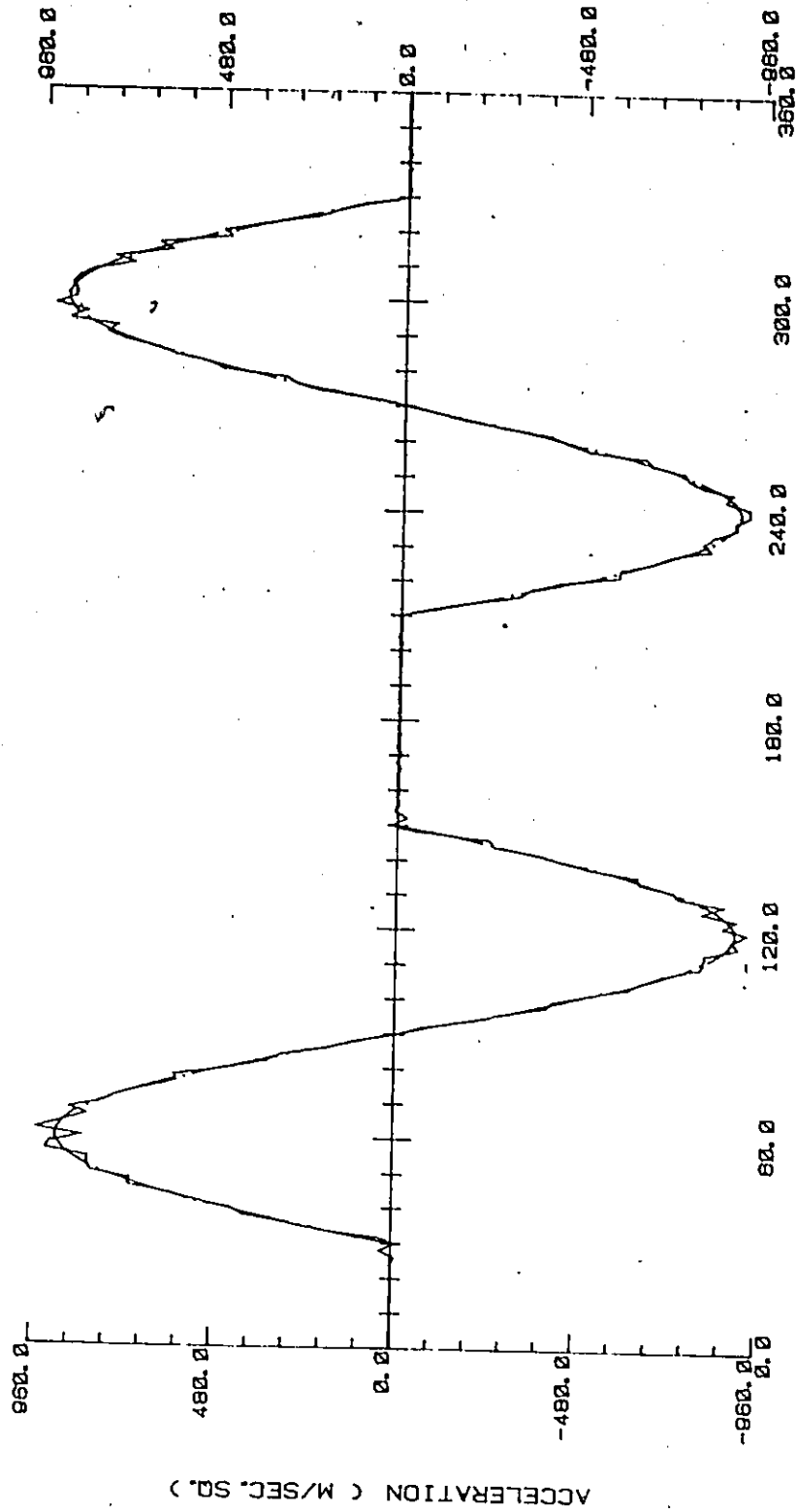


CAM ANGLE ( DEG. )

Fig. 6.6 Tolerance effects on follower acceleration - SH motion, 1500 RPM.

TOLERANCE  
 ACCELERATION  
 THEORETICAL ACCEL.

CYCLE - 1



CAM ANGLE ( DEG. )

Fig. 6.7 Tolerance effects on follower acceleration - Cycloidal motion, 1500 RPM.

### 6.2.3 Comparison Based on the Combined Flexibility and Tolerance Effects

This is the most general, and least studied, case of practical interest. Because of the importance of the combined effects, studies have been made with the simulated lift error at cam speeds of 1500 and 1900 RPM, and also with the inspection lift error data acquired from industry.

The response characteristics at the cam speed of 1500 RPM are given in Tables 6.6 and 6.7, and a few selected plots are shown in Figs. 6.8 to 6.11. The comparison of various motions, with ratings excellent (1) to bad (7), is presented in Table 6.8. It is easily recognized that, for the semi-rigid system under investigation, the combined effects of system dynamics (flexibility) and cam profile errors (tolerance) are significantly greater than for either flexibility or tolerance alone. The dynamic effects on follower acceleration, and the response characteristics at the cam, are discussed under the following five headings.

#### 1. Transient Vibrations

For most motions, the RMS deviation in follower acceleration is increased about four times the deviation due to the kinematic effects of profile errors alone. Deviations at peak acceleration are similarly magnified, because of the superimposed pulse transients generated due to cam profile irregularities. The RMS deviations, for different motions, are not significantly different except for very rough motions. Smooth motions, which have been shown to give very small follower oscillations due to the flexibility



TABLE 6.6 (FLEX. + TOLR.) EFFECTS ON FOLLOWER ACCELERATION

Cam Speed -- 1500 RPM

Size Tolr. = 0.0127 mm, Waviness SD = 0.000762 mm, SM = 35.0

Max. Rate of Deviation = 0.00092 mm/deg.

Motion	Deviation at Peak Acceleration (m/sec.sq.)		RMS Deviation (m/sec.sq.)
	Max. Rise	Max. Return	
1. Parabolic	475.10	386.61	152.46
2. Simple Harmonic	336.68	329.67	106.68
3. Cycloidal	150.99	129.08	75.42
4. Modified Trap.	274.25	179.44	80.93
5. 3-4-5 Poly.	188.01	125.38	77.46
6. 4-5-6-7 Poly.	157.17	133.96	74.36
7. Modified Sine	272.03	184.45	80.73

TABLE 6.7 (FLEX. + TOLR.) EFFECTS AT THE CAM

Cam Speed — 1500 RPM

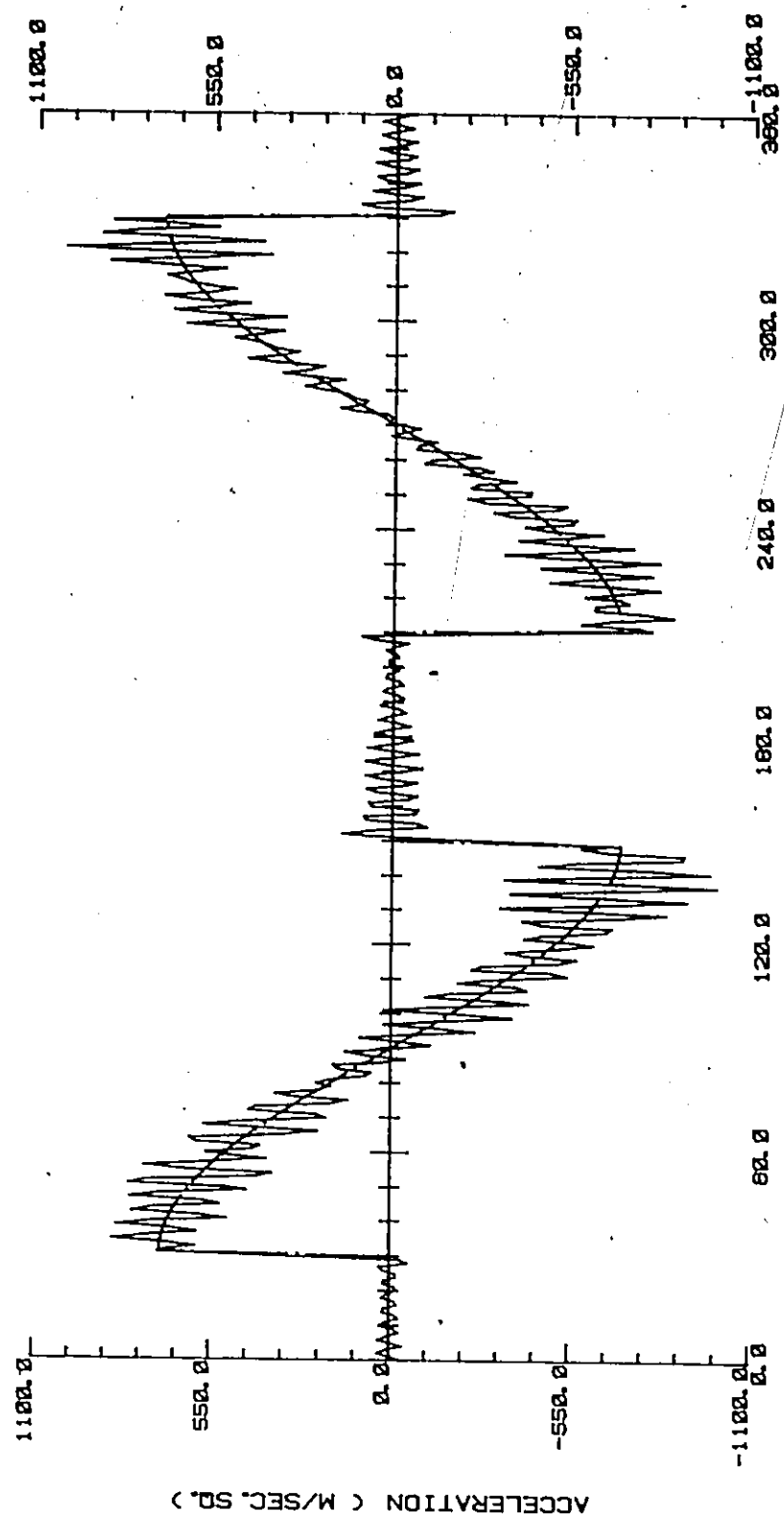
Size Tolr. = 0.0127 mm, Waviness SD = 0.000762 mm, SM = 35.0

Max. Rate of Deviation = 0.00092 mm/deg.

Motion	Contact Force (N)					Max. Cam Torque (N.m)	
	Rise Min.	Rise Max.	Upper Dwell Max.	Return Max.	Return Min.	Rise	Return
1. Parabolic	271.4	991.5	850.3	762.8	297.0	22.0	-16.1
2. Simple Harmonic	420.2	679.9	851.9	636.7	440.6	12.4	-9.7
3. Cycloidal	387.2	840.2	827.6	675.1	349.4	16.4	-12.9
4. Modified Trap.	368.6	851.6	843.1	683.0	338.1	17.7	-13.7
5. 3-4-5 Poly.	427.1	785.2	830.8	644.1	392.9	14.8	-11.7
6. 4-5-6-7 Poly.	310.9	927.5	827.1	728.8	283.6	19.0	-14.8
7. Modified Sine	410.4	732.3	836.2	615.6	426.7	13.7	-10.8

**FLEX. + TOLR.**

— ACCELERATION  
 - - - THEORETICAL ACCEL.      CYCLE - 3



CAM ANGLE ( DEG. )

Fig. 6.8 Combined flexibility and tolerance effects on follower acceleration  
 - SH motion, 1500 RPM.

FLEX. + TOLR.

ACCELERATION

THEORETICAL ACCEL.

CYCLE - 3

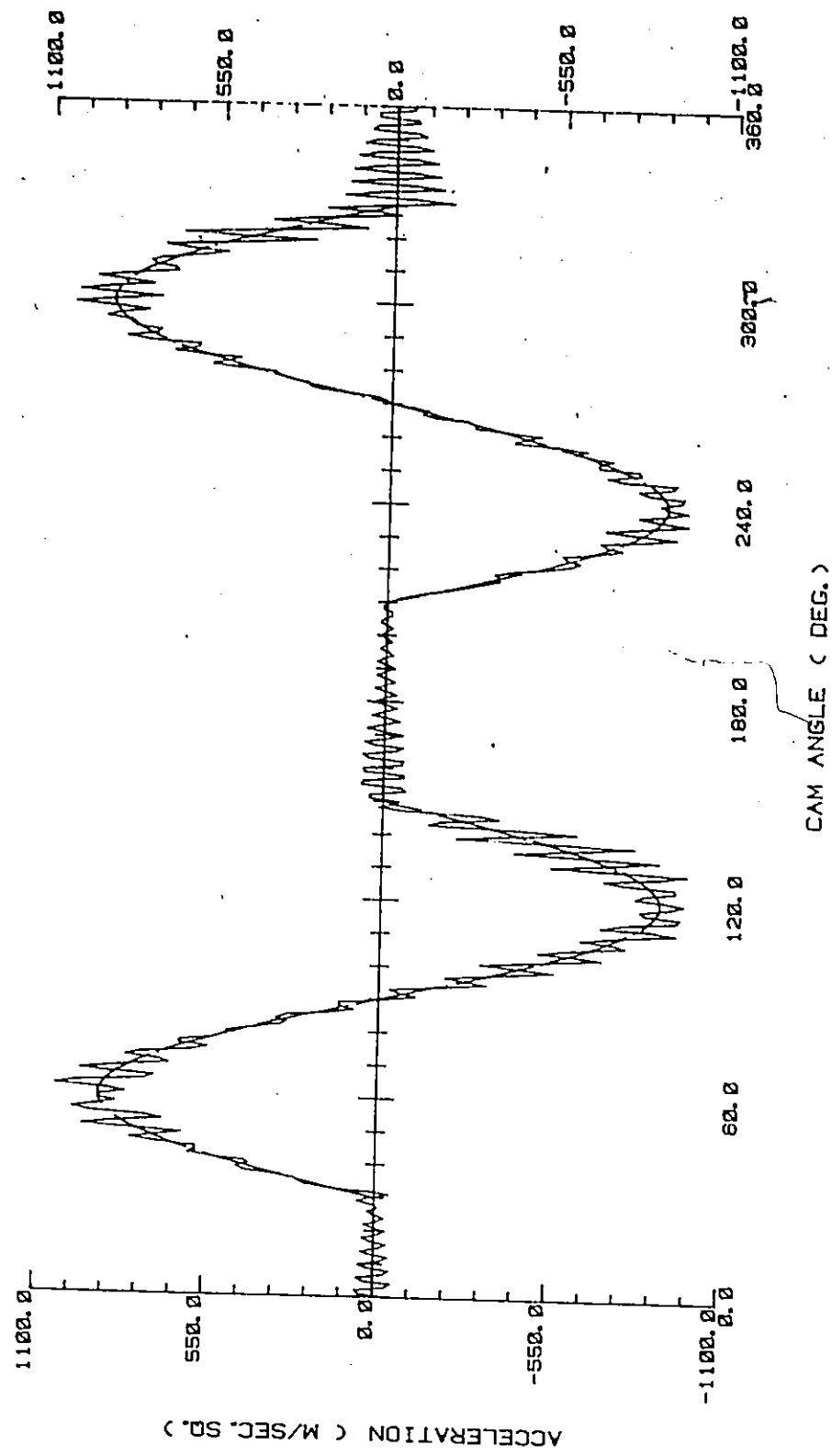
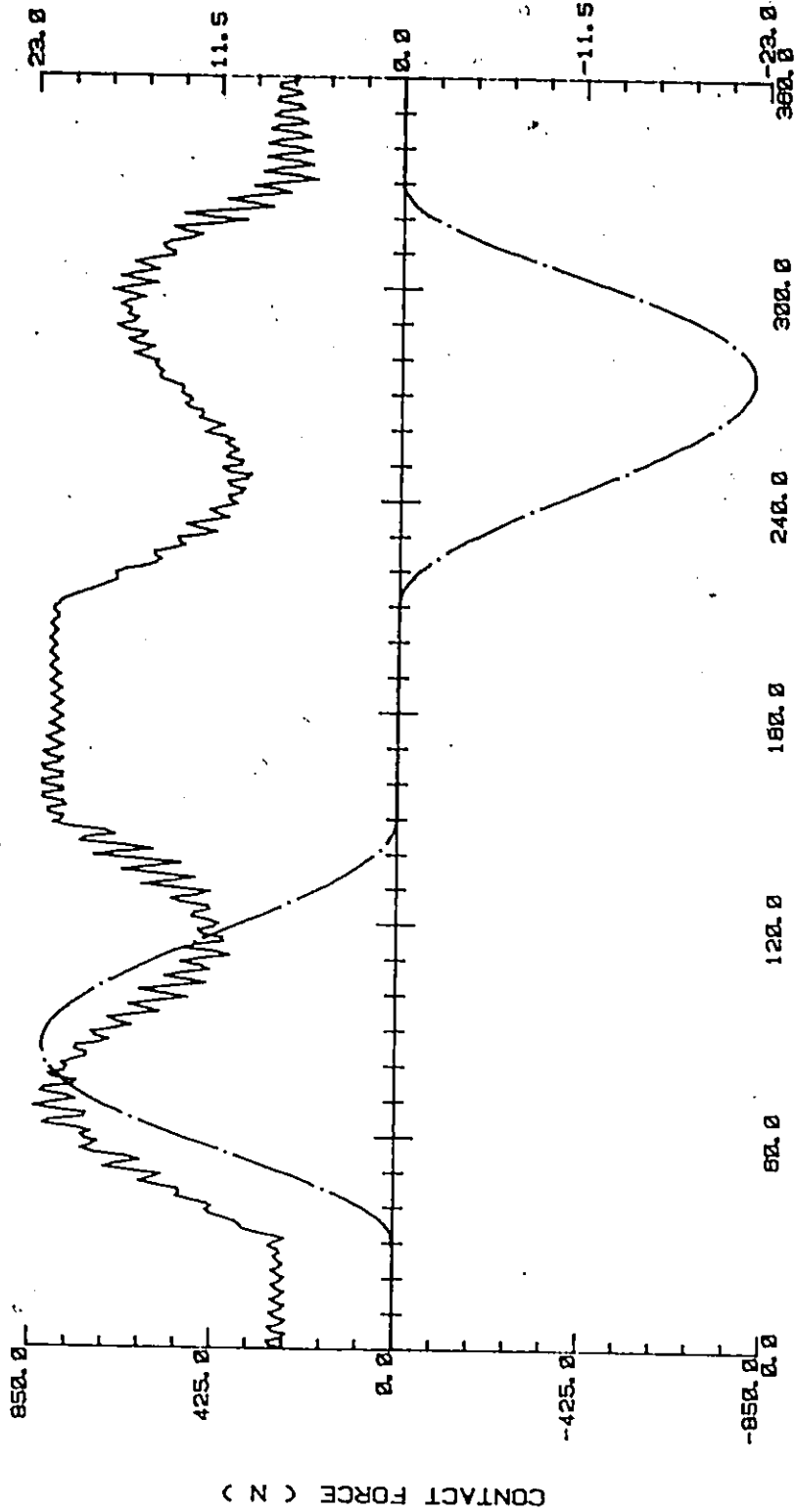


Fig. 6.9 Combined flexibility and tolerance effects on follower acceleration  
- Cycloidal motion, 1500 RPM.

FLEX. + TOLR.

— CONTACT FORCE  
 - - - - - PRESSURE ANGLE

CYCLE - 3



CAM ANGLE ( DEG. )

Fig. 6.10 Combined flexibility and tolerance effects on contact force  
 - Cycloidal motion, 1500 RPM.

FLEX. + TOLR.

— CAM TORQUE  
 - - - CAM SPEED

~ CYCLE - 3

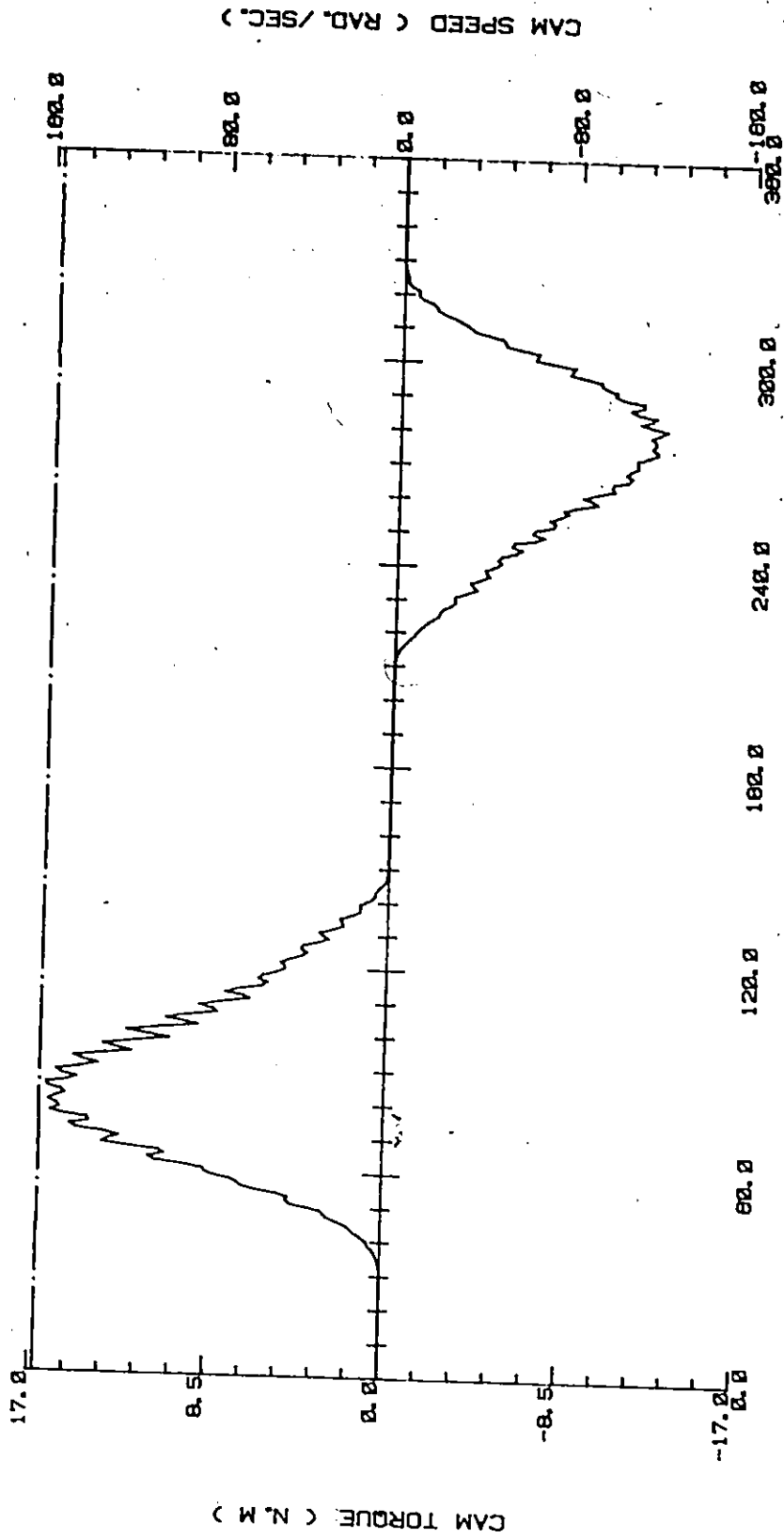


Fig. 6.11 Combined flexibility and tolerance effects on cam torque and speed  
 - Cycloidal motion, 1500 RPM.

TABLE 6.8 COMPARISON OF CAM MOTIONS - (FLEX. + TOLR.) EFFECTS

Cam Speed -- 1500 RPM

Motion	1-Excellent		7-Bad		Torque Requirement
	Transient Vibration	Pitting Tendency	Jump Rise	Return	
1. Parabolic	7	7	7	6	7
2. Simple Harmonic	6	1	2	1	1
3. Cycloidal	2	4	4	4	4
4. Modified Trap.	5	5	5	5	5
5. 3-4-5 Poly.	3	3	1	3	3
6. 4-5-6-7 Poly.	1	6	6	7	6
7. Modified Sine	4	2	3	2	2

effects alone, no longer have that advantage when the cam profile errors are also considered. The effects of manufacturing errors in the cam profile dominate the combined effects of system dynamics and profile errors on the system performance. The vibrational characteristics of the Parabolic and SH motions are much improved because the profile errors result in finite jerks to occur at the transition points to dwells - Fig. 6.8. The response plots of Figs. 6.8 and 6.9 indicate that high amplitude vibrations occur at locations of sharp lift errors. No significant return spring vibrations are observed at this cam speed.

## 2. Pitting Performance - Maximum Contact Force

The Parabolic and SH motions have their pitting performance improved because the maximum contact force on rise is reduced due to the smoothing of sudden jumps in the acceleration. In fact, the SH motion is observed to give the best pitting performance because of its low maximum acceleration (hence low inertia) which occurs at the beginning and the end of rise and return periods. The spring force has its lowest value early on the rise period, and its sum with the inertia force is, therefore, small. The same reasoning holds for the superior pitting performance of the Modified-Sine motion. In the order of increased pitting tendency on the rise portion, the motions are rated as follows:

Simple Harmonic, Modified-Sine, 3-4-5- Poly., Cycloidal,  
Modified-Trapezoidal, 4-5-6-7 Poly., Parabolic.



### 3. Jump Characteristics

The jump characteristics are also changed in a similar way. The Parabolic motion, which was observed to produce jump on the rise due to flexibility effects alone, has now a significant contact force available and a much less tendency to jump. The SH motion is observed to give the best jump behaviour, indicated by the greatest minimum contact force on return. This is due to the fact that the vibration amplitudes in the beginning of the return have been greatly reduced due to the smoothing effect of profile errors at the transition points - Fig. 6.8. However, the minimum contact force on the rise has reduced due to increased vibrations at the location of the maximum deceleration on the rise period caused by the sharp profile errors there (Fig. 6.8). Consequently, the jump is more likely to occur on the rise period. The 3-4-5 Polynomial motion also has good jump characteristics because of its low peak acceleration and small vibrations.

In the order of increased jump tendency, the motions are listed as follows:

Simple Harmonic, Modified-Sine, 3-4-5 Poly., Cycloidal,  
Modified-Trapezoidal, Parabolic, 4-5-6-7 Poly.

### 4. Maximum Torque Requirements

The maximum torque on rise and return is increased for most motions because of the increased maximum contact force. The torque on return for the Parabolic motion is much decreased because of a significant reduction in the maximum contact force. The motions are

rated according to the cam torque requirements as follows:

Simple Harmonic, Modified-Sine, 3-4-5 Poly., Cycloidal,  
Modified-Trapezoidal, 4-5-6-7 Poly., Parabolic.

#### 5. Cam Speed Variations

The cam speed fluctuations are observed to be less than 0.3% (Fig. 6.11) and for the Parabolic motion the deviation is reduced to less than 1.9% because of the smoothing action of the profile errors.

#### Comparison of Cam Motions Based on Combined Flexibility and Tolerance Effects - at 1900 RPM

The comparison of motions based on the combined effects of system dynamics and cam profile errors, at a cam speed of 1900 RPM, is given in Tables 6.9 and 6.10. The Parabolic motion gives rise to jump because of high vibrations occurring at the transition points.

#### 1. Transient Vibrations

The RMS deviation in acceleration is increased, but again it is not significantly different for various smooth motions. But since the theoretical maximum acceleration also increases, the relative increase is not very high. The high value of acceleration vibration for the Parabolic motion result from jump.

The response characteristics at the cam are greatly changed at this high speed.

TABLE 6.9 (FLEX. + TOLR.) EFFECTS ON FOLLOWER ACCELERATION

Cam Speed -- 1900 RPM

Size Tolr. = 0.0127 mm, Waviness SD = 0.000762 mm, SM = 35.0

Max. Rate of Deviation = 0.00092 mm/deg.

Motion	Deviation at Peak Accel. (m/sec.sq.)		Theoretical Max. Accel. (m/sec.sq.)	RMS Deviation (m/sec.sq.)
	Max. Rise	Max. Return		
1. Parabolic	983.62	848.84	916.94	420.53
2. Simple Harmonic	317.54	499.73	1131.23	243.18
3. Cycloidal (IRS=0)	363.74	214.81	1440.33	143.39
	364.37	213.89	1440.33	143.19
4. Modified Trap.	431.63	299.09	1120.53	149.27
5. 3-4-5 Poly.	374.31	257.66	1323.28	145.37
6. 4-5-6-7 Poly.	362.38	215.79	1722.21	145.62
7. Modified Sine	263.37	203.81	1267.20	149.54

TABLE 6.10 (FLEX. + TOLR.) EFFECTS AT THE CAM

Cam Speed -- 1900 RPM

Size Tolr. = 0.0127 mm, Waviness SD = 0.000762 mm, SM = 35.0

Max. Rate of Deviation = 0.00092 mm/deg.

Motion	Contact Force (N)					Max. Cam Torque (N.m)	
	Rise		Upper Dwell	Return		Rise	Return
	Min.	Max.	Max.	Max.	Min.		
1. Parabolic	0.0	1352.7	1038.0	1062.8	0.0	28.2	-21.2
2. Simple Harmonic	322.3	970.3	861.0	801.7	187.1	16.4	-11.8
3. Cycloidal (IRS=0)	137.6	1178.8	894.9	901.8	122.0	22.4	-15.1
	165.6	1157.2	887.8	870.0	143.2	22.2	-14.9
4. Modified Trap.	169.9	1165.0	880.6	816.7	122.2	23.9	-16.2
5. 3-4-5 Poly.	205.7	1082.5	894.2	870.0	174.4	19.7	-13.3
6. 4-5-6-7 Poly.	30.2	1331.6	899.4	983.7	16.8	27.0	-18.4
7. Modified Sine	253.8	1002.8	894.0	834.1	231.1	17.6	-12.3

## 2. Pitting Performance - Maximum Contact Force

The maximum contact force occurs on the lower flank of rise for all the motions, because at high speed the inertia force is increased. The motions are rated in the order of increasing maximum contact force as follows:

Simple Harmonic, Modified-Sine, 3-4-5 Poly., Modified-Trapezoidal, Cycloidal, 4-5-6-7 Poly., Parabolic.

Very high contact forces occur with the Parabolic motion because of jump, and for the 4-5-6-7 Polynomial motion because of high inertia.

## 3. Jump Characteristics

The minimum contact force on rise and return decreases for all motions because of the high inertia force and increased vibrations. For the Parabolic motion, the contact force reduces to zero on both the rise and return periods, and jump is indicated as shown in Fig. 6.12. The follower jump results in significant camshaft vibrations, and maximum speed fluctuations of the order of 3% occur during the cycle. Very small contact force is available on both the rise and return periods for the 4-5-6-7 Polynomial cam, and it will give rise to jump just above this speed. The motions are rated on the basis of jump criteria as follows:

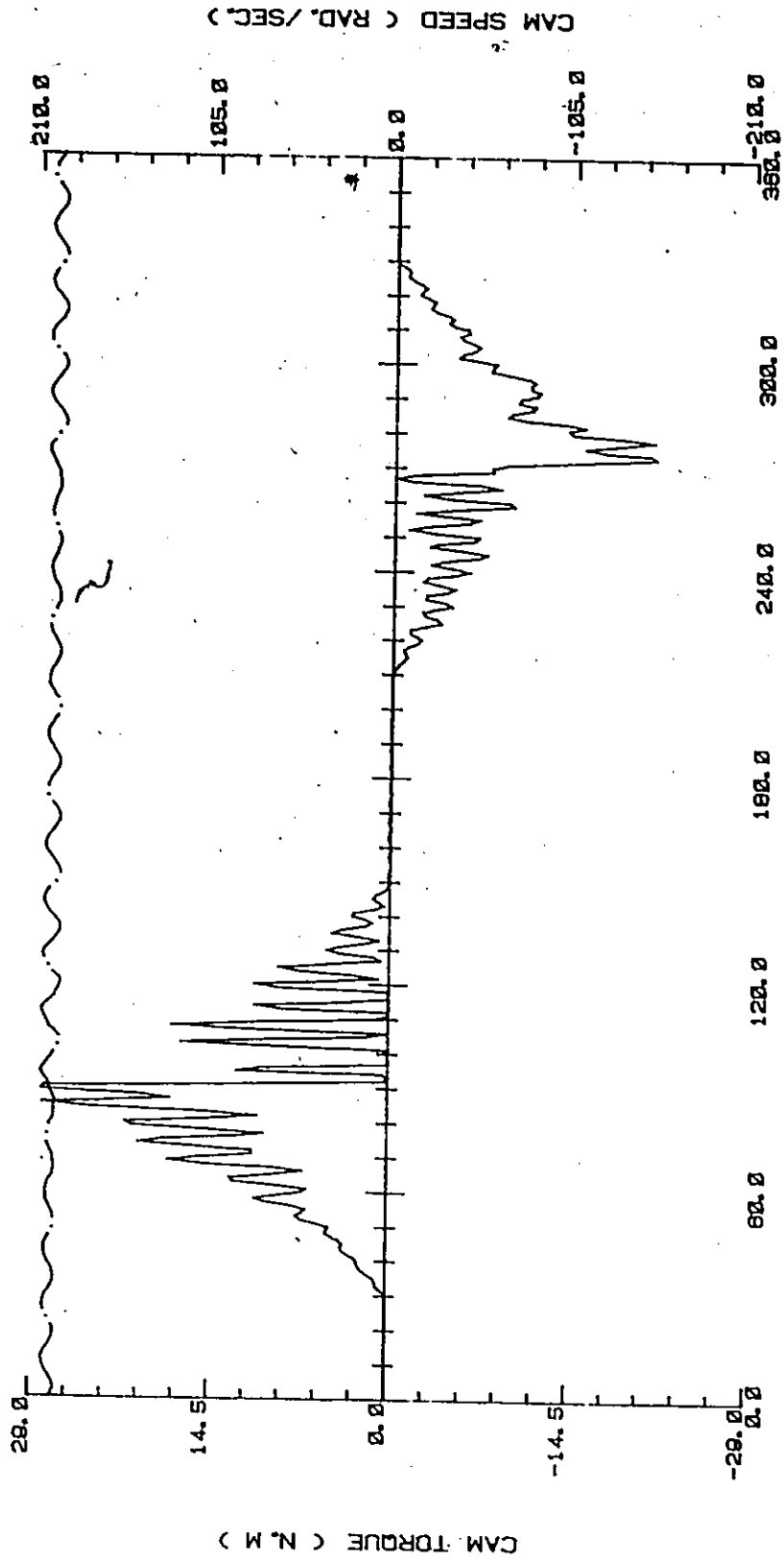
Modified-Sine, Simple Harmonic, 3-4-5 Poly., Modified-Trapezoidal, Cycloidal, 4-5-6-7 Poly., Parabolic.

However, there is little to choose between the Cycloidal and Modified-Trapezoidal motions.

FLEX. + TOLR.

— CAM TORQUE  
 - - - CAM SPEED

CYCLE - 3



CAM ANGLE ( DEG. )

Fig. 6.12 Combined flexibility and tolerance effects on cam torque and speed  
 - Parabolic motion, 1900 RPM.

TABLE 6.11 COMPARISON OF CAM MOTIONS - (FLEX. + TOLR.) EFFECTS

Cam Speed — 1900 RPM

1-Excellent

7-Bad

Motion	Transient Vibration	Pitting Tendency	Jump		Torque Requirement
			Rise	Return	
1. Parabolic	5	7	7 (YES)	6 (YES)	7
2. Simple Harmonic	4	1	1	2	1
3. Cycloidal	1	4	5	4	4
4. Modified Trap.	3	3	4	4	5
5. 3-4-5 Poly.	2	5	3	3	3
6. 4-5-6-7 Poly.	2	6	6	5	6
7. Modified Sine	3	2	2	1	2

#### 4. Maximum Torque Requirements

The maximum torque values are also greatly increased because of higher velocity and high contact forces. The motions are rated according to increasing torque requirements as follows:

Simple Harmonic, Modified-Sine, 3-4-5 Poly., Cycloidal,  
Modified-Trapezoidal, 4-5-6-7 Poly., Parabolic.

Although the return spring vibrations do not change the acceleration response much, the dynamic characteristics at the cam are significantly changed and the effects are different for different cam motions. The results for  $IRS=0$  (no spring vibrations) are given for the Cycloidal motion during the third cycle of cam rotation and indicate significant differences in the contact force values - Table 6.10. The pitting and jump tendencies increase, and more cam torque is required when spring vibrations are accounted for. These differences were not observed at the lower cam speed of 1500 RPM.

The comparison of cam motions at the cam speed of 1900 RPM - Table 6.11 indicates a little change in the ratings based on different performance criteria, but still the SH and Modified-Sine motions remain as superior choices. The 3-4-5 Polynomial motion also has good high-speed performance. The Parabolic and 4-5-6-7 Polynomial motions are poor choices at high speeds.



Comparison of Cam Motions Based on the Combined Flexibility and Tolerance Effects - Inspection Lift Error

Fig. 6.13 shows a plot of the lift error produced by an actual cam profile. The lift error data was obtained from Eonic, Inc., Detroit, in tabular form for  $1^\circ$  cam angle interval. The discrete data has been smoothed by spline interpolation to obtain a continuous lift error function. The plot indicates sharp high frequency errors in the lift function.

To investigate the dynamic effects, the following input data and system parameters were changed to suit the particular rise and return periods of the measured cam so as to keep the maximum acceleration and contact force to reasonable values.

Cam Angle Interval(deg.)	Lower Dwell	Rise	Upper Dwell	Return	Lower Dwell
	0-70	70-140	140-220	220-290	290-360
	Rise				: 0.0127 m
	Return Spring Stiffness, $K_{rs}$				: 3.15E+4 N/m
	Smoothing Parameter, SM				: 0.0
	Cam Speed				: 1200 RPM

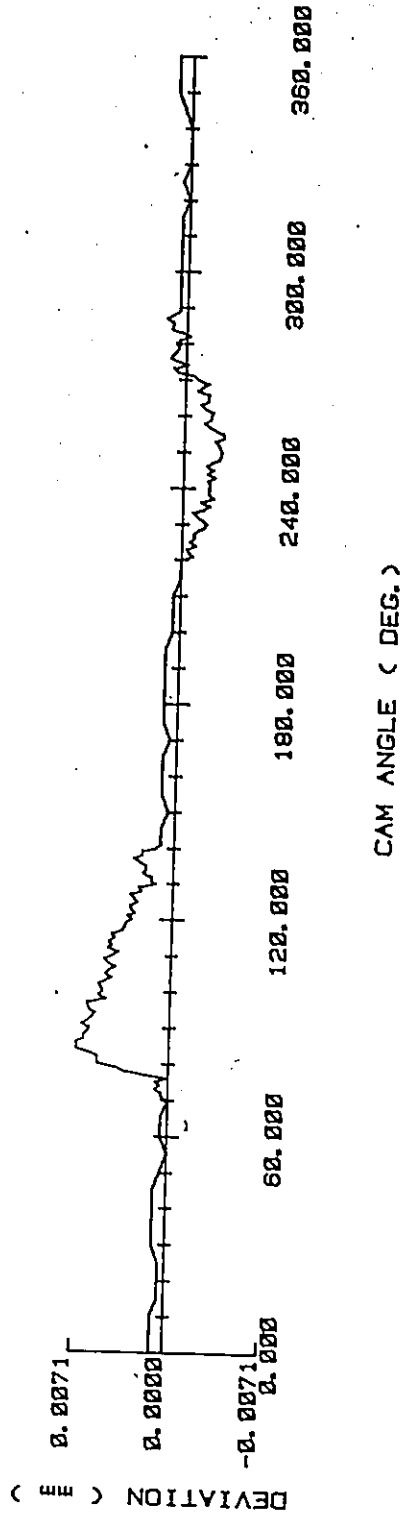


Fig. 6.13 Inspection lift error [Eonic, Inc., Detroit].

The combined effects of system dynamics and inspection lift error are given in Tables 6.12 and 6.13 and the response characteristics for the Cycloidal motion are shown in Figs. 6.14 to 6.16. The observed dynamic behaviour is discussed under the following four headings.

#### 1. Transient Vibrations

Vibrations are observed to occur at the follower system natural frequency - Fig. 6.14. The observed frequency and the calculated frequency (14410 rad/sec) match quite closely. The amplitude of vibrations is high because of the sharp high frequency profile errors. For various smooth motions, the RMS deviations in acceleration are not significantly different. For the Parabolic and Simple Harmonic motions, the vibrations are only marginally increased from those due to flexibility alone.

#### 2. Pitting Performance - Maximum Contact Force

The maximum contact force is significantly increased because of high vibrations, and it occurs on the lower flank of the rise - Fig. 6.15, except for the SH motion, where it occurs on the upper dwell due to the sudden jump in acceleration at the transition. The motions are rated according to the maximum contact force as follows:

Simple Harmonic, Modified-Sine, Parabolic, 3-4-5 Poly.,  
Cycloidal, Modified-Trapezoidal, 4-5-6-7 Poly.

TABLE 6.12 (FLEX. + TOLR.) EFFECTS ON FOLLOWER ACCELERATION

-- Inspection Lift Error

Cam Speed -- 1200 RPM

Max. Rate of Deviation = 0.001825 mm/deg. , SM = 0.0

Motion	Deviation at Peak Acceleration (m/sec.sq.)		RMS Deviation (m/sec.sq.)
	Max. Rise	Max. Return	
1. Parabolic	971.99	621.24	228.59
2. Simple Harmonic	551.78	342.27	196.62
3. Cycloidal	346.99	320.52	151.91
4. Modified Trap.	418.53	325.07	145.40
5. 3-4-5 Poly.	407.82	310.38	149.83
6. 4-5-6-7 Poly.	317.40	376.52	150.16
7. Modified Sine	386.96	342.21	145.18

TABLE 6.13 (FLEX. + TOLR.) EFFECTS AT THE CAM

-- Inspection Lift Error

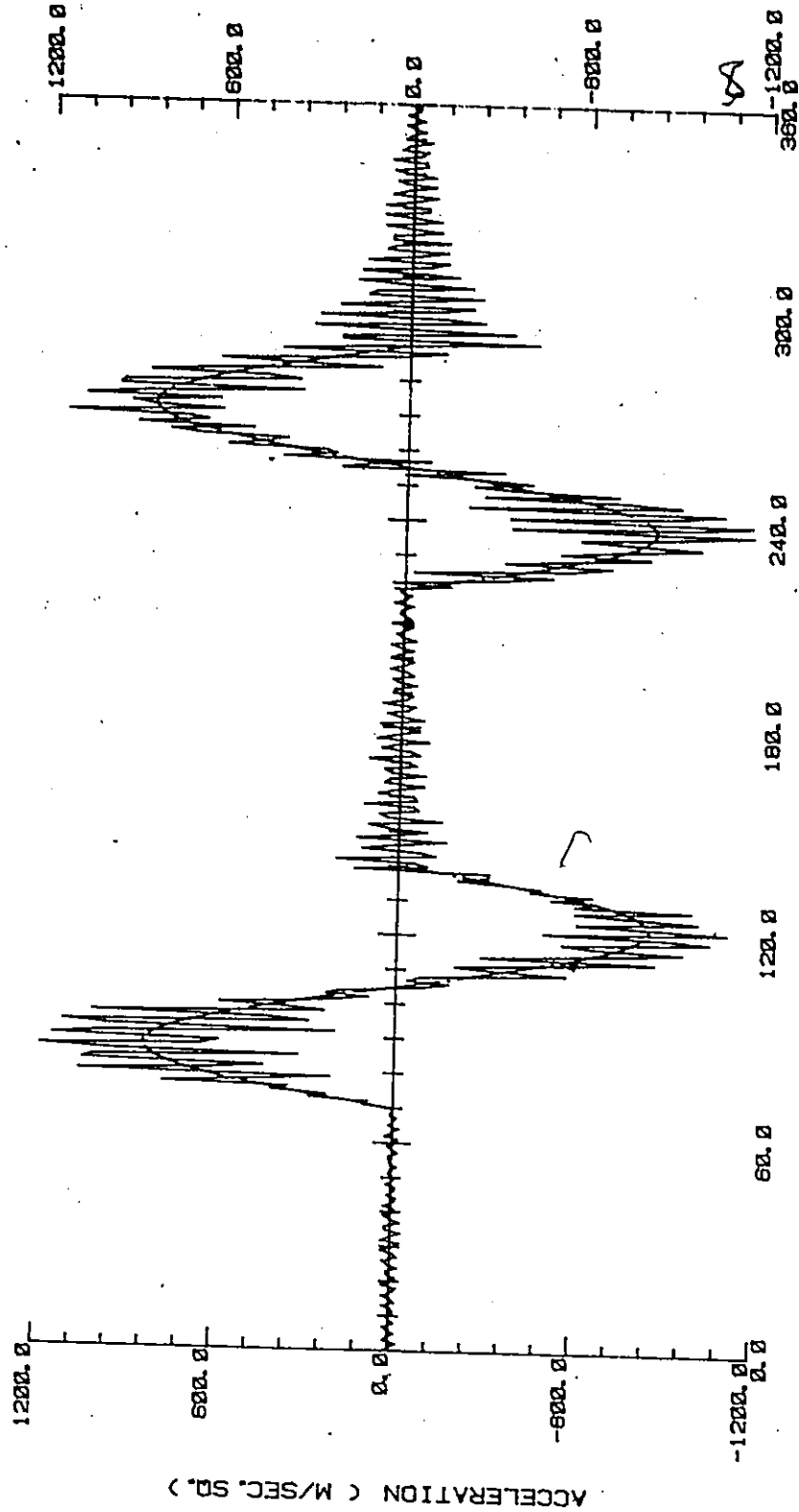
Cam Speed -- 1200 RPM

Max. Rate of Deviation = 0.001825 mm/deg. , SM = 0.0

Motion	Contact Force (N)					Max. Cam Torque (N.m)	
	Rise Min.	Rise Max.	Upper Dwell Max.	Return Max.	Return Min.	Rise	Return
1. Parabolic	116.6	964.1	955.2	861.9	351.2	18.7	-15.4
2. Simple Harmonic	464.1	869.2	1012.2	750.1	373.8	12.4	-9.7
3. Cycloidal	372.9	1051.1	872.0	839.2	300.2	18.1	-13.0
4. Modified Trap.	380.6	1077.0	870.7	770.8	347.2	17.7	-13.6
5. 3-4-5 Poly.	413.3	984.5	867.0	804.9	346.2	16.3	-11.9
6. 4-5-6-7 Poly.	293.3	1120.5	876.3	883.4	226.6	20.2	-14.8
7. Modified Sine	456.9	924.8	864.2	784.9	392.0	14.8	-11.0

FLEX. + TOLR.  
 ACCELERATION  
 THEORETICAL ACCEL.

CYCLE - 3



CAM ANGLE ( DEG. )

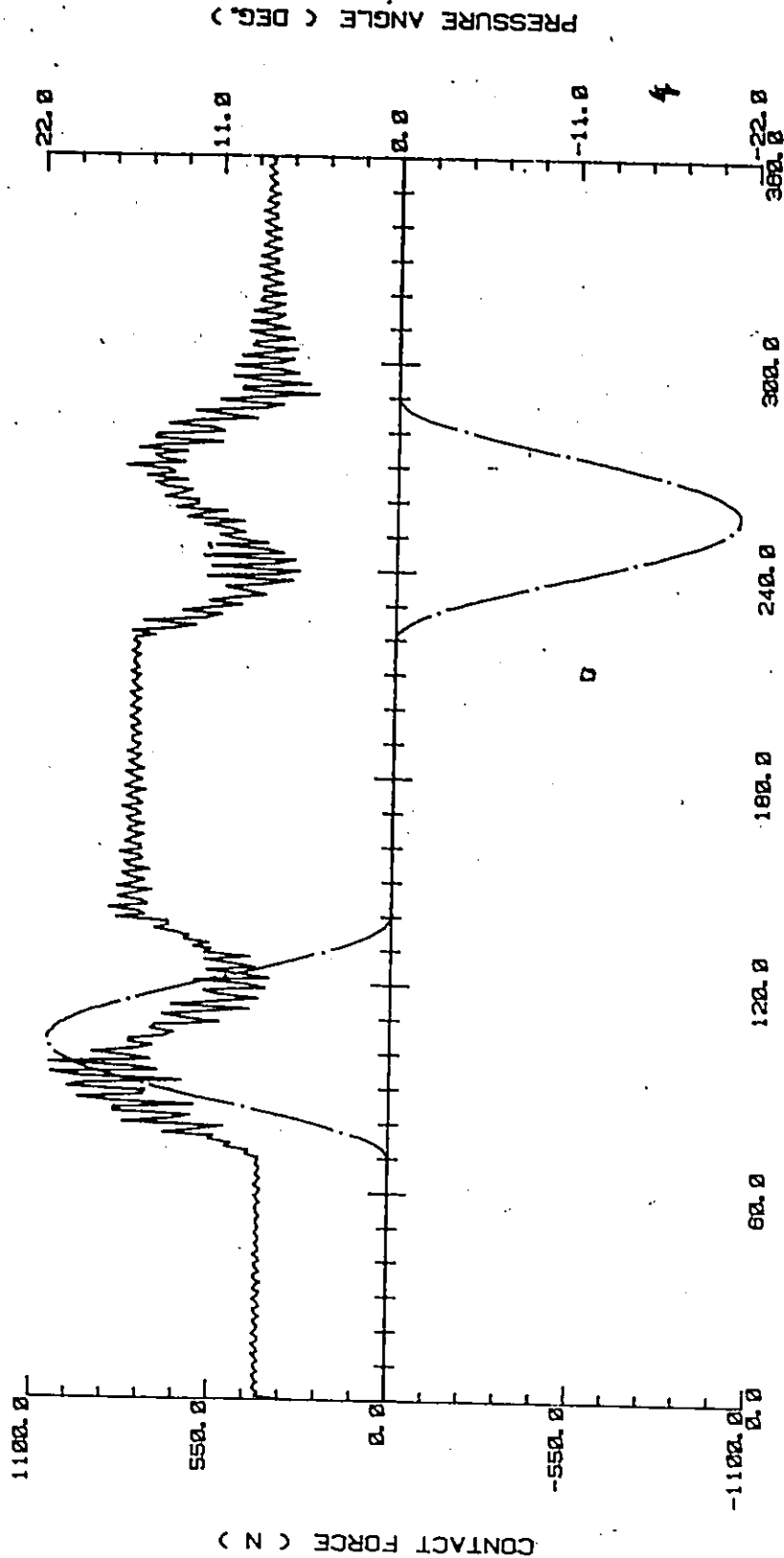
Fig. 6.14 Combined flexibility and tolerance effects on follower acceleration - Inspection lift error, Cycloidal motion, 1200 RPM.

FLEX. + TOLR.

— CONTACT FORCE

- - - - - PRESSURE ANGLE

CYCLE - 3



CAM ANGLE ( DEG. )

Fig. 6.15 Combined flexibility and tolerance effects on contact force  
- Inspection lift error, Cycloidal motion, 1200 RPM.

FLEX. + TOLR.

— CAM TORQUE  
 — CAM SPEED

CYCLE - 3

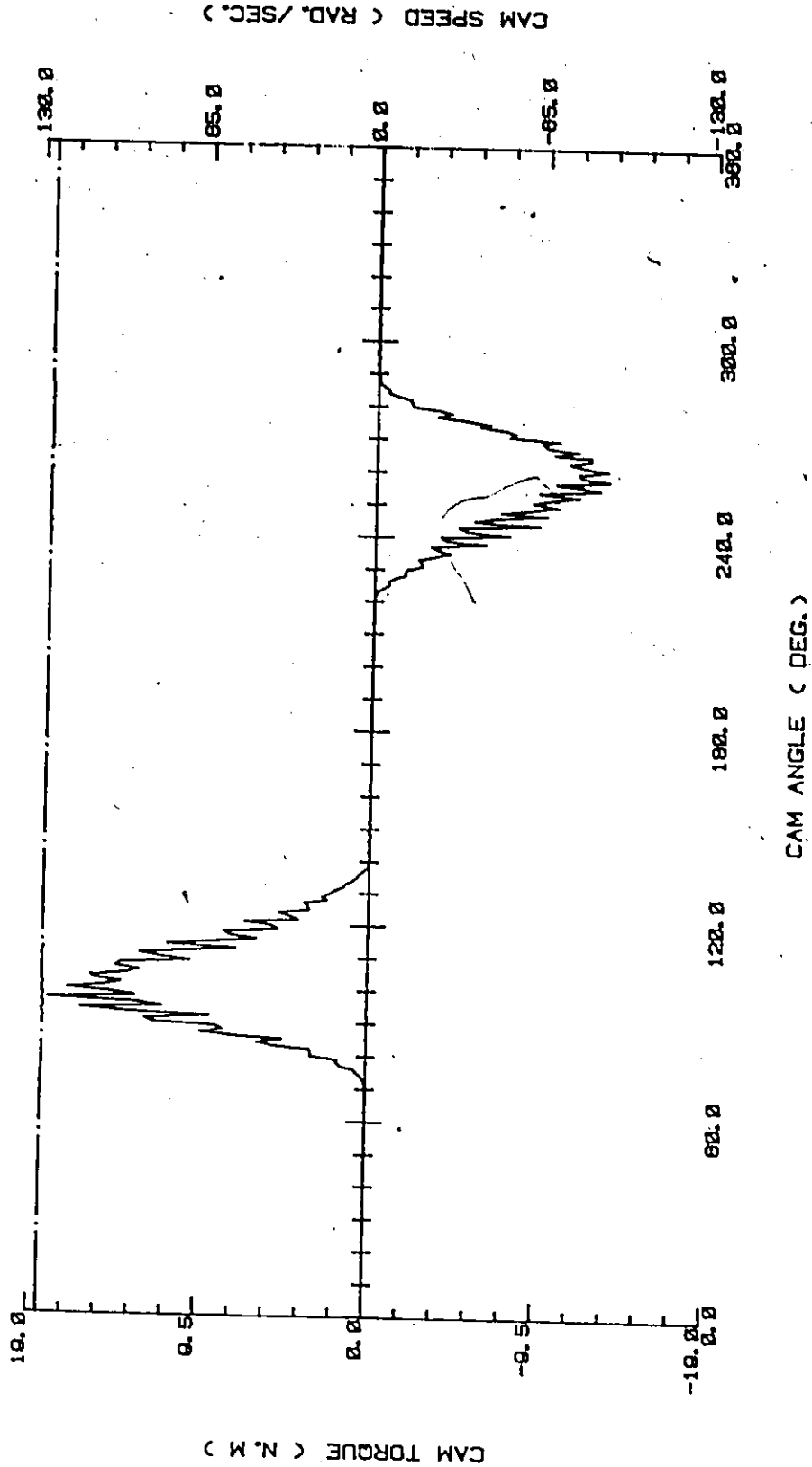


Fig. 6.16 Combined flexibility and tolerance effects on cam torque  
 - Inspection lift error, Cycloidal motion, 1200 RPM.



TABLE 6.14 COMPARISON OF CAM MOTIONS - (FLEX. + TOLR.) EFFECTS

- Inspection Lift Error

Cam Speed -- 1200 RPM

Max. Rate of Deviation = 0.001825 mm/deg. , SM = 0.10

1-Excellent 7-Bad

Motion	Transient Vibration	Pitting Tendency	Jump		Torque Requirement
			Rise	Return	
1. Parabolic	7	3	7	3	6
2. Simple Harmonic	6	1	1	2	1
3. Cycloidal	5	5	5	6	5
4. Modified Trap.	2	6	4	4	4
5. 3-4-5 Poly.	3	4	3	5	3
6. 4-5-6-7 Poly.	4	7	6	7	7
7. Modified Sine	1	2	2	1	2

### 3. Jump Characteristics

The available minimum contact force reduces significantly due to high vibration amplitudes. In order of increased jump tendency, the motions are listed as follows:

Modified-Sine, Simple Harmonic, 3-4-5 Poly., Modified-Trapezoidal, Cycloidal, 4-5-6-7 Poly., Parabolic.

### 4. Maximum Torque Requirements

The maximum torque values are also increased and the motions are rated as follows:

Simple Harmonic, Modified-Sine, 3-4-5 Poly., Modified-Trapezoidal, Cycloidal, Parabolic, 4-5-6-7 Poly.

Speed fluctuations are below 0.5% for most motions and less than 2.4% for the Parabolic motion.

The Simple Harmonic and the Modified-Sine are observed to be the superior motions, with the latter giving the best overall performance based on both the vibrational behaviour and the dynamic characteristics at the cam - Table 6.14.

### Comparison of Cam Motions Based on Combined Flexibility and Tolerance Effects - Simulated Lift Error at 1° Cam Angle Intervals

As has already been remarked in Section 5.3, the simulation of lift error with a cam incremental angle of 1° gives a closer approximation to the waviness frequency observed in inspection lift error - Fig. 6.13. The simulated lift error plot is given in Fig. 6.17, and its dynamic effects on the follower acceleration and

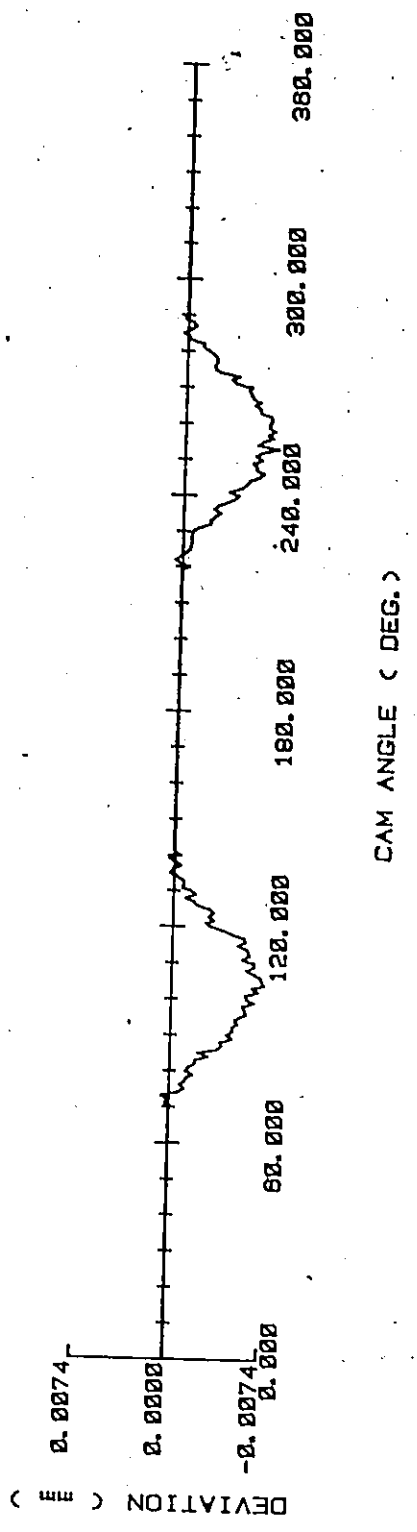


Fig. 6.17 Simulated lift error function - Size Tolr. = 0.0068 mm, Waviness SD = 0.000508 mm, SM = 5.0, 1° cam angle interval.

TABLE 6.15 (FLEX. + TOLR.) EFFECTS ON FOLLOWER ACCELERATION

- Simulated Lift Error at 1° Cam Angle Intervals

Cam Speed — 1200 RPM

Size Tolr. = 0.00680 mm, Waviness SD = 0.000508 mm, SM = 5.0

Max. Rate of Deviation = 0.001615 mm/deg.

Motion	Deviation at Peak Accel. (m/sec.sq.)		Theoretical Max. Accel. (m/sec.sq.)	RMS Deviation (m/sec.sq.)
	Max. Rise	Max. Return		
1. Parabolic	543.29	696.86	537.44	220.28
2. Simple Harmonic	592.42	499.52	663.04	207.35
3. Cycloidal	325.18	598.33	843.37	167.18
4. Modified Trap.	402.65	575.20	656.77	169.96
5. 3-4-5 Poly.	343.23	617.45	775.61	174.85
6. 4-5-6-7 Poly.	327.47	481.81	1008.87	159.80
7. Modified Sine	320.32	581.21	742.66	172.58

FLEX. + TOLR.

ACCELERATION

THEORETICAL ACCEL.

CYCLE - 3

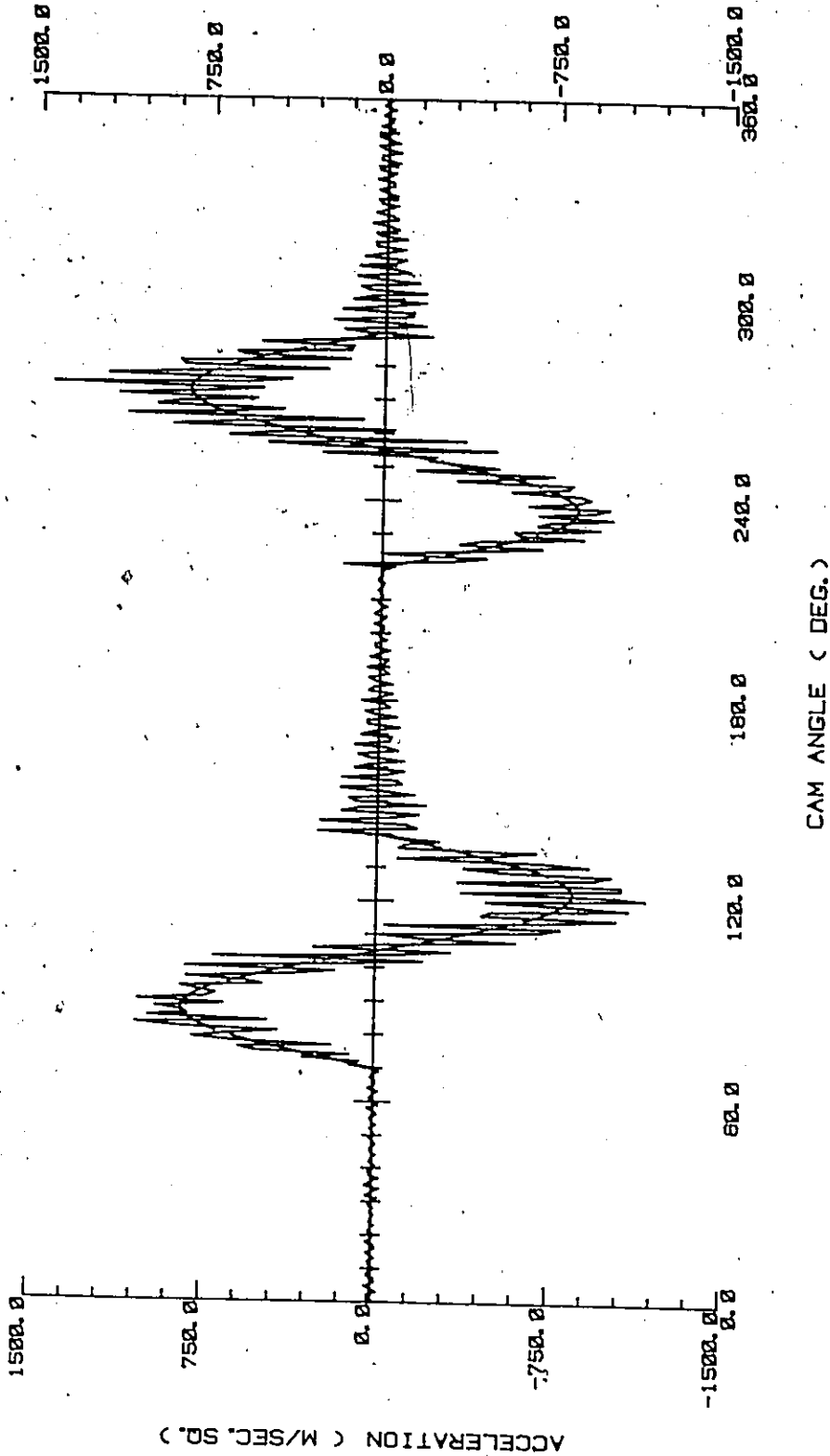


Fig. 6.18 Combined flexibility and tolerance effects on follower acceleration - simulated lift error at 1° cam angle intervals.

TABLE 6.16 (FLEX. + TOLR.) EFFECTS AT THE CAM

-Simulated Lift Error at 1° Cam Angle Intervals

Cam Speed -- 1200 RPM

Size Tolr. = 0.00680 mm , Waviness SD = 0.00508 mm , SM = 5.0

Max. Rate of Deviation = 0.001615 mm/deg.

Motion	Contact Force (N)					Max. Cam Torque (N.m)	
	Rise Min.	Rise Max.	Upper Dwell Max.	Return Max.	Return Min.	Rise	Return
1. Parabolic	347.4	1087.8	979.0	960.0	253.6	19.9	-17.1
2. Simple Harmonic	415.8	886.3	943.7	764.0	371.0	13.2	-11.3
3. Cycloidal	345.2	1019.7	890.4	920.7	374.1	19.3	-14.5
4. Modified Trap.	370.1	1094.9	901.0	860.9	334.4	19.8	-15.1
5. 3-4-5 Poly.	378.6	988.9	892.4	908.2	395.5	17.9	-13.2
6. 4-5-6-7 Poly.	279.1	1095.9	884.1	931.5	318.4	21.8	-16.5
7. Modified Sine	404.4	952.6	896.4	862.1	401.9	16.3	-12.1

TABLE 6.17 COMPARISON OF CAM MOTIONS - (FLEX. + TOLR.) EFFECTS

-Simulated Lift Error at 1° Cam Angle Intervals

Cam Speed -- 1200 RPM

Size Tolr. = 0.00680 mm , Waviness SD = 0.00508 mm , SM = 5.0

Max. Rate of Deviation = 0.001615 mm/deg.

1-Excellent 7-Bad

Motion	Transient Vibration	Pitting Tendency	Jump		Torque Requirement
			Rise	Return	
1. Parabolic	7	5	5	7	6
2. Simple Harmonic	6	1	1	4	1
3. Cycloidal	2	4	6	3	4
4. Modified Trap.	3	6	4	5	5
5. 3-4-5 Poly.	5	3	3	2	3
6. 4-5-6-7 Poly.	1	7	7	6	7
7. Modified Sine	4	2	2	1	2

the characteristics at the cam are given in Tables 6.15 and 6.16. A typical acceleration response for the Cycloidal motion is shown in Fig. 6.18.

The results in Table 6.15 show high transient vibration amplitudes of the order observed with the inspection lift error - Table 6.11. The higher deviation at peak acceleration on the return period occurs due to the presence of sharp profile errors in that portion. The dynamic characteristics at the cam - Table 6.16 are also similarly affected. The comparison of cam motions given in Table 6.17 indicates the similar rating of motions, with the Simple Harmonic and Modified-Sine motions giving superior overall performance.

### 6.3 Effect of Varying the Cam Profile Error

Figs. 6.19a and 6.19b show the simulated lift error functions for different values of the smoothing parameter - SM, and Fig. 6.19c shows the lift error function when the size tolerance is increased, with the smoothing parameter  $SM = 35.0$ . It is important to note that because of the scale, the waviness error cannot be distinguished in Fig. 6.19c, but it is the same as that in Fig. 6.5. The waviness standard deviation is fixed as  $0.000762$  mm. The effects of varying the smoothness (SM), with the size tolerance fixed at  $0.127E-4$  m and of changing the size tolerance, with the smoothness parameter constant, are tabulated in Tables 6.18 and 6.19. Fig. 6.20 shows the increase in the levels of vibrations with a rougher profile corresponding to  $SM=10.0$ . All previous results correspond to  $SM=35.0$ .



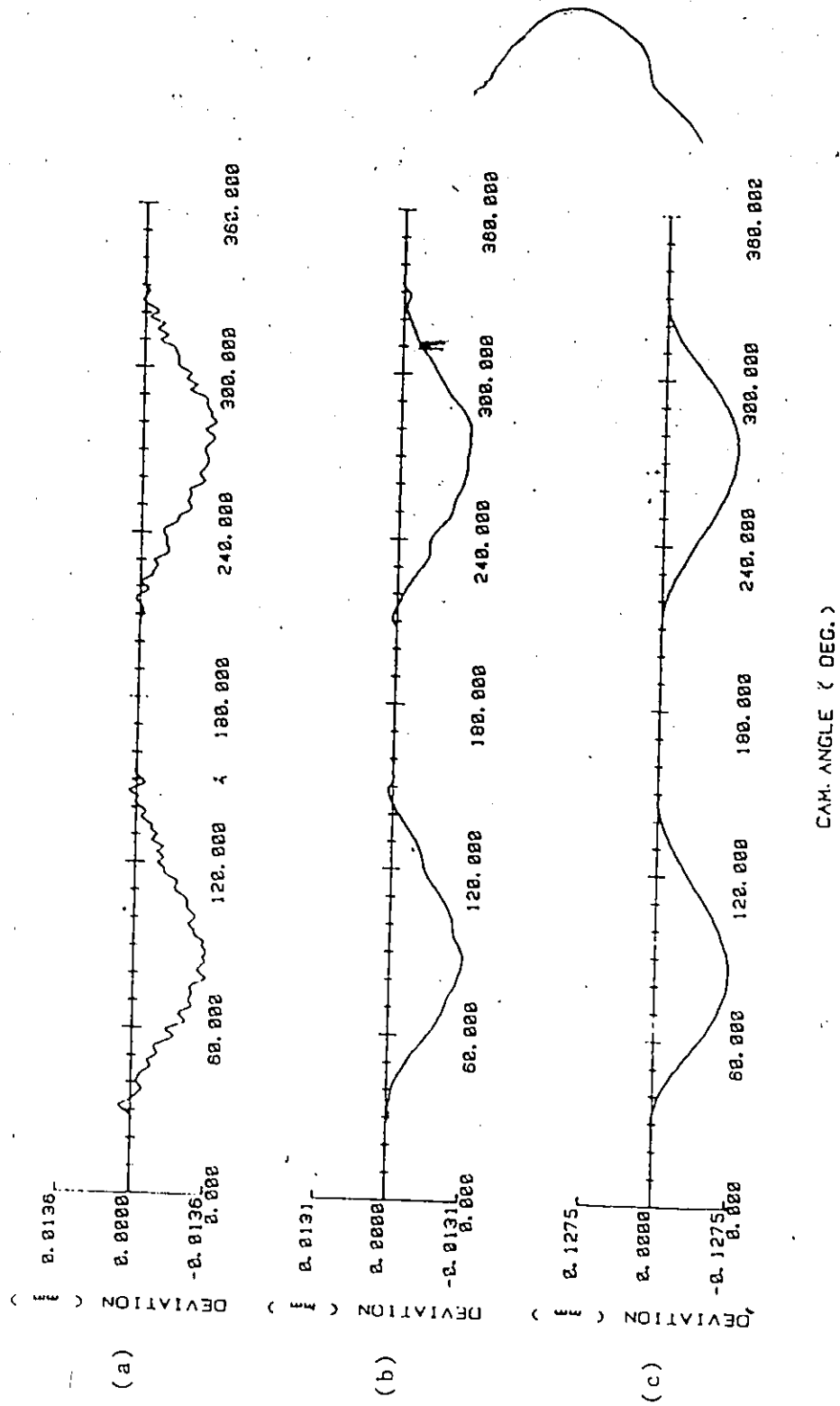


Fig. 6.19 Simulated lift error functions at 2° cam angle intervals  
 (a) Size Tolr. = 0.0127 mm, Waviness SD = 0.000762 mm, SM = 10.0.  
 (b) Size Tolr. = 0.0127 mm, Waviness SD = 0.000762 mm, SM = 100.0.  
 (c) Size Tolr. = 0.127 mm, Waviness SD = 0.000762 mm, SM = 35.0.

TABLE 6.18 SIZE TOLERANCE AND WAVINESS ERROR EFFECTS  
ON FOLLOWER ACCELERATION

Cycloidal Motion, Cam Speed - 1500 RPM  
Waviness SD = 0.000762 mm  
SM -- Smoothing Parameter  
DEVN -- Maximum Rate of Deviation, mm/deg.

SM (DEVN)	Size Tolerance (m)	Deviation at Peak Accel. (m/sec.sq.)		RMS Deviation (m/sec.sq.)
		Max. Rise	Max. Return	
0.0 (0.001838)	0.127E-4	1215.33	1218.22	414.51
10.0 (0.001398)	0.127E-4	449.98	326.05	190.28
20.0 (0.001174)	0.127E-4	236.90	223.50	129.59
35.0 (0.000920)	0.127E-4	150.99	129.08	75.42
50.0 (0.000727)	0.127E-4	93.85	73.30	44.12
100.0 (0.000546)	0.127E-4	16.39	29.07	15.08
35.0 (0.002000)	0.508E-4	154.07	130.92	75.57
35.0 (0.004261)	0.127E-3	160.41	134.61	76.12

TABLE 6.19 SIZE TOLERANCE AND WAVINESS ERROR EFFECTS  
AT THE CAM

Cycloidal Motion, Cam Speed — 1500 RPM  
Waviness SD = 0.000762 mm  
SM — Smoothing Parameter  
DEVN — Maximum Rate of Deviation, mm/deg.

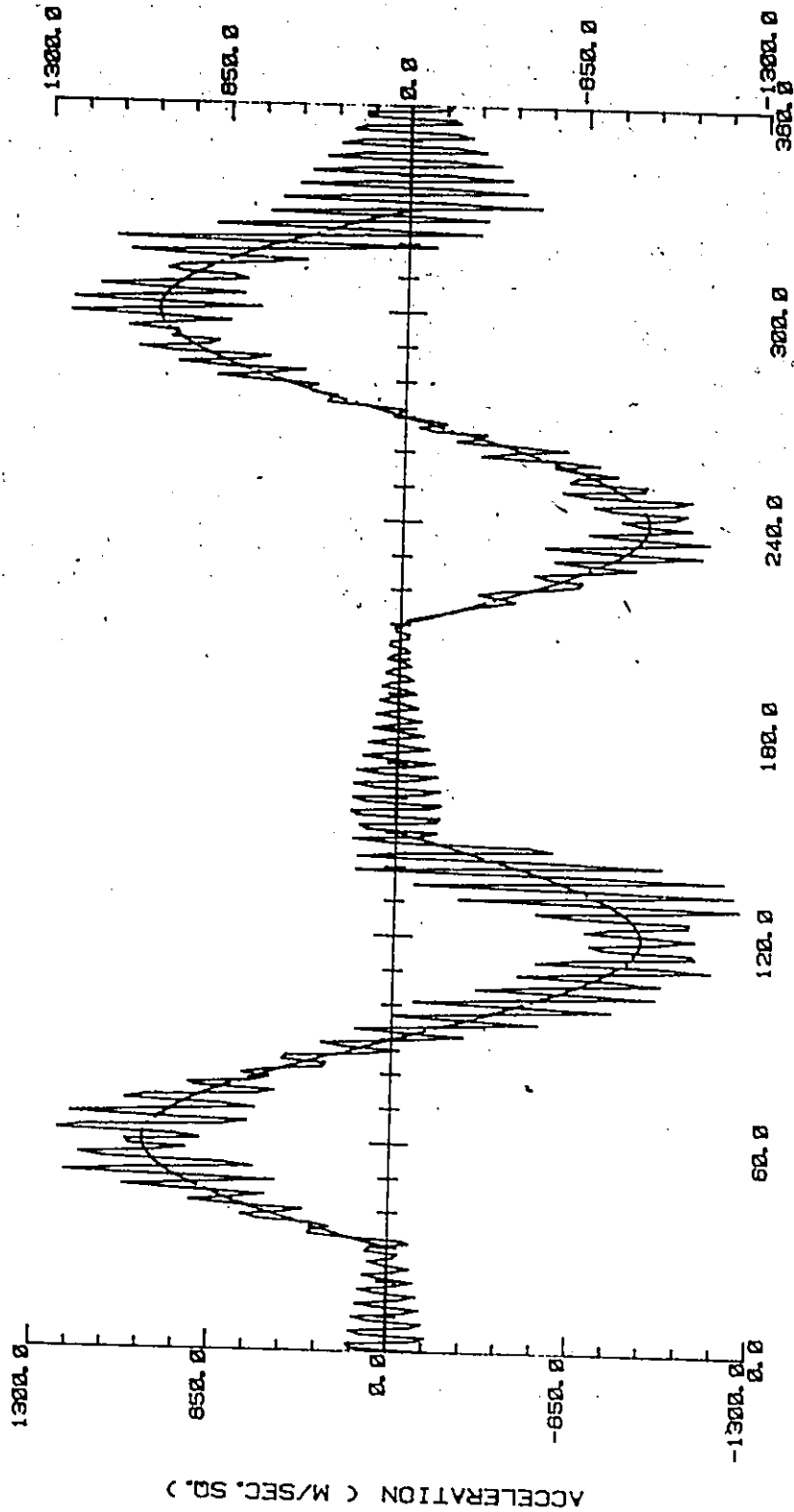
SM (DEVN)	Size Tolerance (m)	Contact Force (N)				Max. Cam Torque (N.m)	
		Rise		Return		Rise	Return
		Min.	Max.	Max.	Min.		
0.0 (0.001838)	0.127E-4	154.2	1074.4	845.1	243.7	19.7	-14.6
10.0 (0.001398)	0.127E-4	306.1	926.7	741.9	307.3	17.2	-13.6
20.0 (0.001174)	0.127E-4	348.5	881.3	707.1	329.4	16.8	-13.3
35.0 (0.000920)	0.127E-4	387.2	840.2	675.1	349.4	16.4	-12.9
50.0 (0.000727)	0.127E-4	410.2	816.6	656.2	360.8	16.1	-12.7
100.0 (0.000546)	0.127E-4	428.0	793.7	640.0	370.9	16.0	-12.4
35.0 (0.002000)	0.508E-4	387.0	840.9	675.0	349.6	16.4	-12.9
35.0 (0.004261)	0.127E-3	386.7	842.3	674.7	350.0	16.4	-13.0

FLEX. + TOLR.

— ACCELERATION

--- THEORETICAL ACCEL.

CYCLE - 3



CAM ANGLE ( DEG. )

Fig. 6.20 Combined flexibility and tolerance effects on follower acceleration - Cycloidal motion, 1500 RPM, SM=10.0.

As can be seen from the tabulated results and the acceleration plot of Fig. 6.20, the dynamic characteristics are highly sensitive to the waviness error. With the increase in profile waviness (maximum rate of deviation), the dynamic response deteriorates rapidly. This is indicated by a sharp increase in vibrations, an increase in the maximum contact force and cam torque, and a greater tendency to jump. Smoothing substantially reduces the follower oscillations, and at a high degree of smoothing (SM=100.0), when very little waviness remains - (Fig. 6.19b), the dynamic characteristics approach those due to flexibility effects alone - Tables 6.2 and 6.3.

The effects of varying the magnitude of the size tolerance are seen to be small, indicating that a high smooth error, without significant waviness, does not change the dynamic characteristics much. Therefore a fairly high deviation in the mean lift error can be accepted for a relatively good performance, provided the waviness in the lift error is closely controlled.

It can be observed that sharp profile errors at the beginning and the end of rise and return periods and the region of maximum acceleration, are critical. Waviness error in these areas must be controlled as closely as possible and should be of low amplitude and low frequency.

#### 6.4 Response Sensitivity to System Parameters

Studies have been made to investigate the effects of important parameters of cam speed, return spring stiffness, follower mass, system damping, and camshaft torsional stiffness on the dynamic performance of the cam system. For the system under investigation, Cycloidal motion is considered and one parameter is changed at a time, keeping all others constant. The basic input data and system parameters given on pages 79 and 80, respectively, have been used. The results are tabulated and graphically presented, wherever necessary. The results of sensitivity studies are discussed in detail.

##### 6.4.1 Speed Effects

The speed effects on follower acceleration are given in Table 6.20. The effects on the dynamic characteristics at the cam are given in Table 6.21 and presented graphically in Fig. 6.21. Some typical response plots at higher speeds are shown in Figs. 6.22 and 6.23. The dynamic performance is observed to deteriorate with an increase in the cam operating speed.

##### Transient Vibrations:

Follower vibrations are increased with an increase in cam speed. However, since the theoretical maximum acceleration also increases, the proportional increase is gradual. This shows that the speed effects on the vibrational characteristics are not critical. A sharp increase at the cam speed of 2020 RPM results due to jump on the rise portion.

TABLE 6.20 SPEED EFFECTS ON FOLLOWER ACCELERATION  
(Flex. + Tolr.)

Cycloidal Motion

Speed RPM	Deviation at Peak Accel. (m/sec.sq.)		Theoretical Max. Accel. (m/sec.sq.)	RMS Deviation (m/sec.sq.)
	Max. Rise	Max. Return		
1500	150.99	129.08	897.71	75.42
1600	177.81	143.84	1021.39	100.90
1700	243.30	230.53	1153.06	121.98
1800	295.97	263.96	1292.70	136.67
1900	363.74	214.81	1440.33	143.39
2020	519.03	289.05	1628.01	229.39

TABLE 6.21 SPEED EFFECTS AT THE CAM  
(Flex. + Tolr.)

Cycloidal Motion

Speed RPM	Contact Force (N)					Max. Cam Torque (N.m)	
	Rise Min.	Max.	Upper Dwell Max.	Return Max.	Min.	Rise	Return
1500	387.2	840.2	827.6	675.1	349.4	16.4	-12.9
1600	333.0	876.4	864.3	725.7	313.1	17.6	-13.4
1700	290.4	967.0	875.4	800.3	240.9	18.9	-14.4
1800	201.8	1058.4	864.9	862.8	178.7	21.3	-14.8
1900	137.6	1178.8	894.9	901.8	122.0	22.4	-15.1
2020	0.0	1331.7	865.6	997.1	73.1	24.5	-17.1



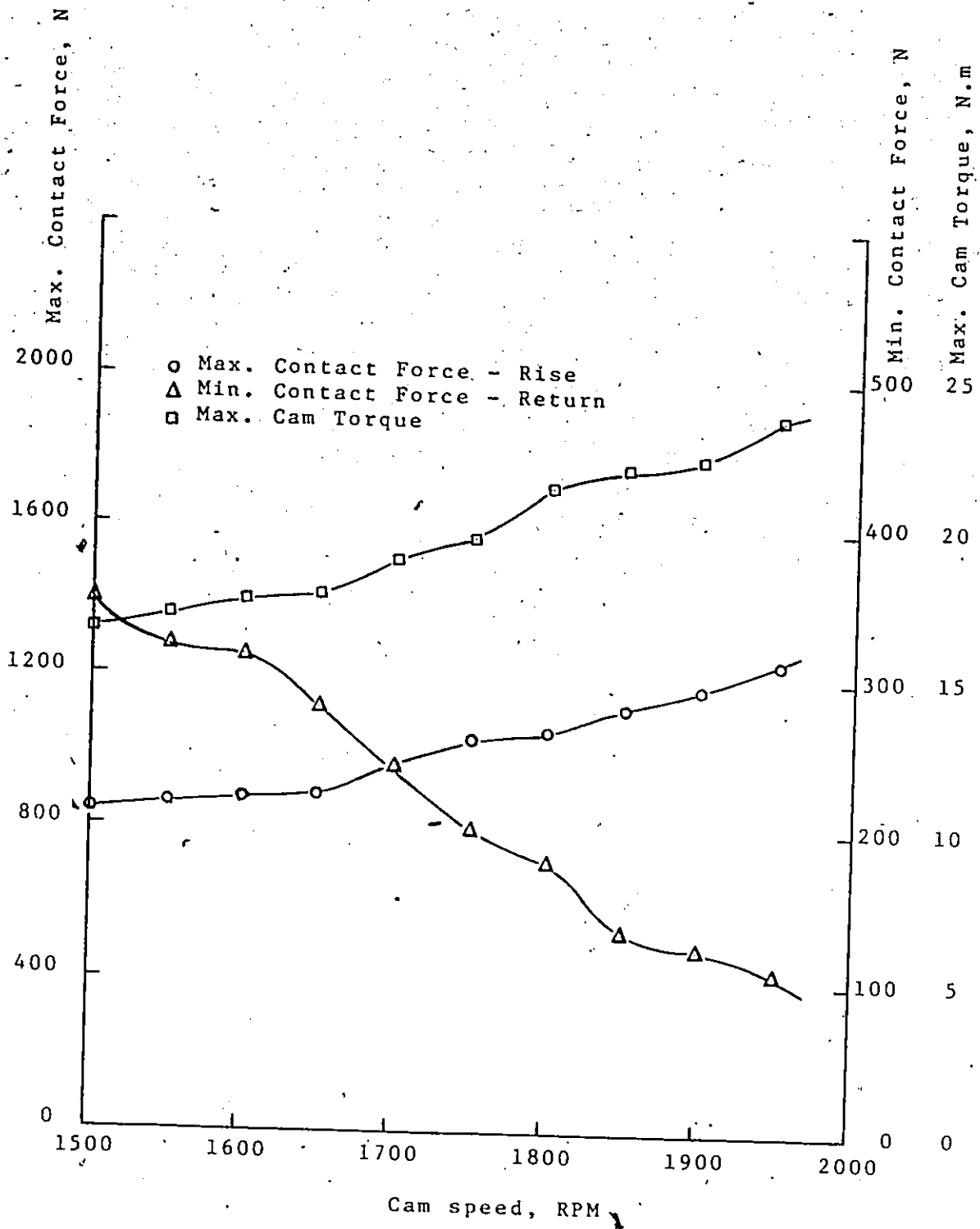


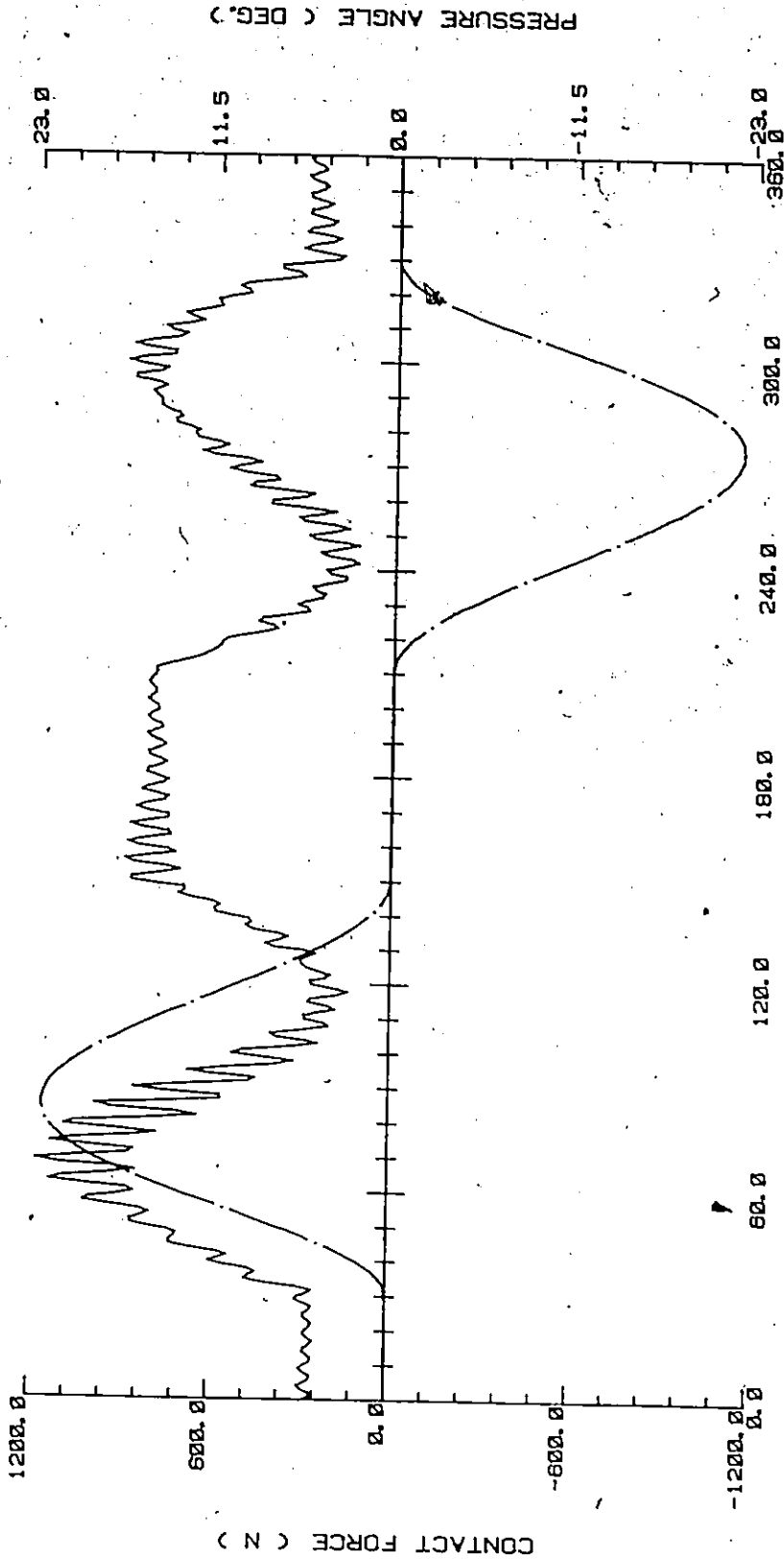
Fig. 6.21 Speed effects on contact force and cam torque - Cycloidal motion.

FLEX. + TOLR.

— CONTACT FORCE

- - - PRESSURE ANGLE

CYCLE - 3



CAM ANGLE ( DEG. )

Fig. 6.22 Speed effects on contact force - Cycloidal motion, 1900 RPM.

FLEX. + TOLR.

CONTACT FORCE

PRESSURE ANGLE

CYCLE - 3

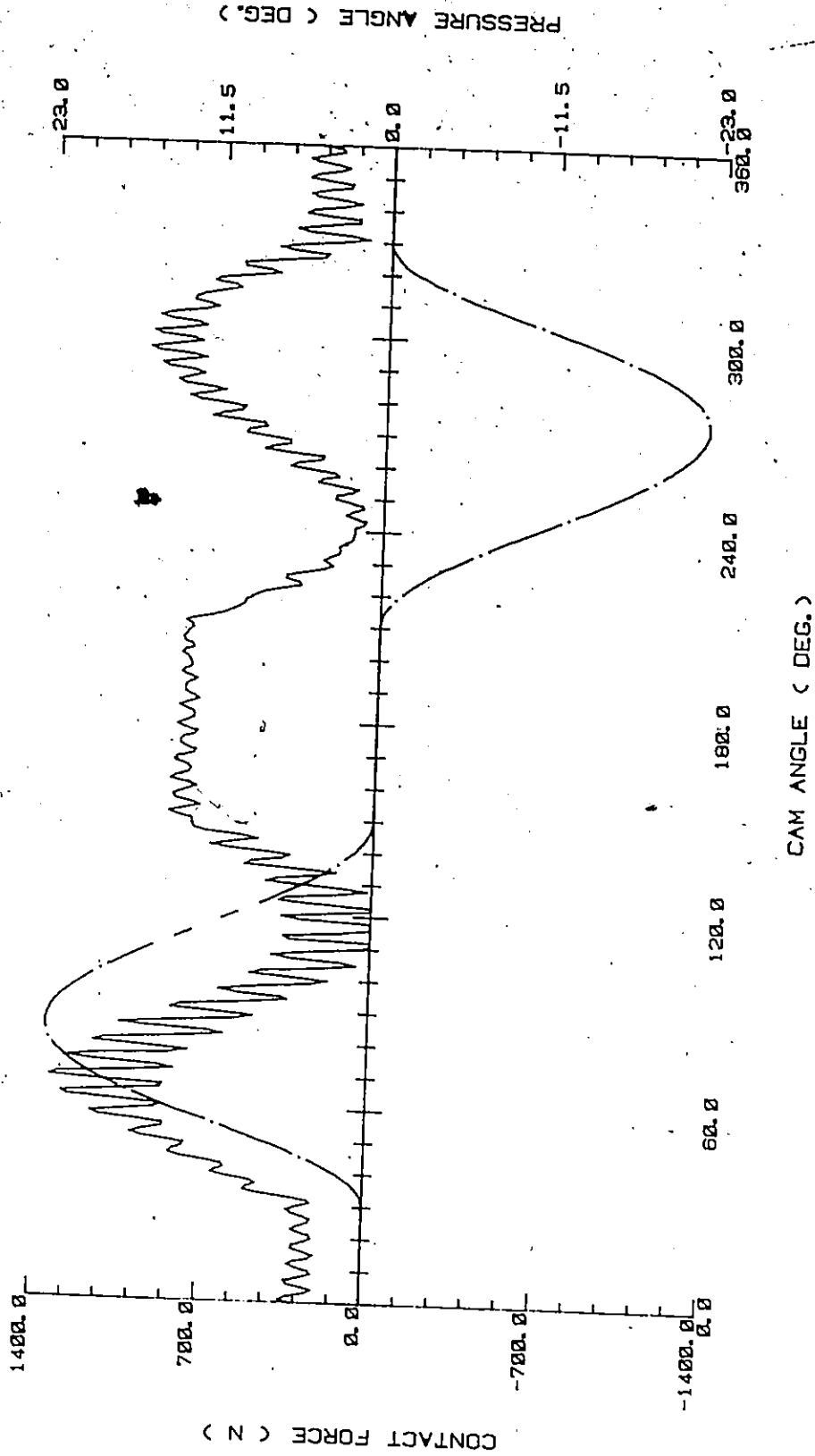


Fig. 6.23 Speed effects on contact force - Cycloidal motion, 2020 RPM.

#### Pitting Performance:

The maximum contact force increases with the increase in cam speed because of high inertia and increased vibrations - Fig. 6.21-6.23.

#### Jump Characteristics:

The available contact force decreases rapidly with speed (Fig. 6.21), and jump occurs just beyond a cam speed of 2000 RPM (Fig. 6.23). Jump occurs on the rise portion because of high vibration amplitudes. At jump, the dynamic response gets much worse. However, the jump on rise is not so critical as on return, because the cam is following the follower on its upward motion.

#### 6.4.2 Effects of Return Spring Stiffness:

Return spring stiffness has been observed to have no significant effect on the vibrational characteristics of the follower because the natural frequency of the follower system does not change. However, the dynamic performance at the cam is greatly affected as shown in Table 6.22 and presented graphically in Fig. 6.24. The available contact force, which is an important indicator of impending jump, decreases quickly as the spring is made more flexible. Whereas a decrease in the maximum contact force and cam torque are useful, the decrease in the minimum contact force on rise and return increases the tendency of the follower to jump - Fig. 6.25. Jump is observed to occur at a 50% reduction in the spring stiffness - Figs. 6.26 to 6.28, with the contact force reducing to zero on both the rise and return. Jump is very severe on the return and the dynamic characteristics get

TABLE 6.22 RETURN SPRING STIFFNESS EFFECTS AT THE CAM  
(Flex. + Tolr.)

Cycloidal Motion, Cam speed — 1500 RPM

Return Spring Stiffness (N/m)	Contact Force (N)					Max. Cam Torque (N.m)	
	Rise		Upper Dwell	Return		Rise	Return
	Min.	Max.	Max.	Max.	Min.		
2.100E+4	387.2	840.2	827.6	675.1	349.4	16.4	-12.9
1.680E+4	233.4	759.9	667.1	614.7	212.4	14.1	-11.2
1.260E+4	73.4	669.7	508.9	551.0	76.3	12.0	-9.5
1.155E+4	34.1	651.0	468.5	534.5	39.0	11.6	-9.0
1.050E+4	0.0	671.5	472.3	629.4	0.0	11.0	-14.7

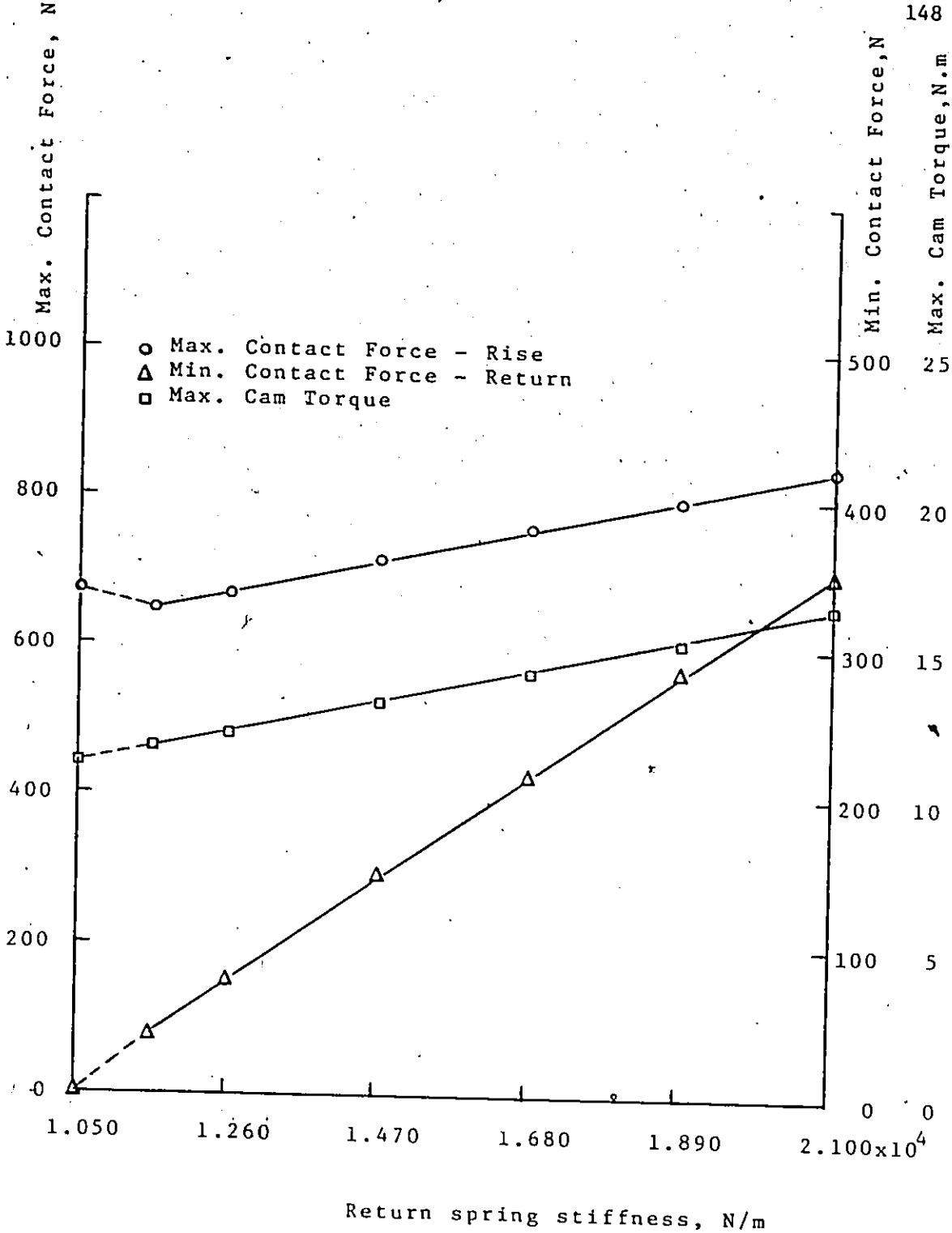


Fig. 6.24 Effects of return spring stiffness on contact force and cam torque - Cycloidal motion, 1500 RPM.

FLEX. + TOLR.

— CONTACT FORCE  
 - - - - - PRESSURE ANGLE

CYCLE - 3

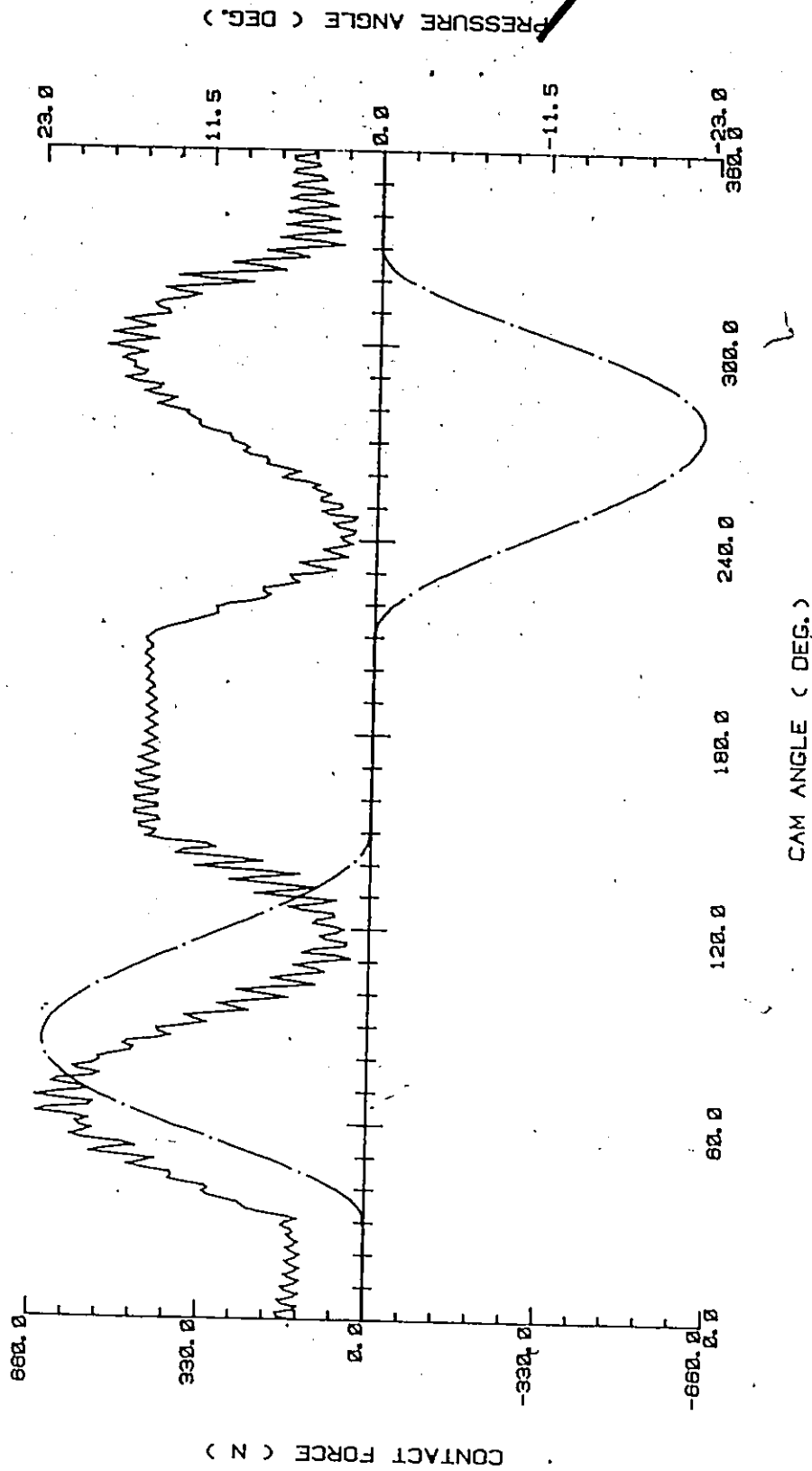


Fig. 6.25 Effects of return spring stiffness on contact force  
 - Cycloidal motion, 1500 RPM,  $K_{rg} = 1.155E+4$  N/m.

FLEX. + TOLR.

ACCELERATION

THEORETICAL ACCEL.

CYCLE - 3

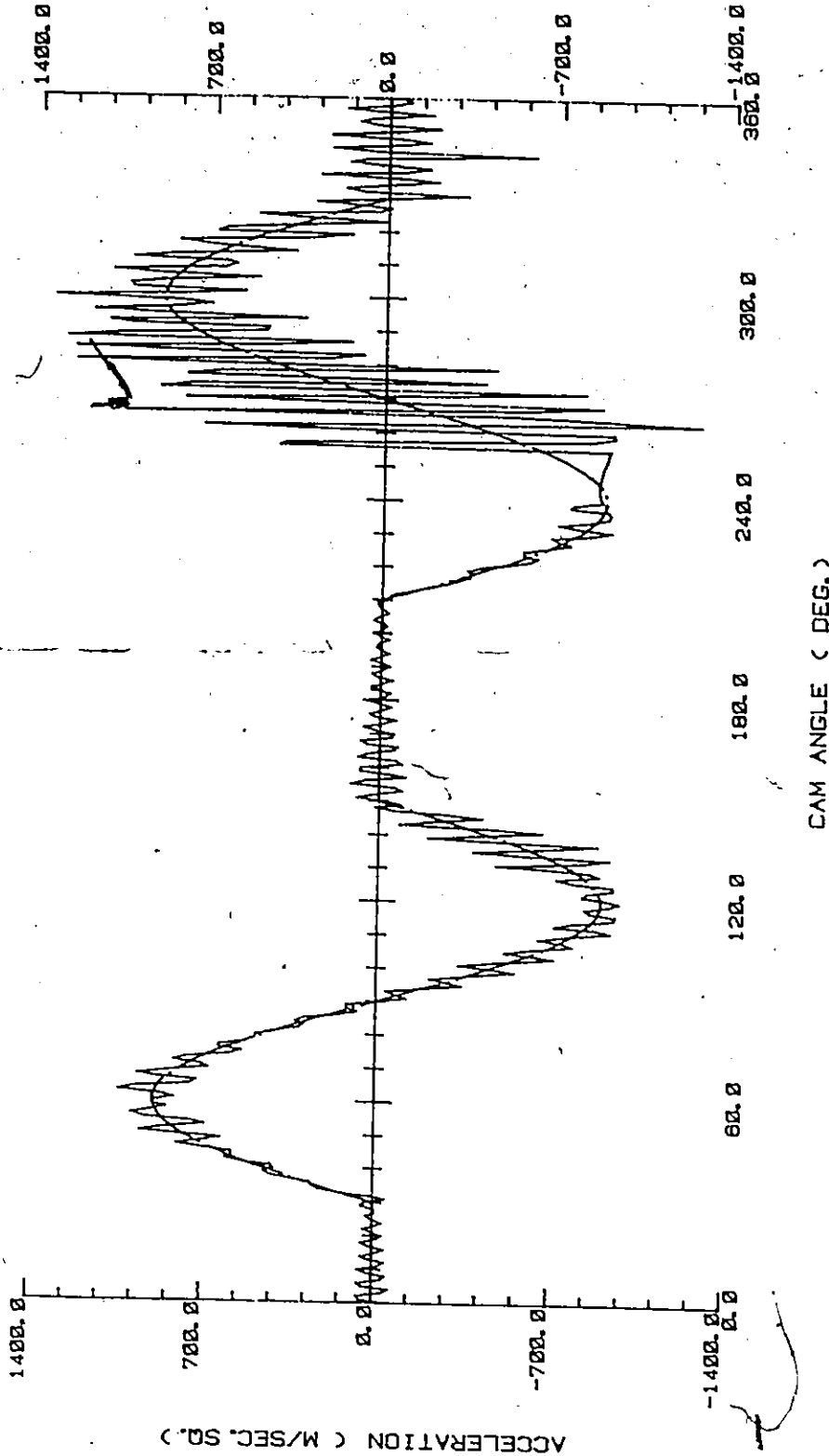


Fig. 6.26 Effects of return spring stiffness on follower acceleration  
- Cycloidal motion, 1500 RPM,  $K_{rs} = 1.050E+4$  N/m.

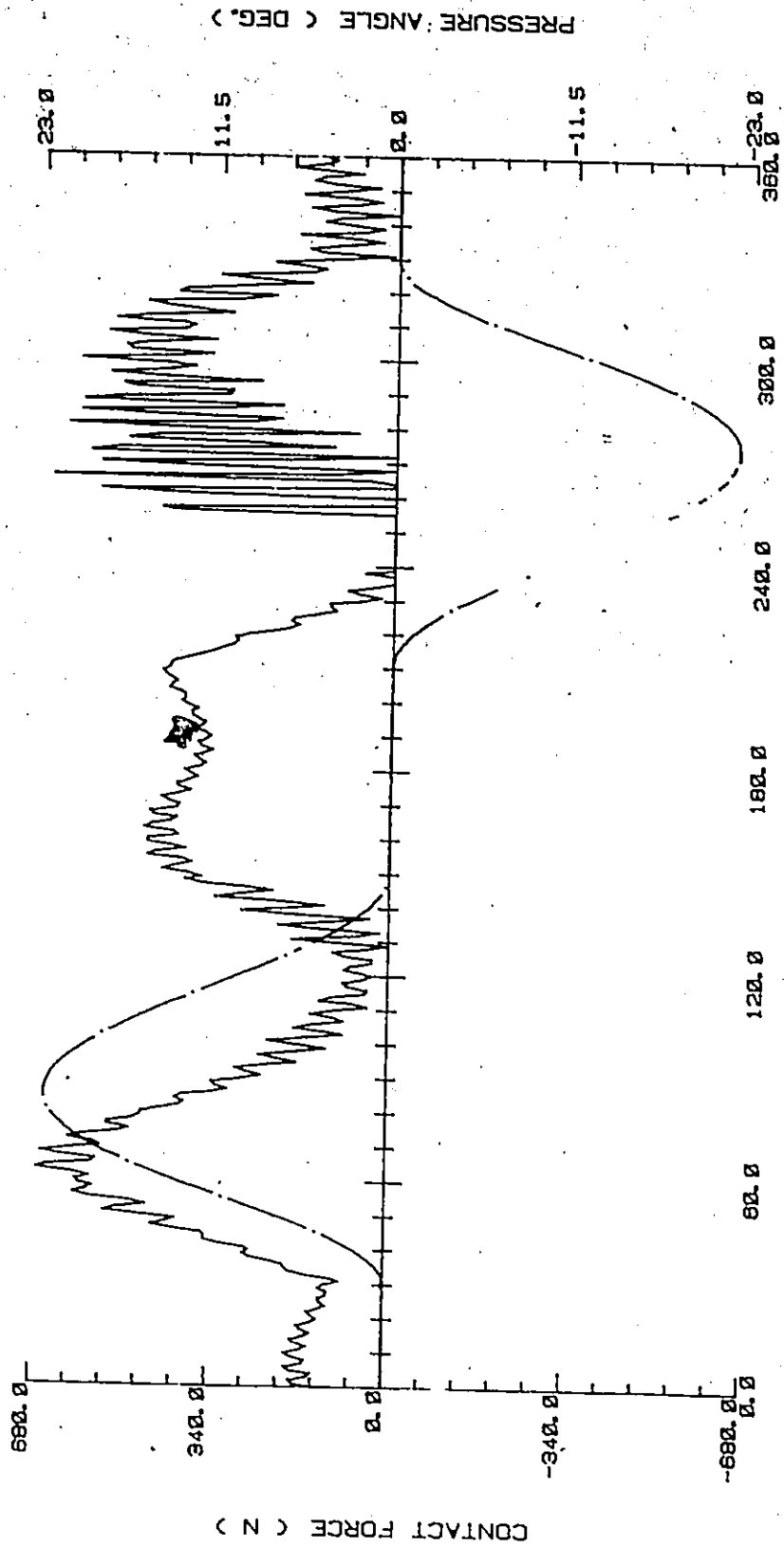


FLEX. + TOLR.

CONTACT FORCE

PRESSURE ANGLE

CYCLE -- 3



CAM ANGLE ( DEG. )

Fig. 6.27 Effects of return spring stiffness on contact force  
 - Cycloidal motion, 1500 RPM,  $K_{rs} = 1.050E+4$  N/m.

FLEX. + TOLR.

— CAM TORQUE  
— CAM SPEED

CYCLE - 3

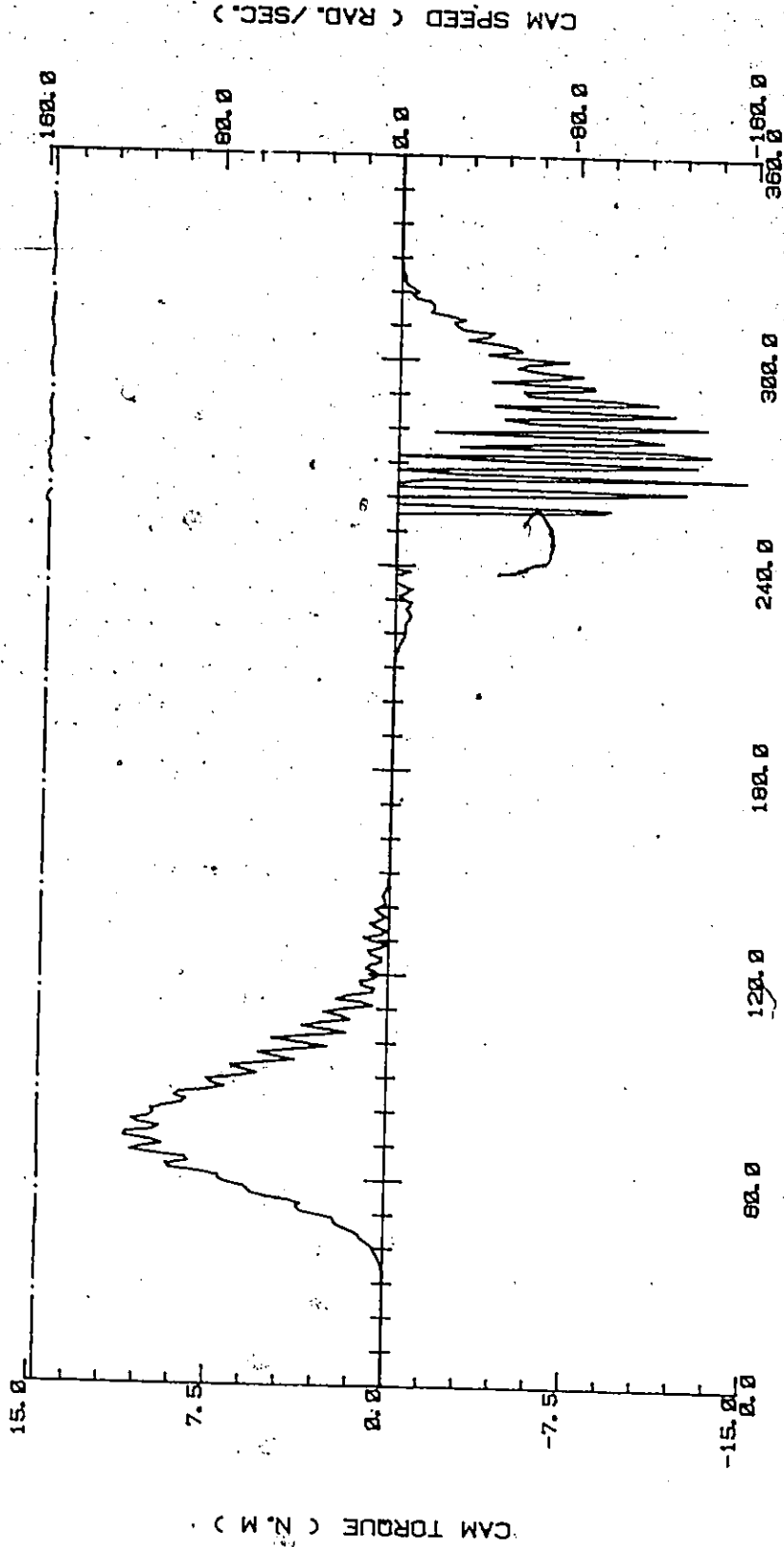


Fig. 6.28 Effects of return spring stiffness on cam torque and speed  
- Cycloidal motion, 1500 RPM,  $K_{rs} = 1.050E+4$  N/m.

really bad. Low frequency return spring vibrations are clearly indicated in Fig. 6.27. Because of sudden changes in cam torque during the return, cam speed fluctuations occur as shown in Fig. 6.28. Camshaft vibrations occur at its natural frequency (4492 rad/sec).

To avoid jump, the return spring should be adequately stiff. Too high a stiffness, however, increases the torque requirements and results in a high contact force on the rise to cause fast wear. The system developed here will enable designers to more accurately forecast a jump problem in any design.

#### 6.4.3 Effects of Follower Mass

The results are given in Tables 6.23 and 6.24, and are presented graphically in Fig. 6.29. Follower mass affects both the vibrational characteristics of the follower as well as the dynamic effects at the cam because the follower natural frequency changes. Follower vibrations, the maximum contact force, and cam torque increase sharply with an increase in the follower mass and the minimum contact force, to avoid jump, decreases. The control of all the desired characteristics requires as small a mass as possible.

#### 6.4.4 Effects of Damping

The effects of changing the internal damping and the rubbing friction at the guides are given in Tables 6.25 and 6.26. The internal friction is useful in controlling the vibration amplitudes and hence the tendency of the follower to jump. But an increase in the Coulomb friction coefficient is observed to worsen the dynamic response characteristics. It results in an increase in the amplitude

TABLE 6.23 EFFECTS OF FOLLOWER MASS ON FOLLOWER ACCELERATION  
(Flex. + Tolr.)

Cycloidal Motion, Cam Speed -- 1500 RPM

Follower Mass (kg)	Deviation at Peak Acceleration (m/sec.sq.)		RMS Deviation (m/sec.sq.)
	Max. Rise	Max. Return	
0.204	130.24	85.97	46.29
0.272	131.02	129.60	83.00
0.340	150.99	129.08	75.42
0.408	166.06	140.95	89.38
0.476	226.98	168.32	95.61

TABLE 6.24 EFFECTS OF FOLLOWER MASS AT THE CAM  
(Flex: + Tolr.)

Cycloidal Motion, Cam Speed — 1500 RPM

Follower Mass (kg)	Contact Force (N)					Max. Cam Torque (N.m)	
	Rise		Upper Dwell	Return		Rise	Return
	Min.	Max.	Max.	Max.	Min.		
0.204	546.0	710.8	826.1	541.0	465.1	15.4	-11.7
0.272	464.7	752.1	840.7	612.3	419.6	15.7	-12.3
0.340	387.2	840.2	827.6	675.1	349.4	16.4	-12.9
0.408	315.1	873.7	887.4	746.5	288.6	17.6	-13.5
0.476	251.6	1029.6	888.9	826.7	208.0	19.8	-14.5

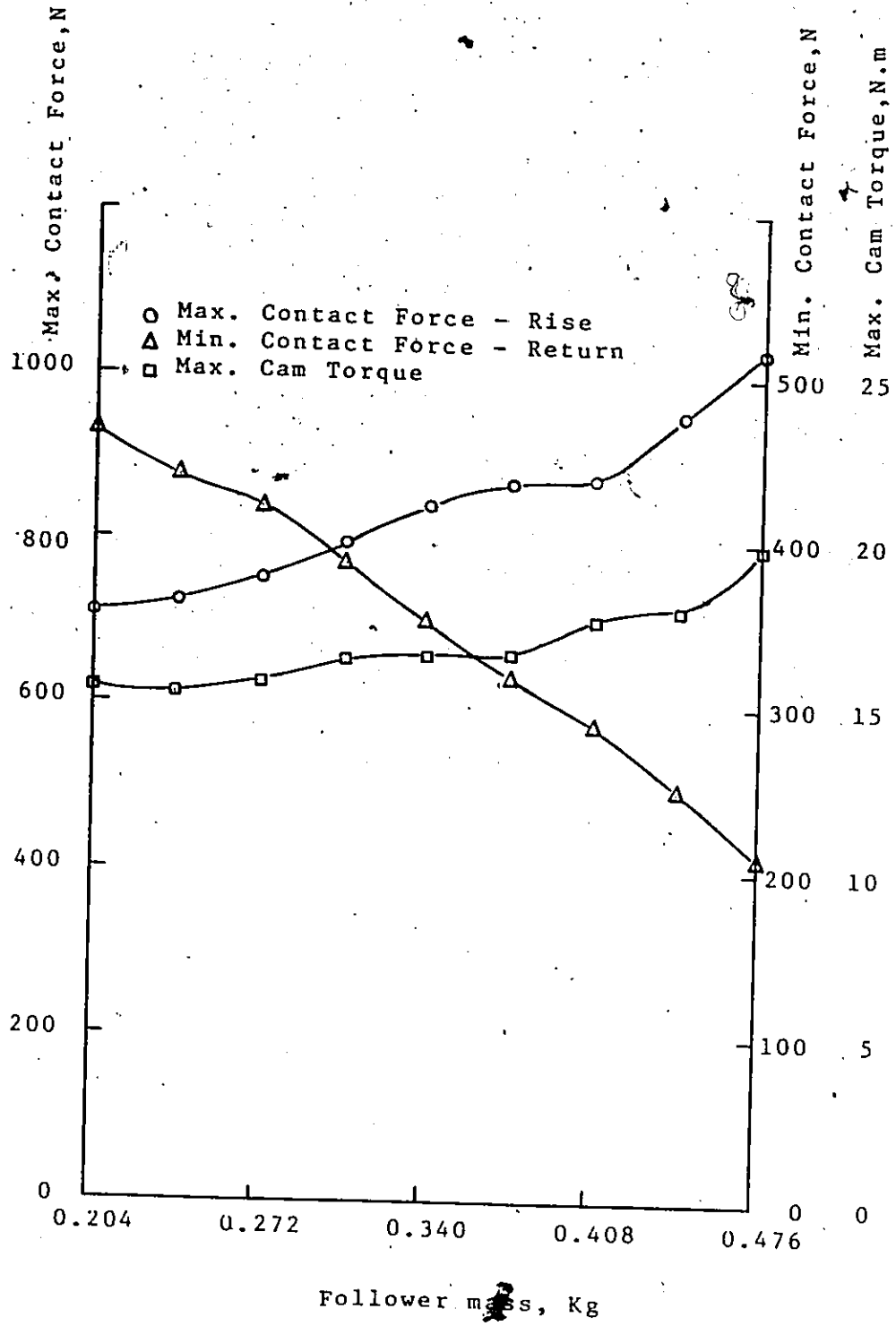


Fig. 6.29 Effects of follower mass on contact force and cam torque - Cycloidal motion, 1500 RPM.

TABLE 6.25 DAMPING EFFECTS ON FOLLOWER ACCELERATION  
(Flex. + Tolr.)

Cycloidal Motion, Cam Speed -- 1500 RPM

Damping Factor (e)	Coulomb Friction Coeff.	Deviation at Peak Acceleration (m/sec.sq.)		RMS Deviation (m/sec.sq.)
		Max. Rise	Max. Return	
0.050		191.36	103.78	103.96
0.075		163.03	121.91	85.79
0.100	0.08	150.99	129.08	75.42
	0.10	224.94	145.98	79.40
	0.12	257.04	165.64	81.89

TABLE 6.26 DAMPING EFFECTS AT THE CAM  
(Flex. + Tolr.)

Cycloidal Motion, Cam Speed -- 1500 RPM

Damping Factor (e)	Coulomb Friction Coeff.	Contact Force (N)					Max. Cam Torque (N.m)	
		Rise Min.	Rise Max.	Upper Dwell Max.	Return Max.	Return Min.	Rise	Return
0.050		355.4	863.4	846.5	676.1	339.8	16.8	-13.0
0.075		375.8	848.7	834.9	672.7	345.2	16.5	-12.9
0.100	0.08	387.2	840.2	827.6	675.1	349.4	16.4	-12.9
	0.10	395.4	865.4	832.9	668.5	345.5	17.0	-12.6
	0.12	404.0	893.7	839.9	663.1	341.9	17.6	-12.3



of vibrations, an increase in the maximum contact force and torque, and a decrease in the minimum contact force. The effects, however, are only marginal.

#### 6.4.5 Effects of Camshaft Torsional Stiffness

Camshaft is generally quite rigid in most applications and has been chosen so in the present investigation. Consequently, the speed fluctuations are small. To study the dynamic effects of a relatively flexible shaft, sensitivity analysis has been conducted for stiffness up to 5% of the original torsional stiffness. The results are tabulated in Tables 6.27 and 6.28. As can be observed, a decrease in stiffness to 20% of the original value causes less than 1% fluctuation in cam speed and an insignificant change in the dynamic characteristics. However, a stiffness of 5% of the original, results in a large variation in the cam speed (6.2%) and a significant change in the dynamic characteristics. The speed fluctuations are shown in the Fig. 6.30, which indicates camshaft vibrations at its natural frequency.

TABLE 6.27 EFFECTS OF CAMSHAFT TORSIONAL STIFFNESS ON FOLLOWER ACCEL.  
(Flex. + Tolr.)

Cycloidal Motion, Cam Speed -- 1500 RPM

Camshaft Stiffness (N.m/rad.)	Deviation at Peak Accel. (m/sec.sq.)		RMS Deviation (m/sec.sq.)	Speed Variation (%)
	Max. Rise	Max. Return		
<del>2.260E+4</del> (original)	150.99	129.08	75.42	0.2
1.808E+4 (80%)	147.47	134.87	76.04	0.2
1.356E+4 (60%)	146.62	182.20	76.68	0.3
0.904E+4 (40%)	149.94	127.86	77.47	0.4
0.452E+4 (20%)	147.40	130.32	78.57	0.8
0.226E+4 (10%)	140.62	109.53	82.33	2.0
0.113E+4 (5%)	278.76	143.00	102.61	6.2

TABLE 6.28 EFFECTS OF CAMSHAFT TORSIONAL STIFFNESS AT THE CAM  
(Flex. + Tolr.)

Cycloidal Motion , Cam Speed — 1500 RPM

Camshaft Stiffness (N.m/rad.)	Contact Force (N)					Max. Cam Torque (N.m) -	
	Rise		Upper Dwell	Return		Rise	Return
	Min.	Max.	Max.	Max.	Min.		
2.260E+4 (original)	387.2	840.2	827.6	675.1	349.4	16.4	-12.9
1.808E+4 (80%)	389.1	841.8	828.2	677.2	349.2	16.4	-13.0
1.356E+4 (60%)	390.2	841.5	829.1	676.0	348.8	16.4	-12.9
0.904E+4 (40%)	392.2	841.8	830.2	674.3	348.5	16.5	-12.9
0.452E+4 (20%)	390.3	839.4	831.8	676.4	344.4	16.6	-12.8
0.226E+4 (10%)	383.0	839.4	831.7	676.4	351.3	17.1	-13.2
0.113E+4 (5%)	320.7	846.8	849.0	698.2	354.9	18.1	-13.2

FLEX. + TOLR.

— CAM TORQUE  
 - - - CAM SPEED

CYCLE -- 3

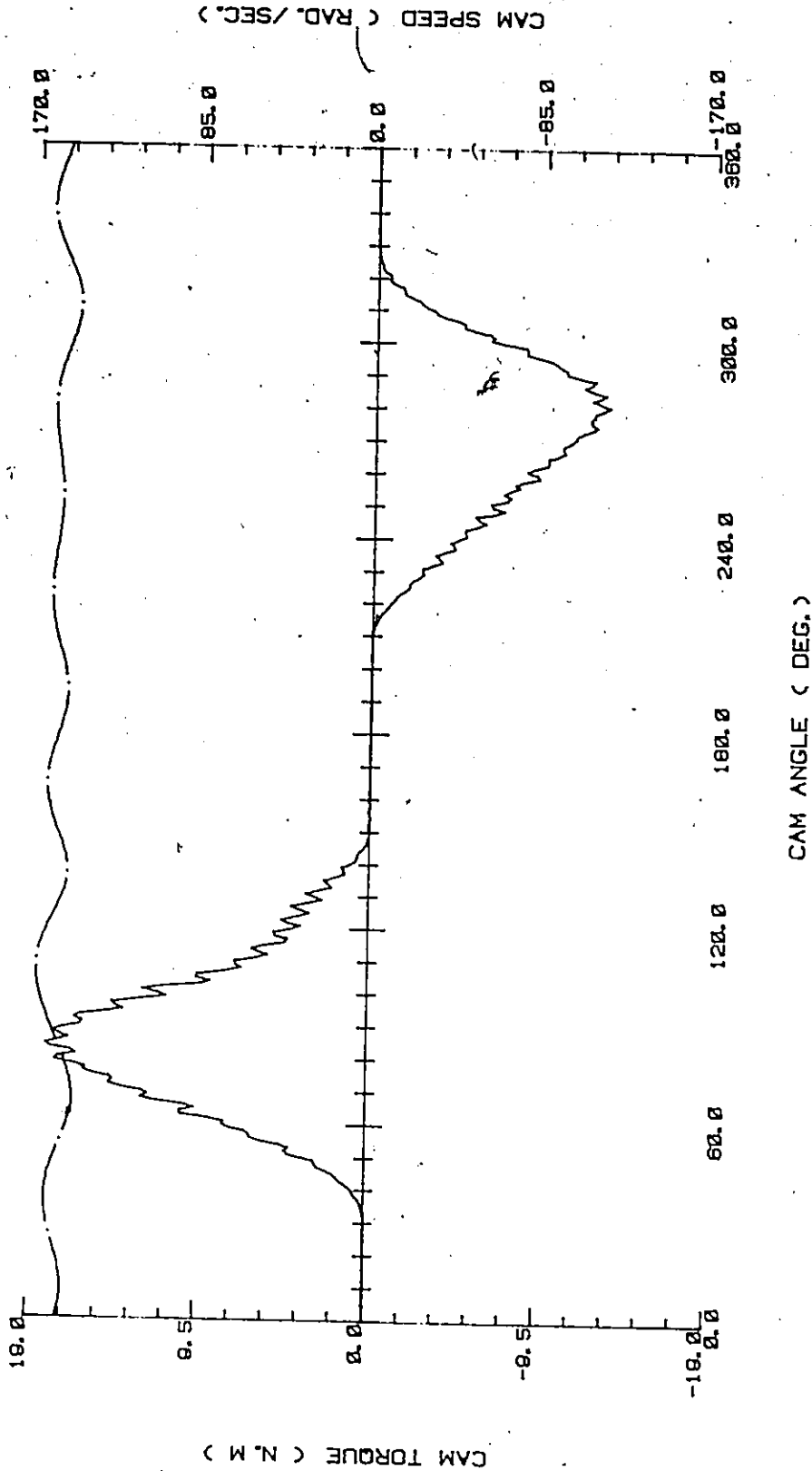


Fig. 6.30 Effects of camshaft flexibility on cam torque and speed  
 - Cycloidal motion, 1500 RPM,  $K_{gf} = 0.113E+4$  N.m/sec.

### 6.5 Effects of System Dynamics and Cam Profile Errors for a Flexible Follower System

The major portion of the present work has been devoted to the studies on a semi-rigid follower system. However, since most earlier investigations have been done on systems with a flexible follower, an analysis is also presented here for such a case. Studies have been performed with follower stiffness in the range of 2.5 to 10% of the original stiffness. This stiffness is typical of the push-rod type automotive valve gear [17,18,27]. The results are presented for the Cycloidal motion in Tables 6.29 to 6.32, and two of the representative plots are given in Figs. 6.31 and 6.32. The results in Table 6.29 show that due to the flexibility effects alone, the transient vibrations increase with a decrease in follower stiffness. However, the dynamic performance due to the combined effects of flexibility and profile errors is much improved because the flexible follower filters out the higher order excitation of frequencies. As the follower is made more flexible the dynamic response due to the combined effects of flexibility and profile errors gets closer to the response due to flexibility effects alone. This shows that the manufacturing errors in the cam profile do not substantially affect the high-speed response of the flexible follower system. This observation supports the results of earlier investigations on the push-rod type automotive cam-follower system.

TABLE 6.29 FLEXIBILITY EFFECTS ON FOLLOWER ACCELERATION

- Flexible Follower

Cycloidal Motion, Cam Speed — 1500 RPM

Follower Stiffness (N/m)	Deviation at Peak Accel. (m/sec.sq.)		RMS Deviation (m/sec.sq.)
	Max. Rise	Max. Return	
1.751000E+8 (original rigid follower)	9.94	13.01	8.86
0.175100E+8 (10%)	7.61	15.96	14.22
0.087550E+8 (5%)	18.92	20.97	21.18
0.043775E+8 (2.5%)	50.29	56.82	34.08

TABLE 6.30 (FLEX. + TOLR.) EFFECTS ON FOLLOWER ACCELERATION

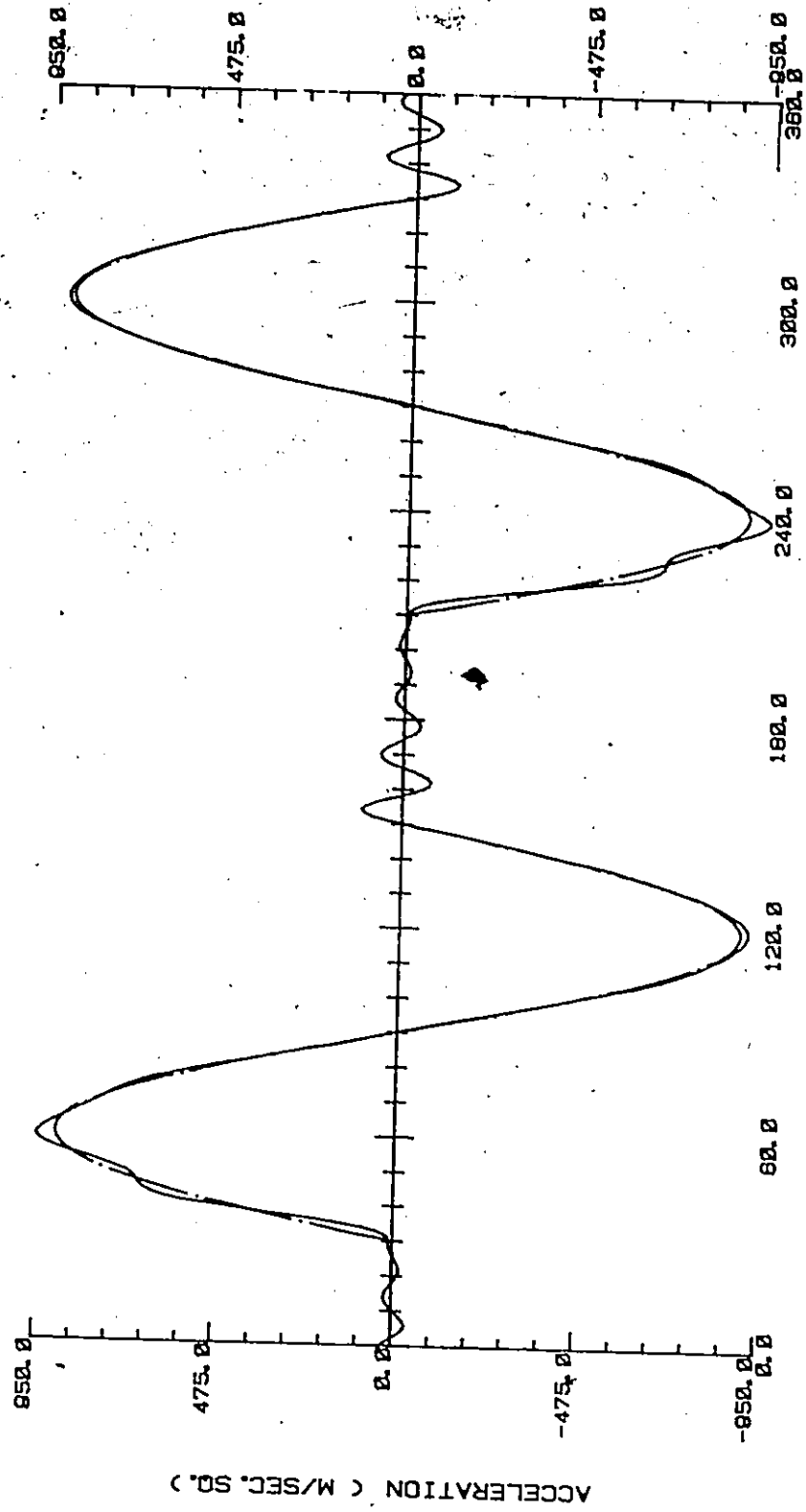
- Flexible Follower

Cycloidal Motion, Cam Speed — 1500 RPM

Follower Stiffness (N/m)	Deviation at Peak Accel. (m/sec.sq.)		RMS Deviation (m/sec.sq.)
	Max. Rise	Max. Return	
1.751000E+8 (original rigid follower)	150.99	129.08	75.42
0.175100E+8 (10%)	80.05	77.51	44.39
0.087550E+8 (5%)	50.15	58.64	33.16
0.043775E+8 (2.5%)	67.42	45.20	37.09

FLEXIBILITY  
ACCELERATION  
THEORETICAL ACCEL.

CYCLE - 3



CAM ANGLE ( DEG. )

Fig. 6.31 Flexibility effects on acceleration for a flexible follower  
- Cycloidal motion, 1500 RPM,  $K_f = 0.043775E+8$  N/m.



FLEX. + TOLR.  
ACCELERATION  
THEORETICAL ACCEL.      CYCLE - 3

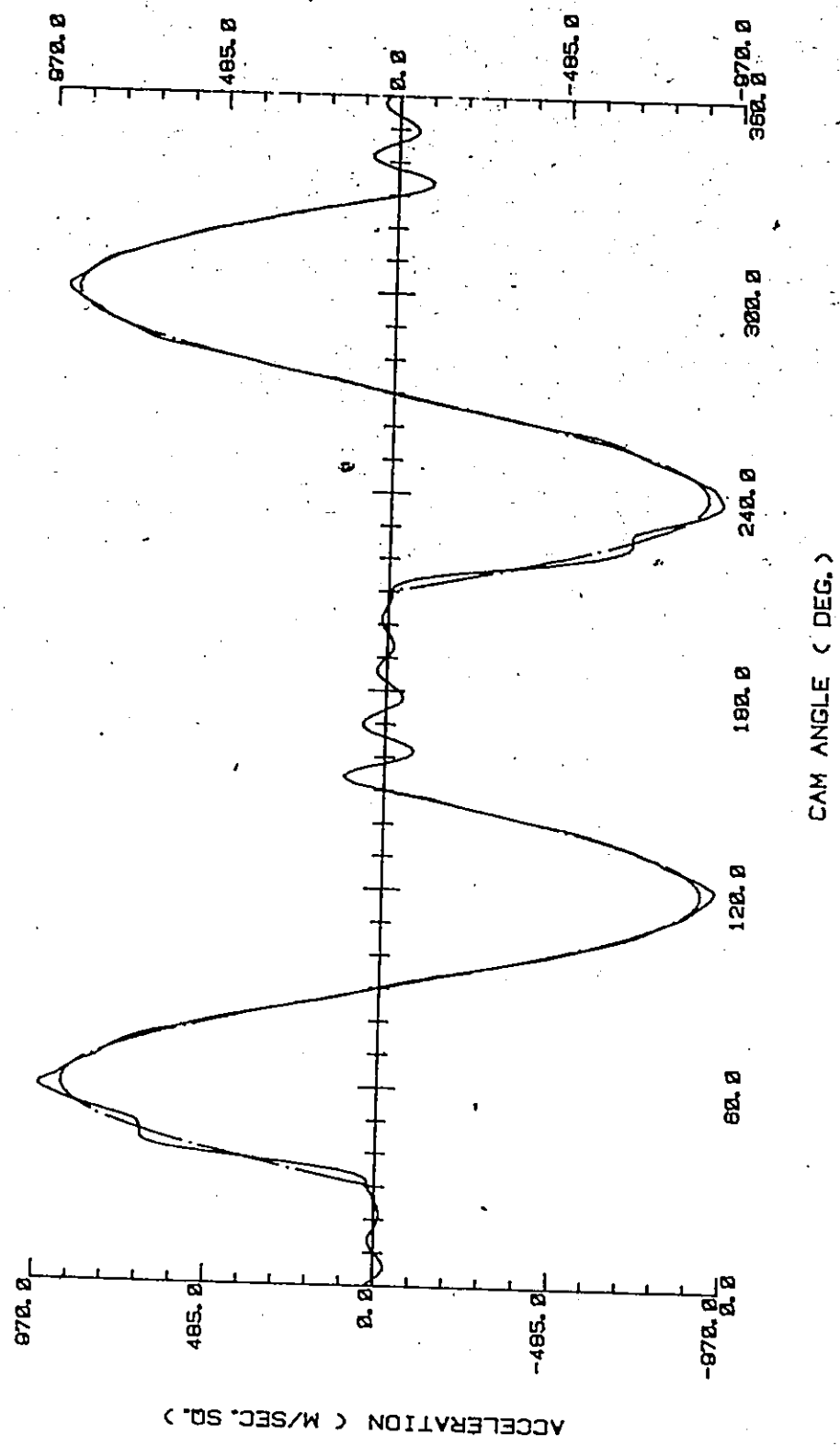


Fig. 6.32 Combined flexibility and tolerance effects on acceleration for a flexible follower - Cycloidal motion, 1500 RPM,  $K_f = 0.043775E+8$  N/m

TABLE 6.31 FLEXIBILITY EFFECTS AT THE CAM

- Flexible Follower

Cycloidal Motion , Cam Speed — 1500 RPM

Follower Stiffness (N/m)	Contact Force (N)					Max. Cam Torque (N.m)	
	Rise		Upper Dwell	Return		Rise	Return
	Min.	Max.	Max.	Max.	Min.		
1.751000E+8 (original rigid follower)	434.6	792.2	812.1	638.3	374.9	16.0	-12.4
0.175100E+8 (10%)	431.5	791.8	817.6	638.4	375.3	16.0	-12.4
0.087550E+8 (5%)	428.1	792.6	823.2	640.3	375.0	16.1	-12.4
0.043775E+8 (2.5%)	425.9	792.2	831.5	638.7	379.0	16.0	-12.4



TABLE 6.32 (FLEX. + TOLR.) EFFECTS AT THE CAM

- Flexible Follower

Cycloidal Motion , Cam Speed -- 1500 RPM

Follower Stiffness (N/m)	Contact Force (N)					Max. Cam Torque (N.m)	
	Rise Min.	Max.	Upper Dwell Max.	Return Max.	Min.	Rise	Return °
1.751000E+8 (original rigid follower)	387.2	840.2	827.6	675.1	349.4	16.4	-12.9
0.175100E+8 (10%)	423.1	803.2	842.9	660.7	364.7	16.6	-12.8
0.087550E+8 (5%)	423.1	801.0	830.7	642.1	362.5	16.5	-12.6
0.043775E+8 (2.5%)	423.4	793.9	834.5	635.5	373.8	16.0	-12.3

## CHAPTER 7

### CONCLUSIONS

#### 7.1 Conclusions and Recommendations

This work involved an investigation of the combined effects of system dynamics and cam profile manufacturing errors on the dynamic performance of a semi-rigid follower cam system. A simulation approach has been employed. A very refined dynamic model has been developed for the mechanism under investigation, which takes into account most of the factors that influence the dynamic behaviour of the system. A stochastic model has been proposed for the generation of the input signal. The input signal consists of the lift function, taking into account the lift error due to manufacturing irregularities. The lift error is considered to be composed of a smooth component and a superimposed waviness error. Results have also been obtained by employing the actual inspection lift error data obtained from industry. The performance criteria include the dynamic response at the output in the form of acceleration deviations and at the cam in the form of jump, contact force, cam torque, and cam speed variations. A fourth order Runge-Kutta method has been programmed and employed to solve the system of equations.

All popular cam motions have been compared for their high-speed dynamic performance. The main emphasis has been laid on the dynamic effects of machining errors in the cam profile. A sensitivity analysis has been performed to study the effects of changes in critical system parameters. The results of the investigation have been

neatly tabulated, and also presented in the form of plots for illustration.

The purpose of the investigation has been to provide more refined qualitative and quantitative information that will be of great value in the manufacture of cams, and to the designer in predicting the system performance during the system development/design stage.

Based on the results of this investigation, many important conclusions are drawn on the design of semi-rigid follower cam systems, and the manufacture of cams. A summary of the conclusions and recommendations is given below:

1. Transient vibrations characterize the system and occur at the fundamental natural frequency of the follower system.
2. Smooth cam motions, which induce very little follower oscillations due to the flexibility effects alone, have their dynamic performance greatly deteriorated when the effects of profile errors are accounted for. The combined effects of system dynamics and cam profile errors are significantly greater because of the superimposed pulse transients due to the profile bumps. Therefore, a mathematically smooth motion is no guarantee for a superior performance at high speeds because of the dynamic effects of manufacturing errors in the profile.
3. The kinematic effects of cam profile errors alone are not critical, and of no practical consequence because system dynamics are always involved.

4. Cam profile errors smooth out the sharp transient points at the beginning and end of the ramps in Parabolic and Simple Harmonic motions, and significantly improve the otherwise poor dynamic performance of these motions. Parabolic motion, which resulted in follower jump on the rise when considering only the system dynamics, gives a significant minimum contact force when the profile errors are accounted for. The Simple Harmonic motion is observed to give very superior jump characteristics for reasons explained in the discussion on results in Section 6.2.3.

5. When the combined effects of system flexibility and cam manufacturing errors are taken into account, the dynamic effects of machining errors are dominating.

6. At high speeds, it is not the vibrational response, but the follower tendency to jump which determines whether or not a particular cam motion has good dynamic performance. Jump occurs at much lower speeds when the effects of profile errors are included.

7. Jump is more likely to occur on the return stroke than on the rise, and if it does occur on the rise, the effects are less severe (Figs. 6.23, 6.26-6.28). The dynamic performance is severely affected during the jump, therefore, this situation must not be allowed to occur by proper choice of the cam motion and system parameters.

8. Return spring vibrations are critical at high speeds and must be accounted for. The dynamic characteristics at the cam are significantly changed as a result of spring vibrations.

9. At high speeds, higher-order Polynomial and Cycloidal cams have inferior jump characteristics and relatively poor performance because of the inherently high maximum acceleration in their theoretical motions, and the resulting high inertia forces. For the best high-speed performance, the choice will be made between the Modified-Sine, Simple Harmonic, and the 3-4-5 Polynomial motions, with the Modified-Sine motion having superior overall characteristics.

Overall, the cam motions can be rated for their high-speed performance as follows:

Excellent :	Modified-Sine, Simple Harmonic, 3-4-5 Poly.
Good :	Cycloidal, Modified-Trapezoidal
Poor :	4-5-6-7 Poly., Parabolic.

10. Dynamic response is critically dependent on the random error (waviness) in the lift function. Sharp, high frequency errors cause high vibration amplitudes, and consequently, a greater tendency to jump, faster wear, and increased power requirements. Waviness error, therefore, should be of low amplitude and low frequency.

11. The smooth size-error has very little dynamic effects, and a fairly high deviation can be accepted for a relatively good performance.

12. Sharp profile errors at the beginning and the end of rise and return periods, and in the region of maximum acceleration are very serious. Waviness error must be closely controlled in these areas.

13. It is difficult to specify a limiting value for the rate-of-deviation error because it depends both on the size tolerance and on limits of the waviness error. Only general rules, as already given, can be prescribed for size and waviness tolerances. Typically, a size tolerance of  $\pm 0.05$  mm (or even more), which can be easily achieved in cam production, may be allowed. However, for good dynamic behaviour of semi-rigid follower systems, the waviness error must be controlled within a band of  $\pm 0.0025$  mm, and the resulting rate-of-deviation be much less than the normally specified value of  $0.005$  mm/deg [26].
14. Return spring stiffness does not influence the vibrational response of the follower, but the characteristics at the cam are greatly changed. Stiffness must be optimized to have a good compromise of an adequate minimum and a small maximum contact force.
15. Follower mass is very important in controlling the cam system dynamics and must be optimized for a minimum.
16. Coulomb friction has adverse effects on the response characteristics and should be minimized.
17. For flexible camshafts, where a speed fluctuation of more than 2% occurs, the effects of cam speed variations must be accounted for.
18. The dynamic effects of cam profile errors are rather small for a flexible follower system defined in [27]. For such systems, the simulation studies, considering a perfect profile, will give quite accurate results.



## 7.2 Comparison with the Results of Previous Work

It is difficult to give specific comparisons because most of the past investigations have been concerned mainly with the dynamics of flexible follower systems. However, in the related discussions, some remarks have been made on the dynamics of semi-rigid follower system. Also in most studies, some of the important factors were not accounted for. Comparisons are made here in the three areas of the present investigation.

### 1. Work on Comparison of Standard Cam Motions

Earlier investigations [2,3] showed that the Cycloidal motion had superior dynamic performance in comparison to the Parabolic and Simple Harmonic motions because of the smooth acceleration curve. Mercer and Holowenko [9] concluded that there was no best-of-all possible motion on the basis of residual vibration characteristics, however, the 7th order Polynomial motion resulted in low vibrations. Simulation studies by Reeve and Rees-Jones [26] indicated the Modified Sine to be the most useful general purpose motion, with the Cycloidal program preferred for relatively flexible systems. Simple Harmonic motion gave the best characteristics of velocity, impact, and input torque. Koester [29] states that for the general D-R-D profile, it was hardly possible to improve upon the Cycloidal cam.

Through experimental investigations with a rigid follower system, Rao and Raghavacharyulu [28] showed the Simple Harmonic motion to give the best jump characteristics. The 7th order Polynomial produced jump at much lower speeds. In a cam seminar given

at a leading cam design and manufacturing company - EONIC, INC. Detroit, it was remarked that the Modified-Sine motion was ideal for high speeds, and was particularly suited for index cams because of its low maximum pressure angle and velocity. Its acceleration and pulse curves were also very acceptable. Simple Harmonic motion was also a very desirable curve when modifications were made to round off the transitions at the dwells. Even manufacturing errors help to remove the infinite pulse at the transitions.

Kim and Newcombe [46] concluded that the Cycloidal curve was the best and most practical motion. Through experimental studies with the Cycloidal, 3-4-5 Poly., Modified-Sine, and 4-5-6-7 Poly. motions, Norton [48], on the basis of vibrational response, concluded that the 5th order Polynomial was the quietest and the 7th order Polynomial, the noisiest motion. This conclusion is based on the RMS average power for six different manufacturing methods taken together. The results with separate manufacturing methods, however, do not show any significant noise differences for various motions as observed in the present investigation. Testing a number of motions cut on a single cam lobe, as done in the study by Norton, is likely to produce erroneous results because the residual vibrations of one motion will influence the following motion. Additionally, the cam motions are produced with different machining errors.

The conclusions from the present investigation, that the Modified-Sine, Simple Harmonic, and the 3-4-5 Polynomial were the preferred motions for high-speed applications, generally agree with

those of earlier works. However, the commonly favoured Cycloidal and Modified-Trapezoidal [26] motions have been shown to give relatively poor performance at high speeds; the former because of its inherently high acceleration, velocity, and pressure angle, and the latter because of its poor vibrational characteristics, high velocity, and pressure angle.

## 2. Work on the Effects of Cam Profile Manufacturing Errors

On the basis of dynamic tests conducted to study the effects of single smooth non-periodic error in the cam profile of a high-speed aircraft valve gear mechanism, Rothbart [34] observed that sharp errors caused large vibration amplitudes. Brittain and Horsnell [37], and Giordana et al. [44] concluded that smooth errors had very little dynamic effects. Studies on the kinematic effects of cam profile errors [36,40] show that cam acceleration errors of 10 to 15% occur due to the waviness error in a tolerance band of 5 tenths.

Many authors [3,5,14] have concluded that the manufacturing errors in the cam profile do not substantially affect the high-speed response of the flexible follower system. At high speeds, the profile errors constituted higher order excitation of frequencies which the soft system was incapable of following. Results of this investigation with a flexible follower support these conclusions.

Tesar in a discussion on papers in Cams and Cam Mechanisms [26, page 60] made the following remarks regarding the dynamics of rigid systems;

" The remarks on Ford's experience should not be lost on the designer of high-speed systems. It concludes, wear is more likely for the overhead-cam system. This system is much stiffer than the push-rod design, and it cannot filter out impacts at the valve as completely - hence, the increased wear".

Results of the present investigation on semi-rigid follower systems indicate high amplitude vibrations and high contact forces, and agree with Tesar's remarks on stiff systems.

The work on the effects of cam lift error, separating out the size-error (size tolerance) and waviness (randomness) components, has been logically performed for the first time. The usual specification of a tolerance band (e.g.  $\pm 0.001$  in.) for the profile errors does not mean much unless the variation within the band is given. Even the tolerance band does not remain uniform over the cam cycle. The use of the smoothing parameter in spline fitting helps to control the severity of the waviness error and study its dynamic effects. The amplitude and frequency of the waviness error can also be changed by manipulating its  $3\sigma$  limits and the cam angle interval for simulation.

### 3. Work on Response Sensitivity to System Parameters

No systematic study appears to have been conducted on the dynamic effects of changes in the system parameters. In a general sense, different authors recommend some general rules for cam system design, and some examples follow.

In the Eonic seminar on cam design [54], the following recommendations were made:

- choose the best possible cam motion,
- design the linkage to be stiff and of minimum mass, and having a natural frequency that is far removed from the machine speed and preferably not a multiple of it, and
- assure quality manufacture.

Matthew and Tesar [27] list the following design rules as guides to the cam designer;

- minimize  $\mu_m$  by decreasing  $M$  or by increasing  $K$ ,
- use higher-order Polynomial motion specification and then manufacture the cam to the highest possible quality (0.0001 in. or better),
- friction should be kept low for efficient operation.

Crutcher [17] studied the effects of changes in internal friction, the Coulomb friction factor, and valve spring stiffness on the dynamics of the valve mechanism. He found that the internal friction of the follower was useful in controlling the amplitude of vibrations, but the Coulomb friction had adverse effects. Results of the present study agree very well with these observations.

Pisano et al. [32], on the basis of experimental studies on the high-speed performance of automotive valve-gear, concluded that the operating speed of the cam-follower system was not limited by excessive dynamic loads or vibrations, but by a loss of load on the push-rod and the resulting valve toss (jump). Results

obtained here on the high-speed performance of cam-follower system, with different cam motions, agree very well with this hypothesis.

This investigation gives useful qualitative and quantitative information on the sensitivity of system performance to the changes in critical system parameters.

#### 4. Work on Return Spring Vibrations

During the discussion on valve symposium papers [5,6], Barkan commented that with highly rigid systems, spring surges were of first order importance at high speeds. Wagstaff [18] concluded that the simulation of the valve spring was a very important factor in obtaining accurate agreement with experimental response, especially at high speeds where the spring vibrations were significant.

These observations are strongly supported by the results of this study. Significant spring vibrations have been observed at high speeds, and they greatly influence the dynamic performance at the cam.

#### 7.3 Contributions in the Area of Research

The original contributions of this research effort to the field of knowledge in the design and manufacture of cam-follower systems are given as follows:

1. Most investigations in the past have been concerned with the dynamics of flexible follower cam systems employed in automotive valve-gear mechanisms. The present research is a significant contribution to the field of study of the dynamics of relatively rigid

follower cam systems typical of production machinery and overhead-cam automotive valve-gear, in which cam manufacturing errors and return spring vibrations play a significant role.

2. A very refined, and yet computationally manageable, system model has been developed that takes into account all the important factors which influence the system dynamics in semi-rigid follower cam systems. Earlier studies employed simple single or two d.o.f. models, and experimental evidence indicated that such models were fairly satisfactory for the study of dynamics of flexible follower cam systems. These studies did not consider the effects of cam profile errors and many other factors.
3. In the system identification process, appropriate expressions have been developed to calculate properties associated with the dynamics of the system such as: contact force, contact stiffness, and the jump criterion.
4. Considering the combined effects of all the important factors, a very comprehensive study has been presented for the comparison of all the popular cam motions regarding their high-speed performance. Studies in the past have generally neglected the effects of cam profile errors. These studies have provided comparisons of a limited number of cam motions based on their vibrational characteristics only. This investigation has demonstrated that at high speeds, it is not the vibrational response, but the jump behaviour and the maximum contact force and torque values which determine the system dynamic performance. The Modified-Sine, SH, and 3-4-5 Polynomial motions have

been shown to give superior performance at high speeds compared to the commonly favoured Cycloidal and Modified-Trapezoidal motions.

5. Another important contribution of this work is the simulation of the excitation (the input signal). This required extensive experimentation and data collection from industry in order to develop a realistic model. The input signal consists of the lift function, and takes into account the profile errors in cam manufacturing. The common practice to define a tolerance band (e.g.  $\pm 0.001$  in.) for the profile error does not mean much unless the rate of deviation per degree of cam angle is considered. The stochastic model developed here considers the lift error to be composed of a variable-mean smooth error (size-error) and a superimposed waviness error (randomness). The simulation process employs the techniques of random number generation and smoothing spline interpolation in which the waviness error can be controlled. The software system developed in this work also allows the use of the actual inspection lift error data available from industry.

6. The investigation on the dynamic effects of cam profile errors, separating out the smooth size-error and the waviness error, has been systematically performed for the first time. The same lift error functions can be used for different motions, which is an impossibility with any experimental study because different cams will be produced with different random errors. It has also been possible to study the kinematic and dynamic effects separately or in combination. An experimental study would necessarily include both of these effects. The results on the dynamic effects of the smooth size-error and the



waviness error provide very useful information for cam manufacturing.

7. The sensitivity analysis is the first such study conducted to determine the effects of changes in system parameters on the dynamic performance characteristics, and important qualitative as well as quantitative information has been provided. Different cam motion programs can be considered so that the optimum profile and the most desirable set of design parameters can be derived.

8. An efficient, versatile, and user-oriented software system - COSCAD has been developed which can be a very useful tool for the cam designer to search for the most desirable cam profile, the system parameters, and the production quality of cams to achieve high overall performance. The system can be conveniently employed to predict the occurrence of jump in any cam system design, and thus help in the selection of an appropriate return spring to avoid jump. The software system provides for the following options - kinematic analysis for a perfectly rigid system; dynamic analysis considering a perfect cam profile; a general case of dynamic analysis accounting for cam profile errors; dynamic analysis with or without return spring vibrations; use of simulated lift error or the actual inspection lift error data obtained from industry; any set of user-defined design parameters; any user-defined cam motion function for rise and return, and for both D-R-D-R or D-R-R-D cams; any work load function; and simulation to any number of cam cycles.

The conclusions and recommendations made in Sec. 7.1 justify the research carried out to investigate the cam-follower system dynamics.

#### 7.4 Suggestions for Further Research

The software system developed in this work can be employed to conduct further studies in cam system dynamics. In particular, following areas can be investigated:

- Any other motion, or suitable motion combinations, can be studied.
- The effects of load functions, camshaft flexibility in bending, and the camshaft inertia can be investigated.
- A comparative study of the cam motions can be made with a flexible follower system.
- The same motion, produced by different cam manufacturing methods can be investigated to compare the quality of manufacture produced by different methods.

The work can be extended to include the effects of clearances where they are essential to the function of a mechanism.

A simulation approach similar to that employed in this investigation could also be used to investigate the dynamic behaviour of other point or line contact mechanisms such as ball or roller bearings and gears.

## REFERENCES

1. Dudley, W.M., "A New Approach to Cam Design", Mach. Des., July 1947, pp. 143-148.
2. Hrones, J.A., "An Analysis of Dynamic Forces in a Cam-Driven System", Trans. ASME 70, 1948, pp. 473-482.
3. Mitchell, D.B., "Tests on Dynamic Response of Cam-follower Systems", Mech. Engg., Vol. 72, 1950, pp. 467-471.
4. Stoddart, D.A., "Polydyne Cam Design", Mach. Des., Vol. 25, Jan. 1953, p. 121; Feb. 1953, p. 146; Mar. 1953, p. 149.
5. Barkan, P., "Calculation of High-Speed Valve Motion With a Flexible Overhead Linkage", SAE Trans., Vol. 61, 1953, pp. 687-700.
6. Turkish, M.C., "Relationship of Valve-Spring Design to Valve Gear Dynamics and Hydraulic Lifter Pump-Up", SAE Trans., Vol. 61, 1953, pp. 707-714.
7. Neklutin, C.N., "Vibration Analysis of Cams", Mach. Des., Dec. 1954, pp. 190-198.
8. Johnson, R.C., "Method of Finite-Differences Provides Simple but Flexible Arithmetical Techniques for Cam Design", Mach. Des. 25, Nov. 1955, pp. 195-204.
9. Mercer, S. Jr., and Holowenko, A.R., "Dynamic Characteristics of Cam Forms Calculated by the Digital Computer", ASME Trans., Nov. 1958, pp. 1695-1705.
10. Freudenstein, F., "On the Dynamics of High-Speed Cam Profiles", Int. J. Mech. Sci. 1, 1960, pp. 342-349.
11. Baumgarten, J.R., "Preload Force Necessary to Prevent Separation of Follower from Cam", Trans. 7th Conf. on Mechanisms, 1962, pp. 213-218.
12. Allais, D.C., "Cycloidal Vs Modified Trapezoidal Cams", Mach. Des., Jan. 31, 1963, pp. 92-96.
13. Eiss, N.S. Jr., "Vibrations of Cams Having Two Degrees of Freedom", Trans. ASME J. Engng. Ind., Nov. 1964, pp. 343-350.

14. Johnson, A.R., "Motion Control for a Series System of N-Degrees of Freedom Using Numerically Derived and Evaluated Equations", Trans. ASME, J. Engng. Ind., 87B, 1965, pp. 191-204.
15. Erisman, R.J., "Automotive Cam profile Synthesis and Valve Gear Dynamics from Dimensionless Analysis", SAE Trans. 75, 1967, pp. 128-147.
16. Meeusen, H.J., "Overhead Cam Valve Train Design Analysis with a Digital Computer", SAE Trans. 75, 1967-68, pp. 418-446.
17. Crutcher, D.E.G., "The Dynamics of Valve Mechanisms", Proc. Instn. Mech. Engrs., Vol. 182, Pt 3L, 1967, pp. 126-136.
18. Wagstaff, P.R., "Analysis of Valve Gear with a Digital Computer", Proc. Instn. Mech. Engrs., Vol. 182, Pt 3L, 1967-68, pp. 137-144.
19. Smith, J.A., "Cams - Local Deformations Between Contacting Surfaces", Proc. OSU's Applied Mechanism Conference, July 31-Aug. 1, 1969, Tulsa, Oklahoma.
20. Sakai, H., and Tsuda, K., "Analysis of Valve Motion in Overhead Valve Linkages", Bulletin of the JSME, Vol. 13, No. 55, 1970, pp. 120-128.
21. Bagci, C., "Stop Designing and Testing Cam-Follower Systems using the Rise Portions of the Displacement Programs Only", Comm. 3rd World Congr. Theory of Machines and Mechanisms, Yugoslavia, 1971, G-25, pp. 347-364.
22. Fawcett, J.N., and Fawcett, G.F., "The Effect of Cam Vibration on Follower Motion", Comm. 3rd World Congr. Theory of Machines and Mechanisms, Yugoslavia, 1971, H-12, pp. 148-158.
23. Matthew, G.K., and Tesar, D., "Formalized Matrix Method for N-th Derivative Trapezoidal Motion Specifications for Cams", Comm. 3rd World Congr. Theory of Machines and Mechanisms, Yugoslavia, 1971, H-19, pp. 247-260.
24. Kanzaki, K., and Itao, K., "Polydyne Cam Mechanisms for Typehead Positioning", Trans. ASME J. Engng. Ind., Feb. 1972, pp. 250-254.
25. Chen, F.Y., "Analysis and Design of Cam-Driven Mechanisms with Nonlinearities", Trans. ASME J. Engng. Ind. 95B, Aug. 1973, pp. 685-694.

26. Reeve, J.E., and Rees-Jones, J., "Dynamic Response of Cam Curves Based on Sinusoidal Segments", Proc. Conf. Mech., Cams and Cam Mech., Liverpool Polytechnic, England, Sept. 1974..
27. Matthew, G.K., and Tesar, D., "The Design of Modelled Cam Systems", Ref. 19.
28. Rao, J.S., and Raghavacharyulu, E., "Experimental Determination of Jump Characteristics in Cam-Follower Systems", I. Mech. E., 1975, pp. 951-955.
29. Koster, M.P., "Digital Simulation of the Dynamics of Cam Followers and Camshafts", I. Mech. E., 1975, pp.969-974.
30. Chen, F.Y., "A survey of the State of the Art of Cam System Dynamics", J. Mech. Mach. Theory 12, 1977, pp. 201-224.
31. Akiba, K., Shimizu, A., and Sakai, H., "A Comprehensive Simulation of High Speed Driven Valve Trains", SAE Paper 810865, 1981.
32. Pisano, A.P., and Freudenstein, F., "An Experimental and Analytical Investigation of the Dynamic Response of a High-Speed Cam-Follower System. Part 1: Experimental Investigation. Part 2: A Combined Lumped/Distributed Parameter Dynamic Model", J. Mechanisms, Trans., and Automation in Des., Vol. 105, Dec. 1983, pp. 692-704.
33. Johnson, R.C., "How Profile Errors Affect Cam Dynamics", Mach. Des., Feb 7, 1957, pp. 105-108.
34. Rothbart, H.A., Cams - Design, Dynamics, and Accuracy. John Wiley and Sons, Inc., N.Y., 1956.
35. Rothbart, H.A., "Which Way to Make a Cam?", Prod. Engg., March 1958, pp. 67-71.
36. Nourse, J.H., "Recent Developments in Cam Profile Measurement and Evaluation", SAE Paper 964A, 1965.
37. Brittain, J.H.C., and Horsnell, R., "A Prediction of Some Causes and Effects of Cam Profile Errors", Proc. Instn. Mech. Engrs., Vol. 182, Pt 3L, 1967-68, pp. 145-151.
38. Dhande, S.G., and Chakraborty, J., "Mechanical Error Analysis of Cam-Follower Systems - A Stochastic Approach", 4th World Congr. Theory of Machines and Mechanisms, I. Mech. E. London, 1975, pp. 957-962.

39. Kawasaki, Y., et al., "Lift Error on Grinding Cam Profile", *Annals of the CIRP*, Vol. 24/1/1975, pp. 253-258.
40. Krawczynski, M., et al., "On the Automation of Cam Profile Control", *Proc. IFAC Symposium on Information Problems in Manufacturing Technology*, Tokyo, 1977, pp. 211-216.
41. Kim, H.R., and Newcombe, W.R., "Stochastic Error Analysis in Cam Mechanisms", *J. Mech. Mach. Theory*, 13(6), 1978, pp. 631-641.
42. Bialkowicz, B., et al., "Changes of the Dynamic Properties of the Real Cam Profile During its Wear", *Proc. 5th World Congr. Theory of machines and Mechanisms*, 1979, pp. 984-987.
43. Grant, B., and Soni, A.H., "A Survey of Cam Manufacture Methods", *J. of Mech. Des.*, Vol. 101, July 1979, pp.455-460.
44. Giordana, F., et al., "The Influence of Construction Errors in the Law of Motion of Cam Mechanisms", *J. Mech. Mach. Theory* 15(1), 1980, pp. 29-45.
45. Sankar, S., and Osman, M.O.M., "Dynamic Accuracy of hybrid Profiling Mechanisms in Cam Manufacturing", *Trans. ASME J. Mech. Des.*, 1980, pp. 1-10.
46. Kim, H.R., and Newcombe, W.R., "The Effect of Cam Profile Errors and System Flexibility on Cam Mechanism Output", *J. Mech. Mach. Theory* 17(1), 1982, pp. 57-72.
47. Norton, R.L., "Manufacturing Considerations in Cam Design", Paper No. 19, OSU's 8th App. Mechanisms Conf., St. Louis, U.S.A., Sept. 19-21, 1983.
48. Norton, R.L., "Effect of Manufacturing Methods on Dynamic Performance of Double Dwell Cams - An Experimental Study, Part II", OSU's 9th Applied Mechanisms Conf., Kansas City, Missouri, Oct 28-30, 1985.
49. Kwakernaak, H., and Smit, J., "Minimum Vibration Cam Profile", *J. Mech. Eng. Sci.* 10(3), 1968, pp. 219-227.
50. Berzak, N., and Freudenstein, F., "Optimization Criteria in Polydyne Cam Design", *Proc. 5th World Congr. Theory of Machines and Mechanisms*, 1979, pp. 1303-1306.
51. Rao, A.C., "Minimum Flexibility Error and Optimum Sensitivity Synthesis of Cam Mechanisms", *J. Mech. Mach. Theory* 14(4), 1979, pp. 209-214.

52. Rao, S.S., and Gavane, S.S., "Analysis and Synthesis of Mechanical Error in Cam-Follower Systems", Trans. ASME J. Mech. Des., Vol. 104, Jan. 1982, pp. 52-62.
53. Chew, M., et al., "Application of Optimal Control Theory to the Synthesis of High-Speed Cam-Follower Systems",  
Part 1: Optimality Criterion.  
Part 2: System Optimization.  
ASME Papers 82-DET-100, 101, 1982.
54. Cam Design Seminar, EONIC, Inc., 464 East Hollywood, Detroit, Michigan 48203 (1980).
55. Koster, M.P., Vibrations of Cam Mechanisms, Macmillan, London, 1974.
56. Chen, F.Y., Mechanics and Design of Cam Mechanisms, Pergamon Press, Inc., N.Y. 1982.
57. Tesar, D., Matthew, G.K., The Dynamic Synthesis, Analysis, and Design of Modeled Cam Systems, Lexington Books, D.C. Heath and Co. Lexington, Massachusetts, 1976.
58. Burr, A. H., Mechanical Analysis and Design, Elsevier, North Holland, Inc., N.Y., 1981.
59. Reinsch, C.H., "Smoothing by Spline Functions", Numer. Math., 10, 1967, pp. 177-183.
60. Vandergrift, J.S., Introduction to Numerical Computations, Second Edition, Academic Press, Inc., 1983.
61. Wold, S., "Spline Functions in Data Analysis", Technometrics, vol. 16, No. 1, Feb. 1974, pp. 1-11.
62. deBoor, C., A Practical Guide to Splines, App. Math. Sc., vol.27, Springer-Verlag, N.Y., 1978.
63. Chai, A.S., "A Fifth-order Modified Runge-Kutta Integration Algorithm", Simulation, vol.18, Jan. 1972, pp. 21-27.
64. England, R., "Error Estimates for Runge-Kutta Type Solutions to Systems of Ordinary Differential Equations", Comput. J. vol. 12, May 1969, pp. 166-170.
65. Hamming, R.W., Introduction to Applied Numerical Analysis, McGraw Hill, N.Y., 1971, p-320.

## APPENDICES

### A.1 Calculation of System Properties

#### Cam Mass and Rotational Inertia:

The mass and rotational inertia of a disk cam can be directly found by using polar coordinates. We require to determine the coordinates of cam profile as function of the cam angle  $\theta$ . Fig. A.1 shows a disk cam with attached system of coordinates. With reference to the moving coordinate system  $\bar{X}-\bar{Y}$  attached to the cam, a point on the cam pitch curve is defined by -

$$\begin{aligned}\bar{x} &= y \sin\theta + e \cos\theta \\ \bar{y} &= y \cos\theta - e \sin\theta\end{aligned}\tag{A.1}$$

where

$$\begin{aligned}y &= y_0 + s(\theta), \quad s(\theta) \text{ is the lift function} \\ y_0 &= \sqrt{(R_b + R_r)^2 - e^2}.\end{aligned}\tag{A.2}$$

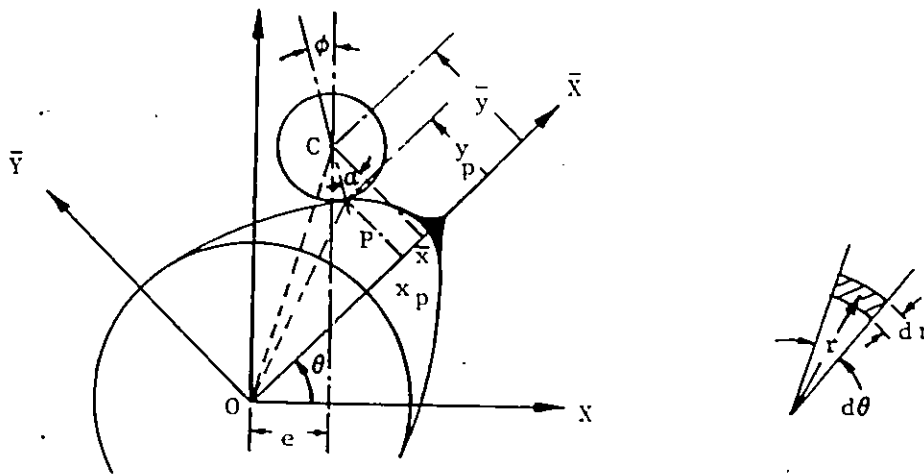


Fig. A.1 Disk cam with a translating offset roller follower.



The cam profile is therefore expressed as -

$$\begin{aligned}x_p &= y \sin\theta + e \cos\theta - R_f \sin\alpha \\y_p &= y \cos\theta - e \sin\theta - R_f \cos\alpha.\end{aligned}\tag{A.3}$$

From the geometry of Fig. A.1

$$\alpha = \theta - \phi\tag{A.4}$$

where

$$\phi = \text{pressure angle.}$$

Therefore, we can write

$$\begin{aligned}x_p &= y \sin\theta + e \cos\theta + R_f \cos(\phi - \theta - \pi/2) \\y_p &= y \sin\theta - e \sin\theta + R_f \sin(\phi - \theta - \pi/2).\end{aligned}\tag{A.5}$$

Consider an element at a radius  $r$  as shown in the figure. The area and mass of this element are

$$dA = r \, dr \, d\theta$$

and

$$dm = \rho \, l \, r \, dr \, d\theta,$$

respectively. The total mass and rotational inertia of the cam are, therefore, expressed as

$$M_c = \int_0^{2\pi c} \int_0^r \rho \, l \, r \, dr \, d\theta$$

$$I_z = \int_0^{2\pi c} \int_0^r r^2 \, dm = \int_0^{2\pi c} \int_0^r \rho \, l \, r^3 \, dr \, d\theta,$$

where  $c$  is the radial distance of a point on the cam profile along the radius  $r$ , and is a function of cam angle  $\theta$ ,

$\rho$  = density of the cam material

$l$  = cam thickness.

Performing the internal integration in above equations, we obtain

$$M_c = \rho t \int_0^{2\pi} c^2/2 d\theta$$

and

$$I_z = \rho t \int_0^{2\pi} c^4/4 d\theta. \quad (A.6)$$

The radial distance  $c$  can be expressed in terms of the system parameters as

$$\begin{aligned} c^2 &= x_p^2 + y_p^2 \\ &= y^2 + e^2 + R_r^2 + 2y R_r \cos\phi - 2e R_r \cos\phi. \end{aligned} \quad (A.7)$$

Numerical integration has been employed to compute the integrals in (A.6). The subroutine computes the mass and rotational inertia of the cam for any standard cam motion defined by the user.

## A.2 Random Number Generation

An approximation to the normally distributed random number  $Y$  can be found from a sequence of uniform random numbers using the formula:

$$Y = \left( \sum_{i=1}^k X_i - k/2 \right) / (k/12)^{1/2} \quad (\text{A.8})$$

where

$X_i$  = a uniformly distributed random number ( $0 < X_i < 1$ )

$k$  = number of  $X_i$ .

$Y$  approaches a true normal distribution asymptotically as  $k$  approaches infinity. Choosing  $k$  equal to 12 gives a distribution for  $Y$  close to normal, having a zero mean and a variance of 1 [65]. It also requires a small computer time. The equation (A.8) then becomes

$$Y = \sum_{i=1}^{12} X_i - 6.0 \quad (\text{A.9})$$

The adjustment for the required mean  $\mu$  and standard deviation  $\sigma$  gives

$$\bar{Y} = \sigma Y + \mu \quad (\text{A.10})$$

where,  $\bar{Y}$  is the required normally distributed random number.

Uniformly distributed random numbers  $X_i$  are generated by employing subroutine RANDU available with the VAX-730 system.

### A.3 Return Spring Idealization

To simulate its vibrational behaviour, the restraining spring has been discretized as a three-mass system - Fig. A.2. This has been shown to fulfil the modelling requirements adequately [31].

$$M_0 = M_{rs}/2, K_0 = K_{rs}$$

$$M_1 = M_3 = 8/15 M_0,$$

$$M_2 = 4/9 M_0$$

$$K_2 = K_3 = 16/3 K_0$$

$$K_1 = K_4 = 16/5 K_0$$

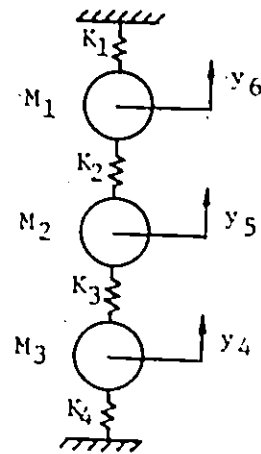


Fig. A.2 A 3-mass model for the return spring.

The spring natural frequencies have been obtained in the following development.

The equations of motion for the system are

$$M_1 \ddot{y}_6 = -K_1 y_6 + K_2(y_5 - y_6)$$

$$M_2 \ddot{y}_5 = -K_2(y_5 - y_6) + K_3(y_4 - y_5)$$

$$M_3 \ddot{y}_4 = -K_3(y_4 - y_5) - K_4 y_4$$

which can be expressed in matrix form as:

$$\begin{bmatrix} M_1 & 0 & 0 \\ 0 & M_2 & 0 \\ 0 & 0 & M_3 \end{bmatrix} \begin{Bmatrix} \ddot{y}_6 \\ \ddot{y}_5 \\ \ddot{y}_4 \end{Bmatrix} + \begin{bmatrix} (K_1 + K_2) & -K_2 & 0 \\ -K_2 & (K_2 + K_3) & -K_3 \\ 0 & -K_3 & (K_3 + K_4) \end{bmatrix} \begin{Bmatrix} y_6 \\ y_5 \\ y_4 \end{Bmatrix} = 0.$$

Assuming a harmonic solution of natural frequency  $\omega$  and its multiples, and substituting in terms of  $M_0$  and  $K_0$ , we have the characteristic equation

$$\begin{vmatrix} (128/15 K_0 - \omega^2 8/15 M_0) & -16/3 K_0 & 0 \\ -16/3 K_0 & (32/3 K_0 - \omega^2 4/9 M_0) & -16/3 K_0 \\ 0 & -16/3 K_0 & (128/15 K_0 - \omega^2 8/15 M_0) \end{vmatrix} = 0. \quad (\text{A.11})$$

This is solved to obtain the following three roots as natural frequencies in rad/sec.

$$\begin{aligned} \omega_1 &= 2\sqrt{K_0/M_0}, \\ \omega_2 &= 4\sqrt{K_0/M_0}, \\ \text{and } \omega_3 &= 6\sqrt{K_0/M_0}. \end{aligned} \quad (\text{A.12})$$

In Hertz, the cyclic frequencies are given as

$$f_1 = 1/\pi\sqrt{K_0/M_0}, \quad f_2 = 2/\pi\sqrt{K_0/M_0}, \quad f_3 = 3/\pi\sqrt{K_0/M_0}. \quad (\text{A.13})$$

COMPUTER SIMULATION OF CAM SYSTEM DYNAMICS  
AND SENSITIVITY STUDIES